1992

A Study of Nuclear Level Structure Using (3He, d) and (3He, p) Reactions

Basher, Md. Abul

University of Rajshahi

A STUDY OF NUCLEAR LEVEL STRUCTURE USING (^{3}He,d) AND (^{3}He,p) REACTIONS

BY

MD. ABUL BASHER

(1992)

DEPARTMENT OF PHYSICS

UNIVERSITY OF RAJSHAHI

BANGLADESH

A STUDY OF NUCLEAR LEVEL STRUCTURE USING (^{3}He,d) AND (^{3}He,p) REACTIONS

A DISSERTATION SUBMITTED TO THE UNIVERSITY OF RAJSHAHI FOR THE

DEGREE OF DOCTOR OF PHILOSOPHY IN PHYSICS FOR THE YEAR 1992.

NUCLEAR RESEARCH LABORATORY
DEPARTMENT OF PHYSICS
UNIVERSITY OF RAJSHAHI
BANGLADESH.

JUNE, 1992.

SUBMITTED BY:

M.A. BASHER

CANDIDATE'S DECLEARATION

I hereby certify that the work which is being presented in the thesis entitled " **A STUDY OF NUCLEAR LEVEL STRUCTURE USING (^{3}He,d) AND (^{3}He,p) REACTIONS**" in fulfilment of the requirement for the award of the Degree of DOCTOR OF PHILOSOPHY IN PHYSICS, submitted to University of Rajshahi, is an authentic record of my won work carried out during the period from July 1986 to June 1992 under the supervision of Dr. Ahmad Husain.

The matter embodied in this thesis has not been submitted by me for the award of any other degree.

mabashe .22/6/92.
(Md. Abul Basher)
Candiate's Signature.

This is to certify that the above statement made by the candidate is correct to the best of my knowledge .

aHusain 22/6/92
(Dr. Ahmad Husain)
Professor of Physics
University of Rajshahi
BANGLADESH.

CONTENTS

ACKNOWLEDGEMENTS

(i)

PREFACE

The present work describes the experimental work performed by the author in candidature for the degree of Doctor of Philosophy. The work was undertaken at the Physics Laboratory, Rajshahi University, during the period from July 1986 to June 1992.

The experimental investigation consists of a study of nuclear level structure using the $(^3He,d)$ and $(^3He,p)$ reactions. For this purpose, the $^{51}V(^3He,d)^{52}Cr$ and $^{62}Ni(^3He,p)^{64}Cu$ reactions have been studied at Helium-3 beam energy of 15 and 18 MeV respectively, using the Tandem Van-de-Graaff accelerator and multichannel magnetic spectrographs. The Ilford L4 type nuclear emulsion plates of 25μm thickness were used to record the tracks of the outgoing particles. A total of 63 levels in ^{52}Cr along with 3 new levels up to $E_x \sim 8.6$ MeV with 20 keV energy resolution and a total of 69 levels in ^{64}Cu along with two isobaric analogue states and three new levels up to $E_x \sim 8.2$ MeV excitations with an overall energy resolution of 36 keV, have been observed.

A comparison of the present results with previous works has been made. Angular distributions have been measured for most of the levels.

The data for angular distributions of cross-sections were analyzed in terms of DWBA theory of direct reaction using the code DWUCK4 and the L-transfers, the parity, the spectroscopic factors and J-limits were determined for most of the levels. Properties of a few low-lying levels in ^{52}Cr and ^{64}Cu were compared with the theoretical predictions based on the shell-model calculations.

The confirmation of the existence of analogue states has also been achieved through the measurements of the angular distributions of the protons populating the 6.821 and 8.188 MeV states in ^{64}Cu.

CHAPTER 1

REVIEW OF THEORETICAL AND EXPERIMENTAL WORK

CHAPTER 1

REVIEW OF THEORETICAL AND EXPERIMENTAL WORK

1.1 General introduction

A nuclear reaction is a process in which a change in the composition, or energy or both of a target nucleus is brought about by the bombardment with a projectile or gamma-ray. Generally, two types of information can be obtained from the study of nuclear reactions: (1) information about the nuclear matter, and (2) information about the special properties such as angular momentum, parity, magnetic moment, etc. of a particular nuclear state formed by the given reaction.

Since the nucleus is a many-body system, it is very difficult to draw a complete picture of its properties. Some simplified models with certain reasonable approximations have been developed in order to remove the complexity. One such model is the compound nucleus model due to Niels Bohr [Bo 36] and the other is the direct interaction model due to Butler [Bu 50].

The nuclear reaction takes place in two steps according to compound nucleus model such as (i) the incident particle is captured by the target nucleus and a metastable compound nucleus is formed; (ii) the compound nucleus subsequently disintegrates to yield the reaction products. These two steps are completely

independent of each other, i.e. disintegration of the compound system is independent of the way in which it was formed. It depends on the energy and angular momentum of the incident particle. The angular distribution of the outgoing particles is symmetric about 90° in the c.m. system. This mechanism is particularly valid in the region of low and medium energy. At higher energies angular distributions are completely different from those obtained by the compound nuclear model. Thus a complementary direct reaction model was first proposed by Butler [Bu 50]. According to this model, the nuclear reaction takes place in a single step. This was first recognized by Oppenheimer and Phillips [Op 35] in analyzing low-energy (d,p) reactions. The main characteristic of direct reaction mechanism is the appearance of the pronounced maxima at the extreme forward angles with oscillatory pattern of distributions. The time required to travel the nuclear dimension by the incident particle is about 10^{-22} sec for direct reaction mechanism, whereas it is about much larger for the compound nucleus process. The existence of the compound nuclear states of relatively long life-time provides an explanation for narrow resonances in nuclear cross-section at low energies (the level width Γ and life-time τ are related by $\Gamma\tau = \hbar$).

The direct interaction model for higher than 10 MeV of incident energy can well explain the experimental data. So, we may hope that the results of the present experiment with

incident energies in the region 15-18 MeV can be explained in terms of the direct reaction model.

A good deal of information on nuclear structure can be obtained from the study of one-nucleon or two-nucleon transfer reactions. In spite of its greater complexity, the two nucleon transfer reaction is a more useful tool to study levels than the single nucleon transfer process.

1.2 Literature review   .

The present work is concerned with the study of the level structure of the nuclei ^{52}Cr and ^{64}Cu. The information on these nuclei is given in this section.

1.2.1 ^{52}Cr nucleus

The excited states of ^{52}Cr were studied by Mazari et al. [Ma 57] through the ^{55}Mn$(p,\alpha)^{52}$Cr reaction and inelastic scattering of protons. By using a 6.51 MeV proton beam from an electrostatic generator and a high resolution magnetic spectrograph, they have found six excited states in ^{52}Cr.

The low-lying states of ^{52}Cr were investigated by Wilson et al. [Wi 62] by studying the decay of ^{52}Mn using scintillation spectrometers and a double-focusing beta ray spectrometer. Three strong lines were observed along with a number of weak transitions. Information on spin and parity of

3

various levels and comparison of experimental observations with theoretical predictions were made by them.

A beam of 22 MeV ^{3}He-ions from the Los Alamos variable energy cyclotron was used by Armstrong et al. [Ar 65] to investigate the (^{3}He,d) reaction on some nuclei including ^{51}V. Energy resolution (100-120 keV) is good enough to resolve levels up to an excitation of 5 to 6 MeV for the nuclei studied, and angular distributions were obtained for the deuterons corresponding to these levels.

Excited states of ^{52}Cr were studied by Monahan et al. [Mo 68] through a p-γ coincidence measurement with a Ge(Li) detector and precise excitation energies of ten levels in ^{52}Cr were obtained.

The (^{3}He,n) reactions on Ca, Ti, Ni isotopes and ^{64}Zn have been studied by Evers et al. [Ev 74] with a time of flight technique at incident energies of 15, 18, and 21 MeV. Angular distributions, spin and parity are analyzed by using DWBA model. Only L=0 and some L=2 transfers have been observed.

Angular distributions of the (^{3}He,d) reaction on ^{51}V have been measured by Pellegrini et al. [Pe 73] at 10.48 MeV with a counter telescope. Spectroscopic factors and L-values of ^{52}Cr states up to 7 MeV excitation energy are obtained by comparing the data with DWBA theory. Shell-model calculations predicted

well the $1f_{7/2}$ spectroscopic strength, but failed in reproducing the observed $2p_{3/2}$ strength.

Energy spectra and angular distributions of neutrons from the (τ,n) reaction on ^{50}Ti, at bombarding energy of 13 MeV have been measured by Bohne et al. [Bo 75] with the time-of-flight facility. The DWBA analysis of angular distributions yielded 26 levels with $J^{\pi}=0^+$ and 27 levels with $J^{\pi}=2^+$. The transitions of 0^+ states have been compared with the shell model and paring model predictions.

The $(^3He,n)$ reactions on ^{46,48,50}Ti, at the incident energy of 15 MeV have been studied by Alford et al. [Al 75] for fp-region of the residual model. Some of the observed states have been identified as analogues of low-lying states in isobaric nuclei and are predicted by pairing vibrational model (PVM). A comparison of the results with (p,t) data suggests that little mixing occurs between states with different PVM configurations.

Differential cross-sections and vector analyzing powers have been measured by Bieszk et al. [Bi 81] for (d,t) reaction induced on ^{53}Cr at E_d = 11 MeV. Transitions with l=0 to 4 are observed. The analyzing power measurements for l=1 transitions exhibit a strong systematic dependence on Q-value. A number of previous spins and parities assignments are confirmed and two new definite assignments are made on the basis of their data.

Nuclear resonance fluorescence experiments with polarized bremsstrahlung have been performed by Berg et al. [Be 81] in order to search for magnetic dipole strength in ^{52}Cr. Thirteen levels of excitation energy ranges from 7.5 to 11.8 MeV have been observed by them.

Smith et al. [Sm 83] have investigated two energy levels in ^{52}Cr which have been excited by resonance fluorescence with linearly polarized, mono-energetic gamma rays of 9.14 MeV. The azimuthal and polar asymmetry of the resonance scattered radiation have led to unique spin-parity assignments of $J^{\pi}=1^-$ for the levels.

Muto et al. [Mu 84] have studied the magnetic dipole excitation in ^{52}Cr in terms of the shell-model which includes configurations with one- and two-particle excitations from $1f_{7/2}$ to $2p_{3/2}$ and $2p_{1/2}$ to $1f_{5/2}$ shell orbits.

A 26.7 MeV beam of α-particles from the Los Alamos cyclotron was used by Armstrong et al. [Ar 67] to study the (α,t) reaction on ^{52}Cr. The triton angular distributions from some low-lying states in the residual nuclei were compared with the predications of the DWBA theory and the resulting spectroscopic information was also compared with similar information obtained by means of the $(^3He,d)$ reaction.

The (α,t) reaction on ^{51}V was studied by Matoba et al.[Ma68] at an incident alpha energy of 29 MeV using an E- $\triangle$E semiconductor detector telescope. Angular distributions were analyzed by the use of zero-range DWBA theory. The L-values and spectroscopic factors are deduced from the transitions leading to 15 low-lying states of ^{52}Cr. The results are compared with seniority scheme and the sum rule of the j-j coupling shell-model.

The excitation functions for alpha particles from the ^{55}Mn(p,α)^{52}Cr reaction from E_p=5.8 to 7.0 MeV at θ_{lab}=90°, 125°, and 180° have been measured by Hsu et al. [Hs 85]. The cross-sections are analyzed by the channel cross-section function, the statistical nuclear theory and the autocorrelation function to determine the number of correlating channels, the average total level width Γ_μ and the ratio Γ_μ/D.

Very recently, Fujiwara et al. [Fu 85] have measured the inelastic scattering of 65-MeV proton on ^{52}Cr for the states up to 11 MeV excitation energy. The systematic decrease in excitation strength of the first 3$^-$ state has been observed. Many 1$^-$ and possible 1$^+$ states have been identified at E_x=5-10 MeV and 1$^+$ assignments are in agreement with those of previous works.

The elastic and inelastic scattering of 15 MeV polarized deuterons from ^{52}Cr has been investigated by Baker et al.[Ba 74] and angular distributions of the cross-section and vector

analyzing power have been measured. Anomalous behaviour of the N=28 nuclei found in the inelastic scattering of polarized protons is not present for deuterons and the distorted spin-orbit term effect is found to be negligible.

Measurements are reported by Huis Kamp et al. [Hu 56] for the anisotropy of the intensity of the gamma radiation emitted by ^{52}Mn nuclei oriented at low temperature. From the results, it has been concluded that the spins of the 3 excited states in ^{52}Cr are 2, 4, and 6.

1.2.2 ^{64}Cu NUCLEUS

The low-lying excited states of ^{64}Cu have been the subject of several investigations over the last few decades. Figueiredo et al. [Fi 58] are one of the early investigators. They investigated the ^{63}Cu(d,p)^{64}Cu reaction at deuteron energies between 6.00 and 6.55 MeV. Sixty-five levels in ^{64}Cu were measured upto E_x~3.8 MeV. They however did not give any information about spin-parity of the states.

Toit et al. [To 61] measured the half-life of the states excited by slow neutron capture in various nuclei. The half-lives of the first and second excited states in ^{64}Cu were found to be ≤0.3 nsec.

The low energy gamma spectra of ^{64}Cu were studied by Skliarevskii et al. [Sk 58] using thermal neutrons. They observed lines at 155±5, 205±10, and 276±10 keV.

Vervier [Ve 61] studied the level structure in ^{64}Cu through circular polarization of gamma-rays following the capture of polarized neutrons. The high energy part of the neutron capture γ-ray spectrum in copper [Ba 53] shows a 7.91 MeV line which is the ground state transition in ^{64}Cu as well as 7.63 and 7.30 MeV γ-rays which are probably transition to 0.277 and 0.607 MeV states in ^{64}Cu [Tr 57, Ba Un]. The capturing state in ^{64}Cu may be 1^- or 2^- and the ground state is known to be 1^+.

Kopecky et al. [Ko 65] and Shera and Bolotin [Sh 68] investigated the level structure of ^{64}Cu by using thermal neutron capture ^{63}Cu(n,γ)^{64}Cu reactions. A number of new transitions are reported. Tentative spin assignments for excited states below 1 MeV are proposed on the basis of the gamma ray decay modes of the levels. The low-lying excited states in ^{64}Cu are discussed in terms of the $2p_{3/2}$, $1f_{5/2}$ and $2p_{1/2}$ proton-neutron configurations.

The ^{62}Ni(^{3}He,p)^{64}Cu reaction was investigated by Young and Rapaport [Yo 68]. Angular distributions are studied for the strongly excited states and L-values are determined for the neutron-proton transferred pair; but no J^{π} assignment has been reported.

9

The most remarkable work on the low-lying excited levels in ^{64}Cu is due to Park and Daehnick [Pa 69] who investigated the levels of the same nucleus with 12.08 MeV deuteron from the ^{66}Zn(d,α)^{64}Cu reaction with an energy resolution of about 11-12 keV and via ^{63}Cu(d,p)^{64}Cu reaction with and energy resolution of about 7-8 keV. About 85 levels in ^{64}Cu up to excitation of 3 MeV energy were identified by them. Angular distributions of ^{66}Zn(d,α)^{64}Cu reaction were obtained over the range $15° \leq \theta \leq 90°$ and angular distributions of ^{63}Cu(d,p)^{64}Cu reaction were also obtained over range $8° \leq \theta \leq 50°$; ℓ-values and spectroscopic factors were also extracted from a comparison with the DWBA calculations.

Lu et al. [Lu 69] studied the (α,d) reaction with a beam of 50 MeV alpha-particles on ^{62}Ni.

Angular distributions and Υ-Υ correlation of Υ-rays emitted following the ^{64}Ni(p,n)^{64}Cu reaction were investigated by many authors. Among them, Davidson et al. [Da 70] have studied levels up to 927 keV. Unique spin and parity assignments for several levels were computed by using the theoretical prediction of the compound nucleus statistical model.

Bass and Stelson [Ba 71] studied the ^{64}Ni(p,n)^{64}Cu reaction using the neutron time of flight technique and the energy levels in ^{64}Cu are measred up to an excitation energy of 2757 keV.

The spins for the several levels in ^{64}Cu have been assigned up to an excitation energy of 663 keV from the ^{64}Ni(p,n)^{64}Cu reaction by Litherland and fergeson [Li 61] and Wellborn [We 71].

Nuclear level structure of ^{64}Cu was studied by Black et al. [Bl 72] by the use of γ-ray spectroscopy via ^{63}Cu(d,p)^{64}Cu reaction at an incident deuteron beam energy of 6.5 MeV. Excitation energies up to 1594 keV were identified.

Green et al. [Gr 76] have measured the gamma-ray angular distribution and γ - γ angular correlation for the transition observed following the ^{64}Ni(p,n)^{64}Cu reaction and unique spin assignments are made for several levels.

The compound nucleus contributions to the proton spectra from 8 MeV to 10 MeV ^{3}He induced (^{3}He,p) reactions on even-A Ni isotopes were obtained by Lee et al. [Le 80]. The relative cross-sections for ^{58}Ni/^{60}Ni/^{62}Ni in the high excitation region are in fair agreement with predictions of statistical theory but the absolute cross-sections in the same region are smaller than the prediction by a factor of 3 to 8 and the shapes of the measured spectra for heavier isotopes do not agree with the prediction. These discrepancies between experiment and theory are in sharp contrast to the situation in (p,p'), (p,α), (α,p) and (α,α') reactions where good agreement was found. The proton spectra from the (^{3}He,p) reactions on nuclei in the A=54-68 mass range have a systematic difference in slope between even-A

targets and odd-A targets; it is similar to the systematic difference found previously in (p,p´) and (α,p) reactions but none of these is well explained by theory.

1.3 Approach to the present work

Over the last two decades stripping reactions have been used for nuclear spectroscopic studies. Among them the (d,p) reaction is the simplest and widely used. But it has been observed that all the final nuclei cannot be reached by a single n-transfer via (d,p) reaction on available targets. Sometimes double stripping reaction like (^{3}He,p) is essential for the purpose.

The (^{3}He,p) reaction is good enough to study the final state with a dominant |Core+p+n> configuration, whereas (d,p) or (^{3}He,d) reaction is only used to study the levels of the final nuclei which have a dominant |Core+n> or |Core+p> configuration. The (^{3}He,p) and (^{3}He,d) reactions are expected to show up new levels which may be unobserved with other particles.

The (^{3}He,d) reaction should be equivalent to the (d,n) reaction in the sense that they lead to the same final nucleus; but in the latter case the neutron being a neutral particle, is very difficult to detect. So the (^{3}He,d) reaction is one of the most important tools of extracting spectroscopic information on

levels in ^{52}Cr. Similarly, the (^{3}He,p) reaction is equivalent to (α,d) reaction in the sense that they have the same final nucleus. The spin and isospin selection rules and the antisymmetrization requirement in the two-nucleon transfer reactions allow the transfer of only spin triplet np pair in the (α,d) reaction in contrast to both the spin triplet and a spin singlet in the (^{3}He,p) reaction. So the (^{3}He,p) reaction is also one of the most important tools of extracting nuclear spectroscopic information on the levels in the complex odd-odd nucleus ^{64}Cu.

The present works on the ^{51}V(^{3}He,d)^{52}Cr and ^{62}Ni(^{3}He,p)^{64}Cu reactions are undertaken with the aim of studying the structure of the low-lying levels of ^{52}Cr and ^{64}Cu. Angular distributions are measured for 63 levels in ^{52}Cr and 69 levels in ^{64}Cu up to excitations of 8.6 and 8.2 MeV for the respective nuclei. The data are analyzed in terms of the DWBA theory of direct reaction. Spectroscopic factors for most of the levels are derived from a comparison of the experimental and DWBA cross-sections. Two analogue states are identified and are confirmed through the measurement of the angular distributions of protons populating the 6.821 and 8.188 MeV in ^{64}Cu from the (^{3}He,p) reaction.

CHAPTER 2

EXPERIMENTAL PROCEDURE

CHAPTER 2

EXPERIMENTAL PROCEDURE

2.1 Experimental set up

Experimental investigations of low-lying excited states of even-even nuclide ^{52}Cr and odd-odd nuclide ^{64}Cu are the subject-matter of the present work. For this purpose, two reactions such as ^{51}V(^{3}He,d)^{52}Cr and ^{62}Ni(^{3}He,p)^{64}Cu are employed for investigations. The 15 MeV doubly ionized ^{3}He-beam from the Oxford Tandem Van de Graaff accelerator was used as projectile. The isotonically enriched ^{51}V target of thickness 100μg/cm² was prepared by vacuum evaporation on to a thin carbon backing of Vanadium oxide. The target was oriented at an angle of 45° with respect to the direction of incident beam. The reactions products were magnetically (H=13.26 KG) analyzed in an Oxford Multichannel Spectrograph [Br 56] and were recorded in Ilford L4 type nuclear emulsion plates of 25μm thickness, simultaneously over the angles between 3.75° to 71.25° (lab) in steps of 7.5°. The emulsion was covered with a 0.25 mm polythene foil so as to stop all particles less penetrating than deuterons. The total beam charge was 5210 μCoul.

For the second reaction, the 18 MeV doubly ionized and monoenergetic ^{3}He-beam from Tandem Van de Graaff generator of AERE, Harwell, U.K. was used as projectile on the target

(isotopically enriched to 99% ^{62}Ni; nominally 100 μg/cm² thick). The reaction products entered into a high magnetic field of strength 12.45 KG of a multichannel spectrograph [Br 56] and were recorded in 25 μm thick Ilford L4 emulsions, simultaneously over the angles between 5° to 80° at 7.5° interval. The emulsion was covered with 40 thou thick polythene foil for stopping all particles other than protons. The total beam charge was 10124 μCoul.

2.2 Multichannel magnetic spectrograph

The Multichannel magnetic spectrograph (MMS) has been used for the analyses of nuclear reaction products. The description of the essential features of MMS is given below for better understanding (Fig. 2.1).

The MMS [Br 56., Mi 62] consists of twenty-four broad range single channel magnetic spectrographs with a common magnetic circuit. A toroidal iron ring with twenty-four radial air-gaps cut in an iron at angular intervals of 7.5° from a suitable starting point, is associated with the magnet. So, a single bombardment covers a wide range of angles. In each channel, there is an arrangement for placing nuclear emulsion plate of about one hundred centimeter in length. In order to have the channel configurations, the whole apparatus can be rotated through 3.75° under vacuum. The plates for detection can be moved laterally across the focal planes in order to allowing successive exposures without breaking the vacuum.

MAGNET COILS

NUCLEAR PLATE

PROTON RESONANCE PROBE

TARGET

DEFINING APERTURE

SEGMENT SUPPORTS

WATER MANIFOLDS

LIQUID AIR TRAP

STABILISING SLITS

POLE CLAMPS

POLE SEGMENTS

OBSERVATION PORT

INCIDENT BEAM AXIS
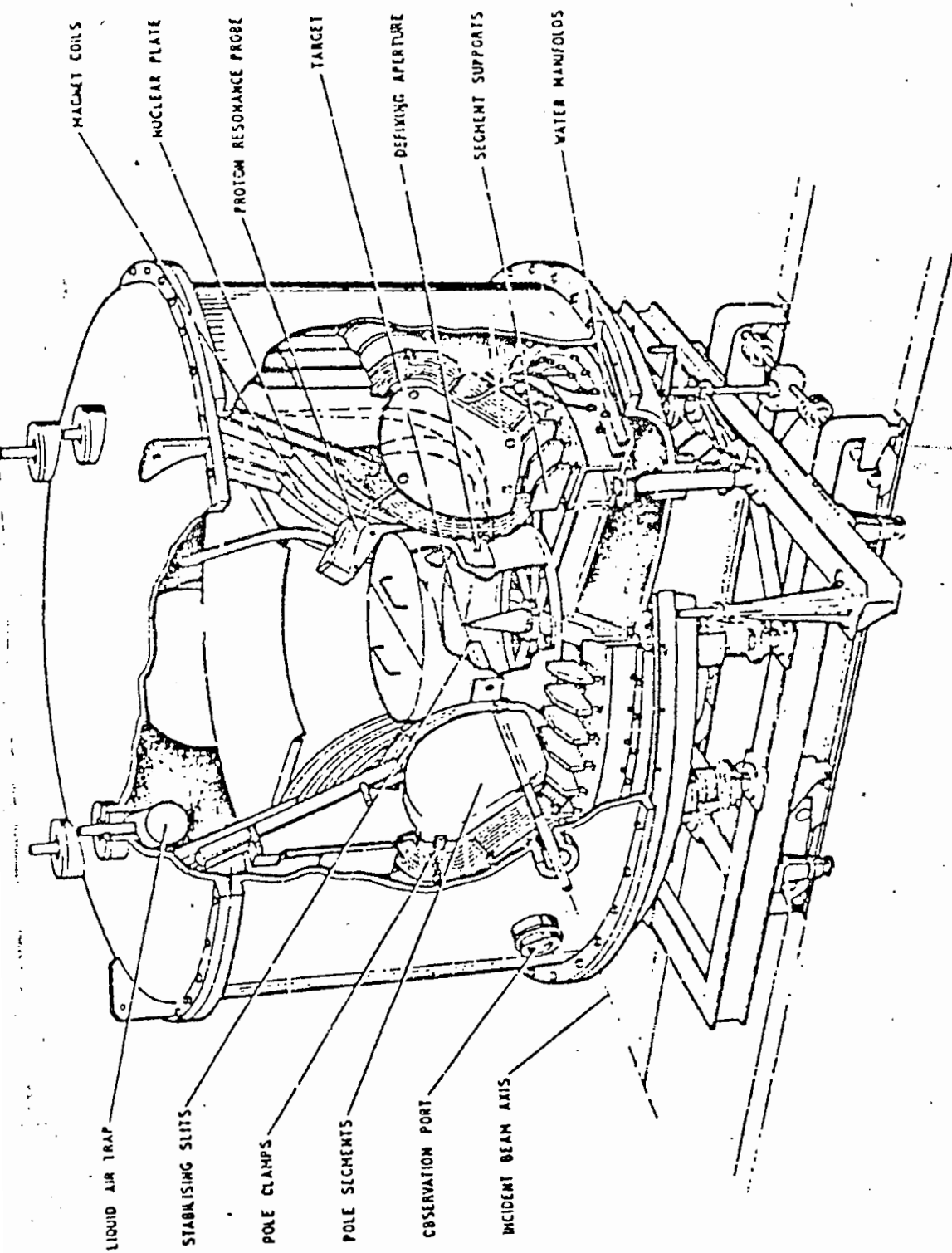
Fig. 2.1. Multi-channel Magnetic Spectrograph.

The incident ion beam from the Van de Graaff generator is allowed to enter the spectrograph through a hole. The beam is collimated by a slit system placed ahead from the central target [Mi 62]. The charge of the ion beam is measured by a Faraday cup which is situated just inside the magnetic fringing field.

The target is mounted on a cone placed at the central part of spectrograph and is also oriented at an angle of 45° with respect to the beam direction. The reaction product emanating from the target is brought to focus on the emulsion plates placed along the hyperbolic focal plane of each magnet. Suitable polythene absorber is placed on the plate for stopping all particles less penetrating than scattering particles (deuterons or protons).

When the experiment is over, the plates are taken out of the spectrograph and are covered with dark lids. Then they are indexed and developed in the usual process.

2.3 Microscope

The rows of black grains of colloidal silver are called tracks which should be measured with great precision. A high resolving power microscope is essential for the analysis of the emulsion plates. A Vickers binocular microscope can be used with great comfort, since a long time has to be spent for the purpose of searching and scanning. The scanning was performed

with 15X eye-piece and 20X objective. Sometimes objective with higher magnification 40X was used for tracks in large numbers.

In order to avoid *back lash* error, the mechanical stage of the microscope is mounted on ball bearing spring loaded. It is achieved by micrometer movements in X- and Y-directions. A green light arrangement with the help of step down transformer of 6 volts is provided with it for the sufficient illumination of the field of view.

2.4 Exposure and scanning of the emulsion plates

The exposure of the emulsion plates had been carried out with a doubly ionized Helium-3 beam of 15 MeV from the Tandem Van de Graaff accelerator of Oxford, U.K. (for the $^{51}V(^{3}He,d)^{52}Cr$ reaction) and of 18 MeV from the Tandem Van de Graaff generator of the AERE, Harwell, U.K. (for the $^{62}Ni(^{3}He,p)^{64}Cu$ reaction) respectively. The plates for exposure and target nuclei for the bombardment were located at the respective positions inside the Multi-channel spetrographs. The total charge of 5210 μc and 10124 μc respectively were collected by Faraday cups situated inside the magnetic fields of flux densities 13.26 KG and 12.45 KG respectively. In the field region, the particles were deflected and were brought to focus according to their energies somewhere along 100 cm long emulsion plates. The Ilford L4 type nuclear emulsion plates of 25 μm thickness were covered with 0.25 mm and 40 thou respectively of

polythene absorber which stopped all particles other than reaction products. At the end of the exposure, the plates were removed covering with dark lids and then they were indexed in the usual process. After processing and drying, the plates were ready for scanning purposes.

The plates were exposed to 24 angles from 3.75° to 176.25° and 5° to 175° respectively at 7.5° intervals. After processing, each plate was marked with eight datum lines perpendicular to the length of it. The indices were labeled by letters A,B,C,D,E,F,G, and H (excluding G and H for Oxford exposure). The extreme three forward angles were stopped down by the following factors in order to cope with high yield in the angles for the stripping reactions:

Channel	Angle	Stop-factor	Remark
1	3.75°	4	Oxford exposure
2	11.25°	2	"
3	18.75°	1.25	"
1	5.0°	4	Harwell exposure
2	12.5°	2	"
3	20.0°	1.33	"

Each of these segment-plates was placed on the table of the Vickers binocular microscope in such a way that one of the datum lines of the plate fell just at the middle of the large square graticule of the eye-piece scale. The datum line was then made

LOW END ← — — — — — — — — — → HIGH END

0	127	254	381	508	635	762	889
A	B	C	D	E	F	G	H

└─INDEX POSITION(mm)   └─SUBPLATE REF

NOT TO BE COUNTED
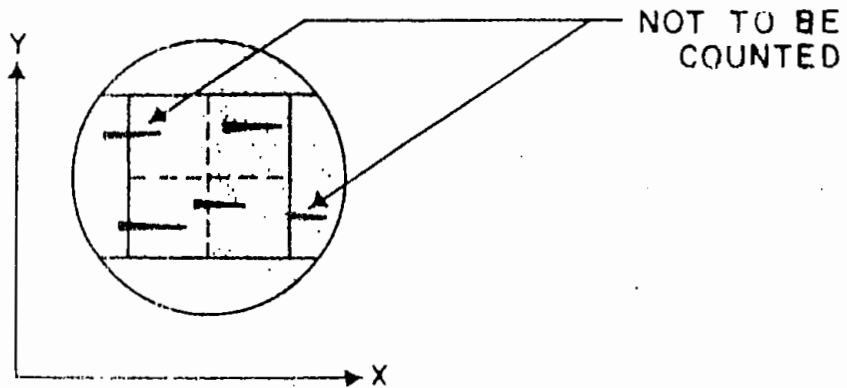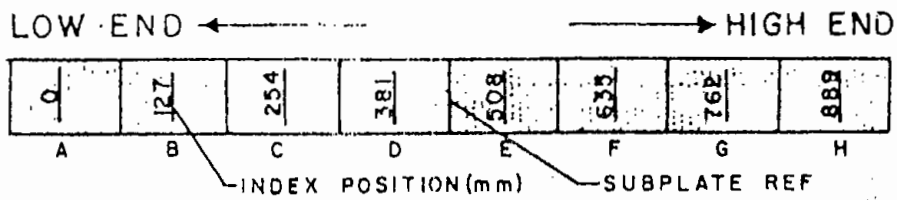
Fig.2.2 Proton or deuteron tracks after magnification.

to coincide with the Y-axis of the cross-wire. The scanning was performed in step of X=0.25 mm. Along Y-axis, a displacement of 9-11 mm. was done by the adjustable screw so that no tracks was missed. The procedure of the scanning could be well understood from Fig. 2.2. The circle represents the field of view under the proper magnification of the microscope. When Y-screw was turned in the forward direction, a number of tracks (say, P,Q,R, etc.) which would move from bottom end of the field of view, would be observed. Those tracks which were not parallel to (0-6) line and those whose entry points were not inside the graticule, should not be counted. X-axis was turned through 0.25 mm. and the total number of the tracks were counted. In this way, the scanning was performed for the whole of the plates.

The plates were obtained through the courtesy of Dr. D.L. Watson [Wa Un] of the University of Bradford, U.K. .The plates were scanned at the Nuclear Physics Laboratory, University of Rajshahi, Bangladesh.

CHAPTER 3

EXTRACTION OF DATA

CHAPTER 3

EXTRACTION OF DATA

3.1 Introduction

The glorious history of nuclear energy levels commenced from 1930 when Rosenblum [Ro 30] discovered the spectra of alpha particles. In the nuclear energy level diagram, the ground state is taken as the lowest energy state depicted by a horizontal line at the bottom on which the other excited levels are located.

3.2 Energy levels

A precise measurement and accurate knowledge of the nuclear energy levels are most essential for the development of the nuclear spectroscopy. The study of nuclear spectroscopy means the mapping of nuclear energy levels and a study of their properties.

The energy of the outgoing particle in the A(a,b)B reaction is given by the expression:

$$E_b = 931.14 \ m_b \left[\left\{ 1 + 1.036598 \times 10^{-7} \times \left(\frac{Hz\rho}{m_b} \right)^2 \right\}^{\frac{1}{2}} - 1 \right] \quad \dots (3.2a)$$

where H is the magnetic field in Kilogauss, m_b, z and ρ are the mass, number of unit charge and the radius of curvature of the outgoing particle respectively. The ρ is given by

$$\rho = \left[a_o + a_1x + a_2x^2 + a_3x^3 + a_4x^4 + \ldots \right]^{\frac{1}{2}} \qquad \ldots (3.2b)$$

where x is the position of the outgoing particle group in unit of 0.5 mm. on the plate. The value of Q in the ith state is given by

$$Q_i = E_b \left(1 + \frac{m_b}{m_B} \right) - E_a \left(1 - \frac{m_a}{m_B} \right) - \frac{2 (m_a \, E_a \, m_b \, E_b)^{\frac{1}{2}}}{m_B} \, Cos\theta \quad ..(3.2c)$$

where m_a is the mass of the incident particle, m_b is the mass of outgoing particle, m_B is the mass of final nucleus, E_a and E_b are the energy of the incident and outgoing particle respectively.

Energy levels of the residual nucleus are obtained from the spectra at different angles. For this purpose, each angle is calibrated in energy using the least squares relation

$$E_b = A_o + A_1x + A_2x^2 + \ldots\ldots\ldots \qquad (3.2d)$$

in which x is the peak-position of the group in the energy spectra of the outgoing particle.

    For the identification of the existing and the new levels, the following criteria were used:

(i)   The excitation energies of levels in residual nucleus obtained at different angles are required to be consistent to within about 20 keV;

(ii)   and the groups due to emitted particles at different angles belonging to the levels have about the same widths.

Energy resolution is one of the most important properties of any energy measuring device. It may be defined as the full width at half maximum (FWHM) or intensity of the peak produced by a number of particles of identical energy. If the resolution is poor, individual peak will not be resolved and information will be lost. For the present experiment, the position of the half-maxima of the peaks were recorded carefully.

3.3 Energy levels in ^{52}Cr

The energy levels in ^{52}Cr were obtained from the $(^{3}He,d)$ reaction on ^{51}V. Details of the exposure are shown in Table 3.1 and the coefficients of the equation (3.2b) from the calculations of the Oxford spectrographs are given in Table 3.2.

The energy levels in ^{52}Cr were obtained by using several well established levels in ^{52}Cr. The least squares values of A_o, A_1, and A_2 in equation (3.2d) for each channel were calculated using the Alpha-Micro AM1000E computer of the University of Rajshahi, Rajshahi, Bangladesh.

After completing the scanning, the energy spectra of the outgoing deuteron of the $^{51}V(^3He,d)^{52}Cr$ reaction at the scattering angles 3.75°, 11.25°, 18.75°, 26.75°, 33.75°, 41.25°, 56.25°, and 71.25° were obtained. The deuteron spectrum at 33.75° (lab.) is shown in Fig. 3.1 as an example.

The calculations of excitation energies of different levels at different angles were carried out with the help of the same computer at Rajshahi University.

In the present work, the levels in ^{52}Cr have been observed up to an excitation energy Ex ≈ 8.6 MeV. The energy resolution was found to be ≈ 20 keV (FWHM). The results of the present study of the energy levels are compared with those of the previous works [Si 84, Pe 73, Fu 85], as shown in Table 3.3. Properties of the levels of ^{52}Cr are summarized in Table 5.2 in Chapter 5.

Table-3.1

Experimental details for the $(^3He,d)$ reaction

Bombarding energy (MeV)	Target enriched	Mag. field (KG)	Frequency (MHz)	Exposure (μC)
15	51_V	13.26	57.16	5210

Table-3.2

The coefficients of eqn. (3.2b) from Oxford spectrosgraph calibration.

$a_o(cm^2)$	$a_1(cm)$	a_2	$a_3 (cm^{-1})$	$a_4 (cm^{-2})$
49.9655	1.04586×10^{-2}	1.15948×10^{-6}	4.04482×10^{-11}	4.36034×10^{-14}

Fig. 3.1—Deuteron spectrum at $\theta_{lab} = 33.75°$

$^{51}V(^{3}He,d)\,^{52}Cr$,
$\theta_{lab.} = 33.75°$
$E(^{3}He) = 15\ MeV$
$H = 13.26\ kG$
Exposure = 5210 µC.
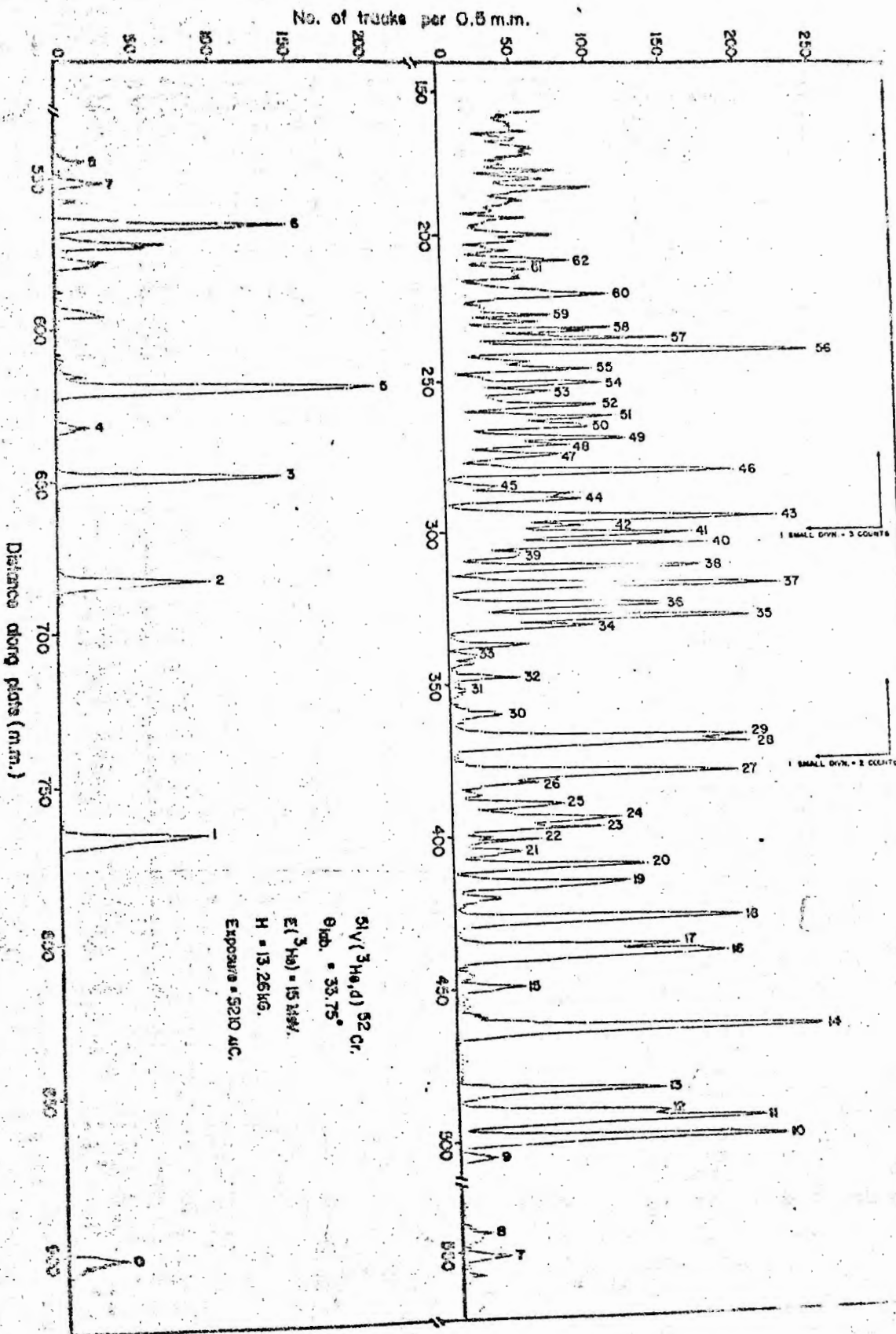
TABLE-3.3

Energy levels in ^{52}Cr

Gr.No.	Excitation energy in ^{52}Cr (MeV)			
	a	b	c	d
00	0.000	0.000	0.000	0.000
01	1.436	1.434	1.430	
02	2.370	2.370	2.360	2.369
03	2.767	2.768	2.770	2.768
04	2.965	2.965	3.110	2.965
05	3.113	3.114		3.114
06	3.770	3.772	3.780	3.772
07	3.938	3.946		3.949
08	4.033	4.038		4.040
09	4.565	4.563		4.563
10	4.628	4.627	4.640	4.630
11	4.701	4.706		4.702
12	4.737	4.741	4.740	4.738
13	4.835	4.837	4.850	4.832
14	5.101	5.097	5.120	5.095
15	5.285	5.281		5.285
16	5.435	5.432		5.425
17	5.467	5.450	5.450	
18	5.594	5.600	5.600	5.569
19	5.751	5.737	5.770	5.727
20	5.828	5.830	5.830	5.811

TABLE-3.3 continued.

Gr.No.	Excitation energy in ^{52}Cr (MeV)			
	a	b	c	d
21	5.891	5.879		5.873
22	5.945	5.953		5.957
23	5.992	5.996		5.996
24	6.026	6.026	6.020	6.055
25	6.089	6.106		
26	6.192	6.193		6.201
27	6.232	6.233	6.240	6.243
28	6.364	6.356	6.370	6.349
29	6.388	6.392		6.382
30	6.500	6.493		6.482
31	6.625			6.637
32	6.676			6.678
33	6.814	6.810		
34	6.894			
35	6.928	6.920	6.920	
36	6.933	7.010	7.010	6.993
37	7.079	7.070	7.070	7.080
38	7.165	7.180	7.180	
39	7.223			7.217
40	7.273			7.278
41	7.322			
42	7.359			

TABLE-3.3 continued.

Gr.No.	Excitation energy in ^{52}Cr (MeV)			
	a	b	c	d
43	7.400	7.400		7.409
44	7.487	7.450		7.482
45	7.536			
46	7.606	7.600		
47	7.686			7.679
48	7.729	7.730		7.738
49	7.760			
50	7.815			7.823
51	7.853			7.848
52	7.905	7.900		7.893
53	7.967			7.967
54	8.020			8.022
55	8.083			8.089
56	8.183			8.181
57	8.234			8.213
58	8.283			8.281
59	8.373			8.374
60	8.451			8.457
61	8.579			8.569
62	8.614			8.617

a. Present work

b. Summary [Si 84]

c. From (^{3}He,d) reaction given by Pellegrini et al. [Pe 73]

d. From (p,p') reaction given by Fujiwara et al. [Fu 85].

3.4 Energy levels in ^{64}Cu

The energy levels in ^{64}Cu were obtained from the ^{62}Ni(^{3}He,p) reaction. Details of the exposure are shown in Table 3.4 and the coefficients of the equation (3.2b) from the calculations of the Harwell spectrograph are given in Table 3.5.

The energy levels in ^{64}Cu are obtained by using several levels in ^{64}Cu as well as contaminant levels arising from (^{3}He,p) reaction on 12_C and 16_O . The contaminant levels used for the calibration are shown below;

^{12}C(^{3}He,p)^{14}N reaction:

E_x =0.0,2.313,3.948,4.915,5.106,5.680,5.832 & 6.444 MeV [Aj 83]

^{16}O (^{3}He,p) ^{18}F reaction:

E_x = 0.0, 0.937, 1.701., 2.101, 1.119, 3.067 and 3.830 MeV [Aj 83]

The least squares values of A_o, A_1 and A_2 in the eqn. (3.2d) for each channel were calculated separately using the Alpha-micro AM1000E computer of the University of Rajshahi, Rajshahi, Bangladesh.

The energy spectra of the outgoing protons of the ^{62}Ni(^{3}He,p)^{64}Cu reaction at the scattering angles 5.0°, 12.5°, 27.5°, 35.0°, 42.5°, 50.0°, 65.0°, 72.5°, and 80.0° were obtained. The proton spectrum at 27.5° (lab.) is shown in Fig. 3.2 as an example.

The calculations of excitation energies of different levels at different angles were carried out with the help of the same computer at the Rajshahi University.

In the present work, the levels in ^{64}Cu have been observed up to an excitation energy $E_x \approx 8.2$ MeV. The energy resolution was found to be ≈ 36 keV (FWHM). The results of the present work are compared with those of the previous works [Si 84, Pa 69, Fi 58], as shown in Table 3.6. Properties of the levels of ^{64}Cu are summarized in Table 6.2 in Chapter 6.

Table-3.4

Experimental details for the (^{3}He,p) reaction

Bombarding energy (MeV)	Target enriched	Mag. field (KG)	Frequency (MHz)	Exposure (μC)
18	^{62}Ni (99%)	12.45	53	10,124

Table-3.5

The coefficients of eqn. (3.2b) from Harwell spectrosgraph calibration.

a_o(cm^2)	a_1(cm)	a_2	a_3 (cm^{-1})	a_4 (cm^{-2})
964.64	0.79606	-2.6399×10^{-5}	-7.8588×10^{-9}	9.5022×10^{-13}
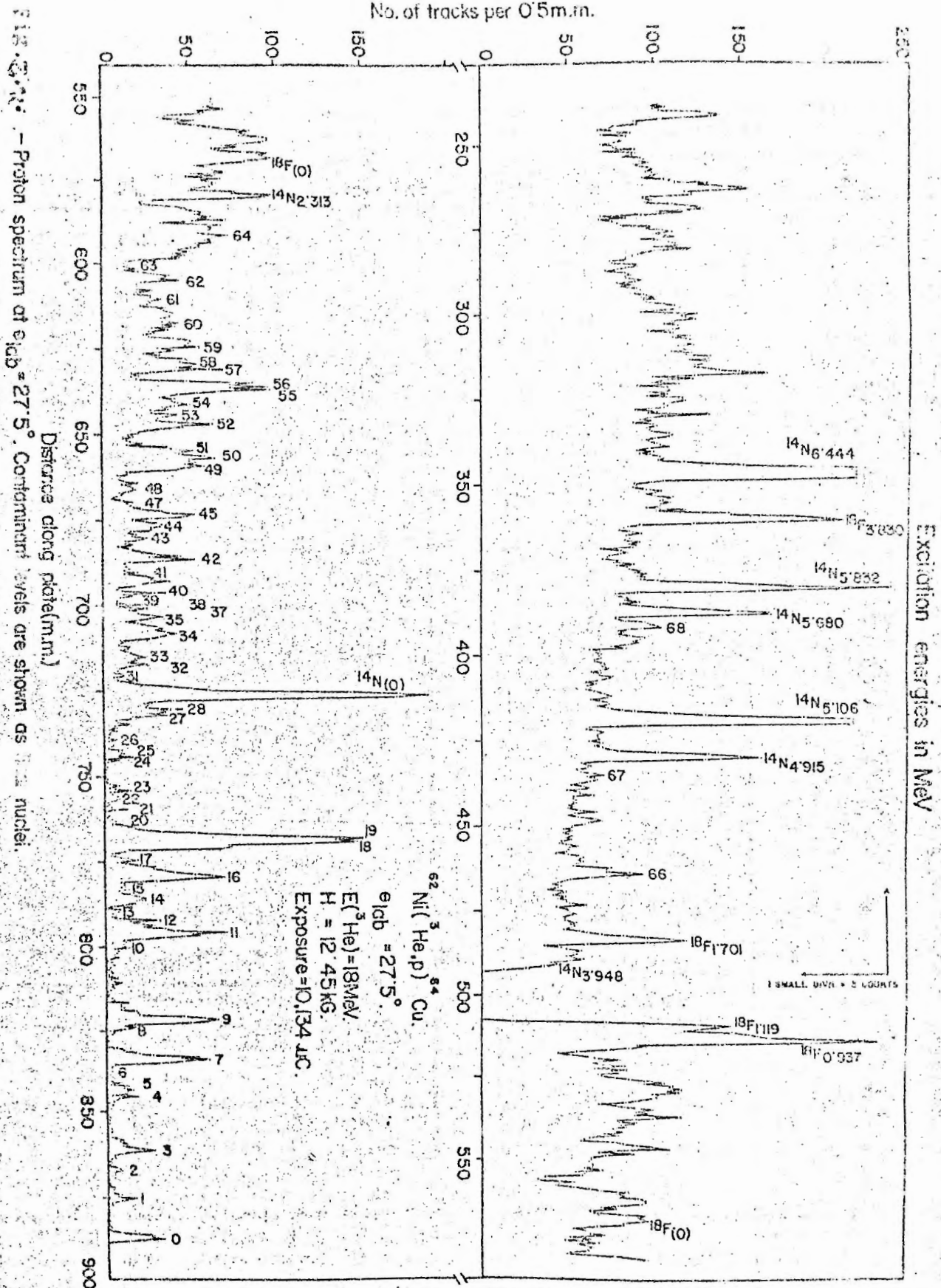
Fig. 2.8. — Proton spectrum at $\theta_{lab} = 27.5°$. Distance along plate(m.m.). Contaminant levels are shown as thin nuclei.

$^{62}Ni(^3He,p)^{84}Cu$.
$\theta_{lab} = 27.5°$.
$E(^3He) = 18 MeV$.
$H = 12.45 kG$.
Exposure = 10,134 μC.

No. of tracks per 0.5 m.m.

Excitation energies in MeV

TABLE-3.4

Energy levels in ^{64}Cu

Gr. No.	Excitation energy in ^{64}Cu (MeV)			
	a	b	c	d
00	0.000	0.000	0.000	0.000
01	0.160	0.159	0.158	0.159
02	0.278	0.278	2.076	0.277
03	0.362	0.362	0.261	0.360
04	0.574	0.575	0.573	0.574
05	0.608	0.609	0.606	0.607
06	0.663	0.663	0.661	0.664
07	0.745	0.746	0.742	0.743
08	0.878	0.879	0.876	0.877
09	0.927	0.927	0.923	0.925
10	1.243	1.241	1.236	1.239
11	1.299	1.298	1.294	1.295
12	1.322	1.320		
13	1.359	1.354	1.349	1.352
14	1.440	1.438	1.435	1.437
15	1.509	1.499	1.495	
16	1.551	1.551	1.546	1.547
17	1.602	1.607	1.607	1.592
18	1.689	1.683	1.678	1.682
19	1.741	1.742		
20	1.775	1.770	1.775	1.779

TABLE-3.4 continued.

Gr. No.	Excitation energy in ^{64}Cu (MeV)			
	a	b	c	d
21	1.853	1.852	1.848	1.852
22	1.907	1.908	1.900	1.904
23	1.952	1.940	1.939	1.939
24	2.047	2.053	2.050	2.020
25	2.092	2.092	2.090	2.072
26	2.146	2.145	2.141	2.145
27	2.246	2.251	2.249	2.232
28	2.290	2.301	2.294	2.268
29	2.323	2.322	2.327	2.316
30	2.369	2.378	2.375	
31	2.414	2.417		
32	2.455	2.457	2.462	2.465
33	2.515	2.522		
34	2.608	2.608	2.596	2.584
35	2.679	2.670	2.670	
36	2.718	2.716	2.720	2.722
37	2.762	2.757	2.760	2.768
38	2.801		2.800	
39	2.827		2.823	2.830
40	2.875		2.876	2.876
41	2.907		2.913	2.934
42	2.990		2.985	2.975

continued...

TABLE-3.4 continued.

Gr. No.	Excitation energy in ^{64}Cu (MeV)			
	a	b	c	d
43	3.066		3.055	3.088
44	3.130	3.127		3.154
45	3.189	3.190		3.192
46	3.231			3.233
47	3.265			3.260
48	3.302			3.290
49	3.397			3.411
50	3.472			3.475
51	3.513			3.515
52	3.607			3.604
53	3.686			3.687
54	3.713			3.712
55	3.767			3.763
56	3.802	3.799		3.791
57	3.902			
58	3.973	3.987		
59	4.028			
60	4.137			
61	4.257			
62	4.316			
63	4.425			

TABLE-3.4 continued.

Gr. No.	Excitation energy in ^{64}Cu (MeV)			
	a	b	c	d
64	4.571	4.570*		
65	6.171			
66	6.821	6.826		
67	7.339	7.320*		
68	8.188			

a. Present work

b. Summary [Si 84]

c. From (d,α) reaction given by Park and Daehnick [Pa 69]

d. From (d,p) reaction given by Figueiredo et al. [Fi 58]

* means ref.[Lu 69]

3.5 Differential Cross-Section

The differential scattering cross-section for the reaction A(a,b)B in the laboratory system is obtained from the following relation:

$$(d\sigma/d\Omega)_{Lab} \propto D \, N(\theta)$$

The differential cross-section $(d\sigma/d\Omega)_{Lab}$ can be converted into the centre of mass system $(d\sigma/d\Omega)_{cm}$ through the relation:

$$(d\sigma/\Omega)_{cm} = f(\theta) \, (d\sigma/d\Omega)_{Lab} \qquad \ldots (3.4a)$$

$$\text{where } f(\theta) = \frac{Sin^2\theta}{Sin^2\phi} \, Cos \, (\phi-\theta) \qquad \ldots (3.4b)$$

and ϕ is the angle in cm. system; $f(\theta)$ is calculated from the kinematics of the reaction.

It has been shown that the differential scattering cross-section in mb/sr is given by

$$(d\sigma/d\Omega)_{Lab} = 0.266 \; \frac{N z A \, cos\theta_t}{Q(\mu c) \; T(\mu g/_{cm}{}^2) \; \Omega(msr)} \qquad \ldots (3.4c)$$

Here, $N = N_A S$

where, N_A — Actual counts

   S — Stopping factor

A — target mass (a.m.u)

Z — charge of a projectile (in e)

T — target thickness

θ_t — target angle = 45°.

The measured angular distributions for the $^{51}V(^3He,d)^{52}Cr$ and $^{62}Ni(^3He,p)^{64}Cu$ reactions are presented in Chapters 5 and 6 respectively.

CHAPTER 4

MATHEMATICAL FORMULATION

CHAPTER 4

MATHEMATICAL FORMULATION

This chapter is devoted to giving an outline of the DWBA theory to be used in the subsequent chapters (chapters 5 and 6) for the purpose of analyzing the angular distributions of the outgoing protons and deuterons for the (^{3}He,p) and (^{3}He,d) reactions respectively. Extensive works on the DWBA theory have been done by many workers. Some of the main points relating to the present works are worth noting.

4.1 DWBA theory for the (^{3}He,p) reaction

Fig.4.1 illustrates the (^{3}He,p) processes calling in general A(a,b)B stripping reaction in this chapter.

As shown in the figure the projectile ^{3}He-represented by 'a' being incident upon the target 'A' stripped off two nucleons. As a result the nuclear reaction occurs and the outgoing proton represented by 'b' moves away leaving the residual nucleus 'B' behind. Let us suppose that the target is of nucleon number A and hence the residual nucleus is that of (A+2).

4.1.1 The transition amplitude

When the incident ^{3}He-particle and the target nucleus are far apart the wave function (w.f.) of the incident system ϕ_i is
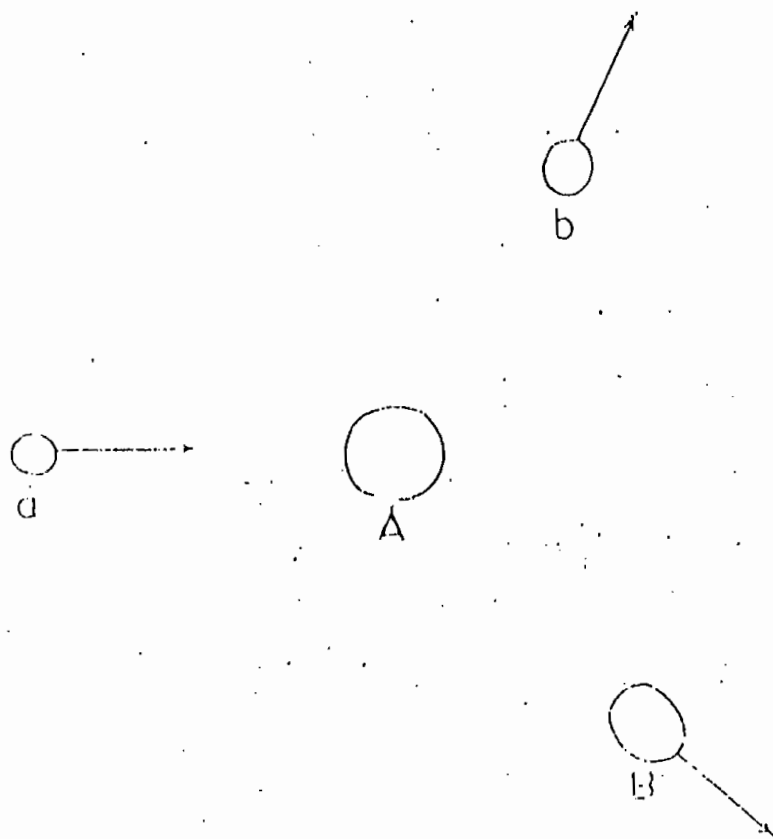
Fig.4.1.- Description of the A(a,b)B stripping reaction

$$a = b + x$$
$$x = x_1 + x_2$$
$$b = b_1 + b_2$$

$$\vec{r}_{bB} = \vec{r}_{bx} + \frac{A}{B}\vec{R}_x$$
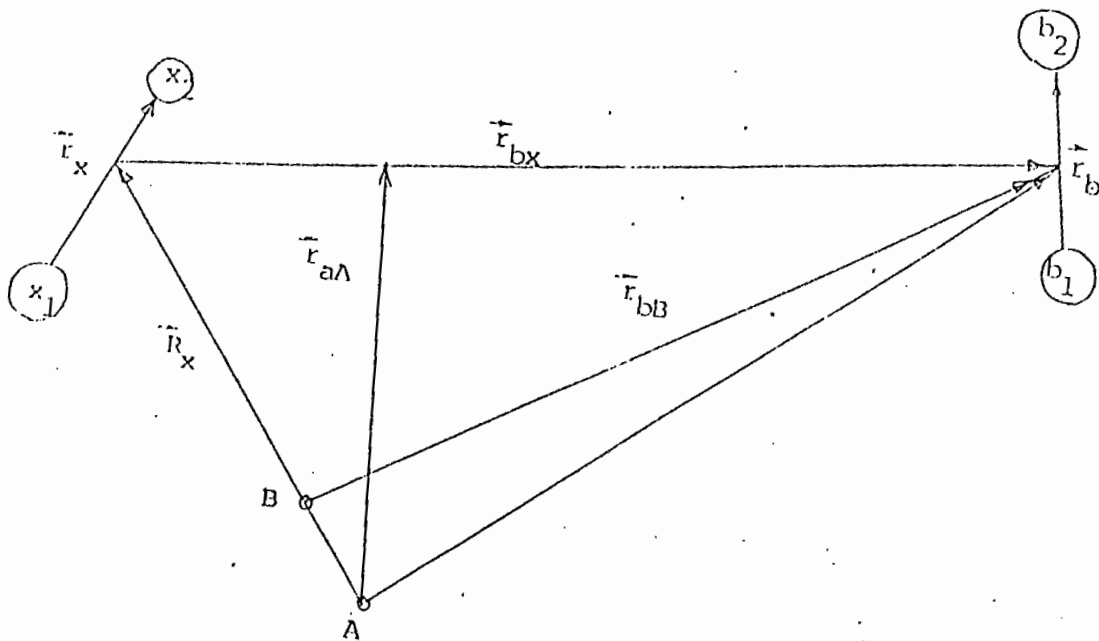
$$\vec{r}_{aA} = \frac{b}{a}\vec{r}_{bx} + \vec{R}_x$$

Fig. 4.2.—The coordinate system used in the $(^3He, p)$ reaction

an eigenfunction of the Hamiltonian H_i;

$$H_i = \sum_{k=1}^{A+3} T_k + \sum_{j=1}^{3} \sum_{k=j+1}^{3} V_{jk} + \sum_{j=1}^{A} \sum_{k=j+1}^{A} V_{jk} + \bar{V}_i$$

and is of the form

$$\phi_i = \mathcal{X}^{(+)}(\bar{k_a}, \bar{r}_{aA}) \, \phi_S \, M \, t \, m \, \phi_J \, M \, T \, M$$

$$= \mathcal{X}_{aA} \, \phi_a \, \phi_A \qquad \qquad \ldots (4.1)$$

Here $\mathcal{X}_{aA}$ is the w.f. describing the relative motion in the incident channel, ϕ_a and ϕ_A are the internal wave functions of the incident and target nuclei and V_i is the optical potential of the 3-body system with target A.

Similarly the wave function of the outgoing channel is,

$$\phi_f = \mathcal{X}^{(-)}(k_b, r_{bB}) \, \phi_S \, M \, t \, m \, \phi_J \, M \, T \, M$$

$$= \mathcal{X}_{bB} \, \phi_b \, \phi_B \qquad \qquad \ldots (4.2)$$

Using eqns. (4.1) and (4.2) and taking into account that the direct reaction theory accepts the optical model as a first approximation but takes a perturbation as an additional interaction which gives rise to non-elastic process the transition amplitude T_{ab} may be written as:

$$T_{ab} = \int d\tau \, \mathcal{X}_{bB}^{(-)} \, \phi_b \, \phi_B \, |V| \, \phi_A \, \phi_a \, \mathcal{X}_{aA}^{(+)} \qquad \ldots (4.3)$$

Here V is the perturbation Hamiltonian. The coordinates of all constituents of the reaction are described in fig.4.2. The two transferred neutrons x_1 and x_2 form a cluster X.

4.1.2   Calculation of the transition amplitude

In order to calculate the transition amplitude the following specific assumptions for some of the terms in the expression (4.3) are made:

a) The spatial part of intrinsic functions ϕ_b and ϕ_a is assumed to be of the Gaussian form for simplicity:

$$\phi_b \ (\ \bar{r}_x, \bar{r}_b, \bar{r}_{bx} \ ) = N_a \ \exp \ (-\eta^2 \ \sum_{i>j} \bar{r}^2{}_{ij} \ )$$

$$= \Psi_{ooo} \ (\ 3\eta^2, \bar{r}_x) \Psi_{ooo} \ (4\eta^2, \ \bar{r}_{bx}) \qquad \qquad \text{(for } {}^3\text{He)}$$

$$\phi_b \ (\ \bar{r}_b \ ) = N_b \ \exp \ (-\delta^2 \ \sum_{i>j} r^2{}_{ij} \ ) = 1 \qquad \qquad \text{(for proton)}$$

Here 'x' is the c.m. coordinate and Ψ_{nlm} a harmonic oscillator wave function with the number 'n' of radial nodes. The size parameters η and δ may be obtained from any electron scattering experiment [Co 63, Sc 64].

b) The perturbation interaction V may be considered a Gaussian form as used by Lin and Yoshida [Li 64]:

$$V = U_o \ \sum_{j_{ex}} \ \exp \ (-\beta^2 \ r^2{}_{ij} \ (\ W + B \ P^{\sigma}_{ij} + MP^{\sigma}_{ij} - HP^{T}_{ij}))$$

40

c) Each of the two nucleons is represented by a Woods-Saxon wave function with the quantum numbers $(N_x l_x)$. This wave function is again expanded in terms of the harmonic oscillator wave funciton.

Using the above assumptions and expanding the nuclear wave function of the residual nucleus 'B' in terms of the nuclear states of 'A' and the extra two nucleons the transition amplitude T_{ab} for the ZRA (zero range approximation) can be written as [Li 73]:

$$T_{ab} = \Sigma(-1)^{M_b - S_b}_{\ b\ \ b} \frac{1}{\sqrt{2}} \langle J_A J M_A M_J | J_B M_B \rangle \langle L S M_L M_S | J M_J \rangle \langle S_a S_b M_a$$

$$-M_b | S M_s \rangle \langle t_b T m_{tb} M_T | t_a m_{ta} \rangle \ B(NLn1)(a/2)^{\frac{1}{2}} \ ((-1+1.5(B+H))$$

$$\delta_{s1}\delta_{to} + (1-0.5(B+H)) \ \delta_{So}\delta_{T1}) \ (2S_a+1)^{\frac{1}{2}} \ / \ (2S+1)^{\frac{1}{2}}$$

$$\int d\bar{R}_x \bar{d} r_{bx} \mathfrak{X}^{(-)*} \ (\bar{K}_b, \ \frac{A}{B}\bar{R}_x + \bar{r}_{bx}) \ (\ NLM_L \ (\ \frac{2A}{A+2}, \bar{R}_x)$$

$$1_{nlml} \ (\bar{r}_{bx})) \ LM1 \ \mathfrak{X}^{(+)} \ (k_a, \ \bar{R}_x + \frac{1}{3}r_{bx} \ ) \qquad \dots (4.4)$$

4.1.3   The differential cross-section

The expression of the cross-section for the stripping reaction A(a,b)B can be obtained by putting T_{ab} in the equation,

$$\frac{d\sigma}{d\Omega} = \frac{\mu_a \mu_b}{(2\pi\hbar^2)^2} \frac{k_b}{k_a} \frac{1}{(2J_A+1) \ (2S_a+1)} \ \Sigma \ |T_{ab}|^2$$

the final expression for the cross-section thus becomes

$$\frac{d\sigma}{d\Omega} = \frac{\mu_a\mu_b}{(2\pi\hbar^2)^2} \frac{k_b}{k_a} \frac{(2J_B+1)}{(2J_A+1)(2S_a+1)} \Sigma_{LSJ} \mid (1/\surd(2L+1))$$

$$\int d\bar{R}_x d\bar{r}_{bx} \chi^{(-)*}(k_b, \frac{A}{B}\bar{R}_x + \bar{r}_{bx}) F_{LSJ}^T(R_x, \bar{r}_{bx}) \chi^{(+)}$$

$$(\bar{k}_a, \bar{R}_x + \frac{1}{3}\bar{r}_{bx})\mid^2 \qquad\qquad ...(4.5)$$

The form factor F_{LSJ}^T is defined as follows:-

$$F_{LSJ}^T(R_x, \bar{r}_{bx}) = \underset{\tilde{N}\tilde{n}}{\Sigma} A_{LSJ}^T(\tilde{N},\tilde{n}) \underset{M_L m_1}{\Sigma} (-1)^{m_1^1} < L1M_L \ -m_1 \mid LM_L >$$

$$\overset{*}{\Psi}_{\tilde{N}\tilde{n}ML} (2Av/(A+2), \bar{R}_x) (aB/x(a+x))^3 \sigma(\bar{r}_{bx}) \sigma_{lo} \quad...(for \ ZRA)$$

where $A_{LSJ}^T(\tilde{N},\tilde{n}) = 2bU_o \cdot (\frac{(2\tilde{n}+1)!!}{2^{\tilde{n}}n!})^{\frac{1}{2}} (\frac{2\pi abvn^4}{(CD)^2})^{3/4} (1 - \frac{v}{2C}$

$$(1 + \frac{B^2}{4CD})) \tilde{n} (\frac{a}{2})^{\frac{1}{2}} ((2S_a+1)/(2S+1))^{\frac{1}{2}} \frac{1}{\surd 2}$$

$$((-1+1.5)(B+H))$$

$$\delta_{S1}\delta_{To} + (1-0.5(B+H))\delta_{So}\delta_{T1})\beta^2 < t_bTm_{tb}M_T \mid t_a m_{ta} >$$

Expression (4.5) can be used for the determination of theoretical curves of differential cross-section in the $(^3He,p)$ reaction analysis. The effect of the choice of different

parameters and the consideration of finite range in numerical
calculations are described in the following sub-section.

4.1.4   Numerical calculations

Effects of the parameters

The effect of the parameters on the overlap integral,
dynamical factor and differential cross-section has been
illustrated by Lin et al. [Li 73] through a study of the ^{12}C
$(^{3}He,p)$ ^{14}N reaction. The summary of the result is described
below.

a) The overlap integral, $C_{\tilde{n}}$ is more sensitive to the change of
    force range parameter β and size parameter η than both the
    dynamical factor $D^{\tilde{n}}\psi_{\tilde{N}L}$ and the differential cross-section.

b) The absolute value of the overlap integral depends strongly
    on the interaction range ζ and the node of the relative
    motion of the two transferred nucleons. The choice of the
    interaction range parameter is, therefore, quite important
    at the time of discussing the absolute value of cross-
    section.

c) The dynamical factor shows the most remarkable difference in
    the calculations done taking different type of interactions.
    This is specially prominent when calculations are done
   considering finite range of interactions.

Finite range consideration

The work of Lin et al. has also been devoted in illustrating the difference in results between the finite range approximation and the zero range approximation calculation.

a) The difference becomes more prominent as the force range, ξ is increased.

b) This difference is not so sensitive to the type of interaction used in the calculation.

4.2 DWBA theory for the (^{3}He,d) reaction

Let us describe the (d,^{3}He) reaction as a pick-up process in which the deuteron, d-particle represented by 'a' being incident upon a nucleus (b+c) takes one proton 'c' from it. A residual nucleus 'b' of the same nucleus as the target but one proton less is thus created. On the other hand, the d-particle combined with picked up proton from the target, forms a ^{3}He, particle represented by (a+c):

a+ (b+c) ---> b+ (a+c) ; 'b' core
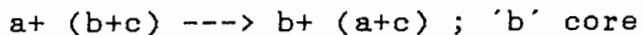
4.2.1   The transition amplitude

As in the previously described (^{3}He,p) reaction the exact matrix element for the pickup process in the distorted wave representation reads:

$$T^{DW} = \langle \Psi^{(-)}_{(a+c),b} |\, V_{ab} + V_{ac} - U^a\, |\, \phi_a \phi_{b+c} \chi_a^{(+)} \rangle \qquad \ldots \,(4.2.1)$$

Here $\Psi^{(-)}_{(a+c),b}$ is the solution of the Hamiltonian $H = T_{b,(a+c)}$

$+V_{ab} + V_{bc}$ and ϕ's denote the internal wave functions. The distorted wave $\chi_a^{(+)}$ is a solution of the Schrodinger equation for the relative motion in the entrance channel with the optical model potential U^a.

4.2.2 Calculation of the transition amplitude

The expression (4.2.1) needs some simplification before it is calculated. Substituting the formal solution of the Lippman-Schwinger [Li 50] equation for $\Psi^{(-)}$:

$$|\Psi^{(-)}_{(a+c)}\rangle = |\chi^{(-)}_{(a+c)}\rangle + (E^{(-)} - H)^{-1}\, (V_{ab} + V_{bc} - U^{(a+c)})$$

$$|\chi^{(-)}_{(a+c)}\, \phi_b \phi_{(a+c)} \rangle$$

We find

$$T^{DW} = \langle \phi_b\, \phi_{(a+c)}\, \chi^{(-)}_{a+c}|\, (1 + (V_{ab} + V_{bc} - U^{(a+c)})\, (E^{(+)} - H)^{(-)})$$

$$(V_{ab} + V_{ac} - U^a)\, |\, \phi_a \phi_{(b+c)} \chi_a^{(+)} \rangle \qquad \ldots \,(4.2.2)$$

Since the cross-section is proportional to the (amplitude)^2, we can find out the cross-section with respect to amplitude.

The cross-section for inverse process, the pick-up reaction, is related to the stripping reaction by the principle of detailed balance.

$$(d\sigma/d\Omega)^{d,\tau}_{\text{pick-up}} = \frac{k^2_{\tau}}{k^2_{d}} \cdot \frac{(2J_{\tau}+1)(2J_f+1)}{(2J_d+1)(2J_i+1)} X(d\sigma/d\Omega)^{\tau,d}_{\text{stripping}}$$

Hence, we can find out the cross-section of the (^{3}He,d) stripping reaction.

Now the expression (4.2.2) can be further simplified by making the following assumptions:

a) The Born approximation consists in disregarding the non-elastic part proportional to $(V_{ab} + V_{bc} - U^{(a+c)})(E^{(+)}-H)^{-1}$, which for $d+(A+n) \longrightarrow A+^3He$ reaction means

$$|| V_{d,A} + V_{p,A} - U^{\tau}_{\text{elastic}}|| = 0$$

Here τ stands for ^{3}He.

b) In addition to the earlier assumption the $V_{ab}-U^a$ i.e., $|| V_{d,A} - U^{\tau}_{\text{elastic}}||$ for $d+(A+p) \longrightarrow A+\tau$ system is put equal to zero. This has the meaning of neglecting the core excitation in the reaction.

Using the above assumptions, the expression for T_{ab} becomes,

$$T_{ab} = \langle \phi_a \phi_{(a+c)} \chi^{(-)}_{a+c} | V_{ac} | \phi_a \phi_{(b+c)} \chi^{(+)}_a \rangle \quad \dots (4.2.3)$$

46

If $V_{p,A}$ is replace by $U_{p,A}$ the above approximations together means the

$$U^T + (A+p) + U^{p,A} \approx U^{T,A} \qquad \dots (4.2.4)$$

which must hold for the optical potentials if one wants to use the simple matrix element (4.2.3) instead of its earlier ones.

The most consistent calculation with the simple DWBA matrix element should use the

i) zero range form together with

ii) the measured elastic scattering parameters which must be used

iii) in combinations as close as possible to the criterion (4.2.4)

As it is difficult to achieve the relation (4.2.4) the introduction of correction terms together with, the zero range calculations has been provocated [St 67].

4.2.2 The finite range corrector factor

If in a stripping reaction

a+A $\longrightarrow$ b+B where a=b+c, B=A+c

Here 'a' stands for ^{3}He- particle, 'A' for target nucleus, ^{51}V, 'B' for residual nucleus, ^{52}Cr, 'b' for outgoing particle, deuteron,d with the transition amplitudes

$$T_{fi} = \iint d\bar{R} \, d\bar{x} \, D(x) \, \mathcal{X}_f^{(-)*}(R+x) \, \phi_C^*(R)$$

$$\mathcal{X}_i^{(+)}(R+ \frac{m_b}{m_a}x)$$

Here,

$\mathcal{X}_f^{(-)} \longrightarrow$ the distorted wave of the c.m. of particle 'b'

$\phi_C \longrightarrow$ the found state wave function of the transferred

particle;

$\mathcal{X}_i^{(+)} \longrightarrow$ the distorted wave of the c.m. of particle 'a'

$D(x) \longrightarrow$ the 'overlap' of 'b' with 'a'

where, $D(x) \longrightarrow \int d\tau_b \, \phi_b^* \, V_{bc} \, \phi_a$

If we define

$$G\ (k^2) = \int e^{i\bar{K}.\bar{x}} \, D(x) \, d\bar{x}$$

then the zero-range normalization is given by

$D_o = G(0),$

and the finite range correction parameter R is given by

$$R^2 = \frac{1}{G(k^2)} \frac{\delta G(k^2)}{\delta(k^2)} \Bigg|_{k^2 = 0}$$

The first order correction factor from the local energy approximation for $D(x)$ which multiplies the form factor is

$$W_o(r) = \{1+A(r)\}^{-1} \qquad \ldots \text{ Hulthen form}$$

$$= \exp(-A(r)) \qquad \ldots \text{ Gaussian form}$$

where

$$A(r) = \frac{2}{\hbar^2} \frac{m_b m_c}{m_a} k^2 [E_b - V_b(r_b) + E_c - V_c(r_c) - E_a + V_a(r_a)]$$

where E_a, E_b, E_c, and V_a, V_b, V_c are the energies and potentials for the three light particles of mass m_a, m_b, m_c. The typical value of the range parameter, R is 0.77 for (^{3}He,d) reaction and 0.80 for (^{3}He,p) reaction.

The non-locality correction factor

The correction needed for the use of an equivalent local potential multiplies the form factor and is of the form

$$W_{NL}(r) = \exp \left((\beta_i^2/8) \ (2m_i/\hbar^2) \ V_i(r) \right)$$

for each of the projectiles and the bound state functions used in this form factor. Here β_i is the non-local parameter and m_i are the masses of particles and the V_i are the potentials for the particles. In the case of bound state, the factor W_{NL} multiplies the bound state function and then the function is re-normalized to unity. The $V_i(r)$ include any Coulomb potentials for the projectiles or particles. Typical values of the β parameter are

$$\beta_p \approx 0.85$$
$$\beta_d \approx 0.54$$
$$\beta_T \approx 0.20\text{-}0.30$$

CHAPTER 5

THE $^{51}V(^3He,d)^{52}Cr$ REACTION

CHAPTER 5

THE $^{51}V(^{3}He,d)^{52}Cr$ REACTION

5.1 Introduction

The level structure of ^{52}Cr has been the subject of a number of experimental studies through varieties of nuclear reactions. Information thus obtained is summarized by Singh [Si 84]. The $^{51}V(^{3}He,d)^{52}Cr$ reaction was studied by Armstrong and Blair [Ar 67] at 22 MeV under an overall energy resolution of 100-200 keV (FWHM) and angular distribution were studied for levels up to $E_x=8.6$ MeV. This includes the levels summed over approximately 300 keV at $E_x = 6.8 -8.7$ MeV. A somewhat more detailed investigation of this reaction is due to Pellegrini et al. [Pe 73] carried out at 10.5 MeV and the energy resolution was about 50 keV. Level structure in ^{52}Cr was studied up to $E_x=7.2$ MeV. The present work was undertaken at a beam energy $(E_x=15$ Mev) intermediate between the above two with a much improved energy resolution of ~ 20 keV. Several new levels are identified at $E_x \geq 6.8$ MeV. Angular distributions are measured in most of the cases for single levels up to E_x ~ 8.6 MeV including the new levels. The data are analyzed in terms of the DWBA theory of stripping reacting and spectroscopic factors are extracted.

5.2 DWBA Analysis

Microscopic DWBA analyses of the stripping angular distributions were carried out using the code DWUCK4 due to Kunz. The optical model potential used with DWBA analysis was of the form

$$V(r) = V_c(r) - V_o f(r,r_o,a) - i[W - 4a_I W_D(d/dr)]f(r,r_I,a_I) + \hbar/m_\pi c)^2$$
$$V_{so}(1/r)(d/dr)f(r,r_{so},a_{so})\sigma.L. \qquad \qquad \dots (5.2.1)$$

where $V_c(r)$ is the Coulomb potential from a sphere of uniform charge density and radius $R_c = r_c A^{1/3}$, V_o is the real part and W and W_D are the imaginary parts of central potentials respectively; V_{so} is the spin-orbit dependent potential; $(\hbar/m_\pi c)$ is the pion-wave length; $f(r)$ is the Woods-Saxon form such as

$$f(r) = \left[1 + \exp (r-R)/a \right]^{-1}$$

where $R = r_o A^{1/3}$ is the nuclear radius and a is the surface diffuseness parameter.

To begin with, detailed DWBA analyses were performed for the following transitions in the $^{51}V(^3He,d)^{52}Cr$ reaction -

$l = 3; E_x = 0.0$ and 2.370 MeV
and $l = 1; E_x = 4.701, 5.101$ and 7.400 MeV.

All these have well-known J^π values [Si 84], except the 7.400 MeV which on the other hand is extremely strong and should be of dominant single particle character. Several sets of

optical-model parameters were used. An overall good description of the above angular distributions is given by the parameters listed in Table-5.1. These are from the global survey by Trost et al. [Ha 87] and Newman et al. [Ne 67] respectively for the entrance and the exit channels. All the angular distributions were then analyzed using this combination of potential parameters.

The bound state wave function was generated by assuming a real Woods-Saxon well with well-matched geometrical parameters given by $r_0 = 1.17$ fm. and a =0.70 fm. A Thomas-Fermi spin-orbit term given below was added to it

$$\frac{V_0 \lambda}{45.2} \cdot \frac{1}{r} \frac{d}{dr} \, f(r, r_0, a) \, \mathbf{L} \cdot \mathbf{s}$$

with $\lambda = 25$ and $f(r, r_0, a)$ as the usual Woods-Saxon form factor. The depth of the potential was adjusted so as to give the transferred proton an appropriate binding energy $E_B = Q(^3He, d) + 5.49$ MeV.

The effect of the finite range interaction and the non-locality of the optical-model potentials can be introduced in the DWBA calculations in the local energy approximation using a finite range correction factor $F_r \approx 0.77$ fm. for the $(^3He, d)$ reaction. The non-locality corrections of the form:

$$\left[1- (\beta^2/4)\ (2m/\hbar^2)\ V(r) \right]^{-\frac{1}{2}}$$

were applied, where the values of $\beta_T \approx 0.22$ fm.for the Helium-3, $\beta_d \approx 0.54$ fm. for deuteron were used for the purpose. No non-locality correction was considered for bound state.

All calculations were carried out with the help of Alpha-micro computer of the Rajshahi University, Bangladesh. The summary of the results on the levels in ^{52}Cr has been shown in the Table-5.2.

Table - 5.1

The optical model parameters

Particle	V_0 (MeV)	r_0 (fm)	a (fm)	$4W_D$ (MeV)	rI (fm)	a_I (fm)	V_{SO} (MeV)	r_{SO} (fm)	a_{SO} (fm)	r_0 (fm)	ref.
^3He	93.86	1.15	0.76	96.36	1.35	0.80				1.40	a)
d	90.60	1.17	0.69	46.40	1.34	0.82	6.18	0.70	0.40	1.30	b)
p	c)	1.17	0.70				λ=25			1.25	

a) Potential parameters for ^3He from Trost et al. [Tr 87];b) Potential parameters for deuteron from Newman et al.[Ne 67]

c) Adjusted to give the transferred proton a binding energy of $Q(^3He,d)$ +5.49 MeV.

5.3 Results and discussion

5.3.1 The angular distributions

The angular distributions have been measured for sixty-three levels observed up to an excitation energy of 8.6 MeV. Thirty-four levels have been analyzed in terms of the local zero range DWBA theory of direct reaction as discussed in Section 5.2. The results are summarized in Table 5.2 including the results from previous works [Si 76].

The measured angular distributions are compared with the DWBA theory as displayed in Figs. 5.1-5.10. Some of the angular distributions are marked NS in Table 5.2. These distributions do not have the characteristics of a direct single-step process of nuclear reaction. A number of levels in ^{52}Cr below $E_x \approx$ 6.6 MeV excited in various other reactions [Si 76] were not observed in the (^{3}He,d) reactions [present work]; ref. [Ar 65], [Pe 73]. These and two NS levels at 6.089 and 6.625 MeV are thus unlikely to have an appreciable single-particle structure. The level at 2.965 MeV could not be analyzed for very poor data and it is marked NA in the table.

A few l=3, two l=0, and a large number of l=1 transitions are observed in the present work covering an excitation energy of about 8.6 MeV. The l=3 transitions to the low-lying levels up to E_x = 3.11 MeV were assumed to correspond to the $1f_{7/2}$

levels. These levels have well established J^{π}-values [Si   76] and have a ono-to-one correspondence with the shell-model predictions [Pe 73].

The angular distributions for the 7.686 and 8.614 MeV states were fitted by $L=1+3$ (Fig. 5.2) and it is reasonable to assume that the $L=3$ components correspond to the $1f_{5/2}$ shell-model state.   The $1f_{5/2}-1f_{7/2}$ separation is then found to be greater than 5 MeV. An insignificant portion of the $1f_{5/2}$ strength thus lies below $E_x = 8.6$ MeV and so does the $3s_{\frac{1}{2}}$ strength.   The $L=0$ angular distributions are shown in Fig. 5.3.

Several levels at $E_x > 6.6$ MeV not hitherto observed in any reaction [Si 76] including the (^{3}He,d) reaction [Ar 65,Pe   73] have been observed in the present work and the angular distributions are measured for them and L-transfer and spectroscopic information are obtained. A few low-lying levels with well established J^{π} values [Si 76], but not observed in the previous (^{3}He,d) studies [Ar 65,Pe 73], have also been observed and angular distributions are measured. The $L=1$ assignment made in the present work is consistent with the J^{π} values of all but the 4.565 MeV level (Table 5.2). The latter level could be a doublet.

Fig.5.1. The measured angular distributions fitted to l=3 DWBA curves.

Fig. 5.2. The measured angular distributions
fitted to l=1+3 DWBA curves.

Fig. 5.3. The measured angular distributions fitted to l=0 DWBA curves.
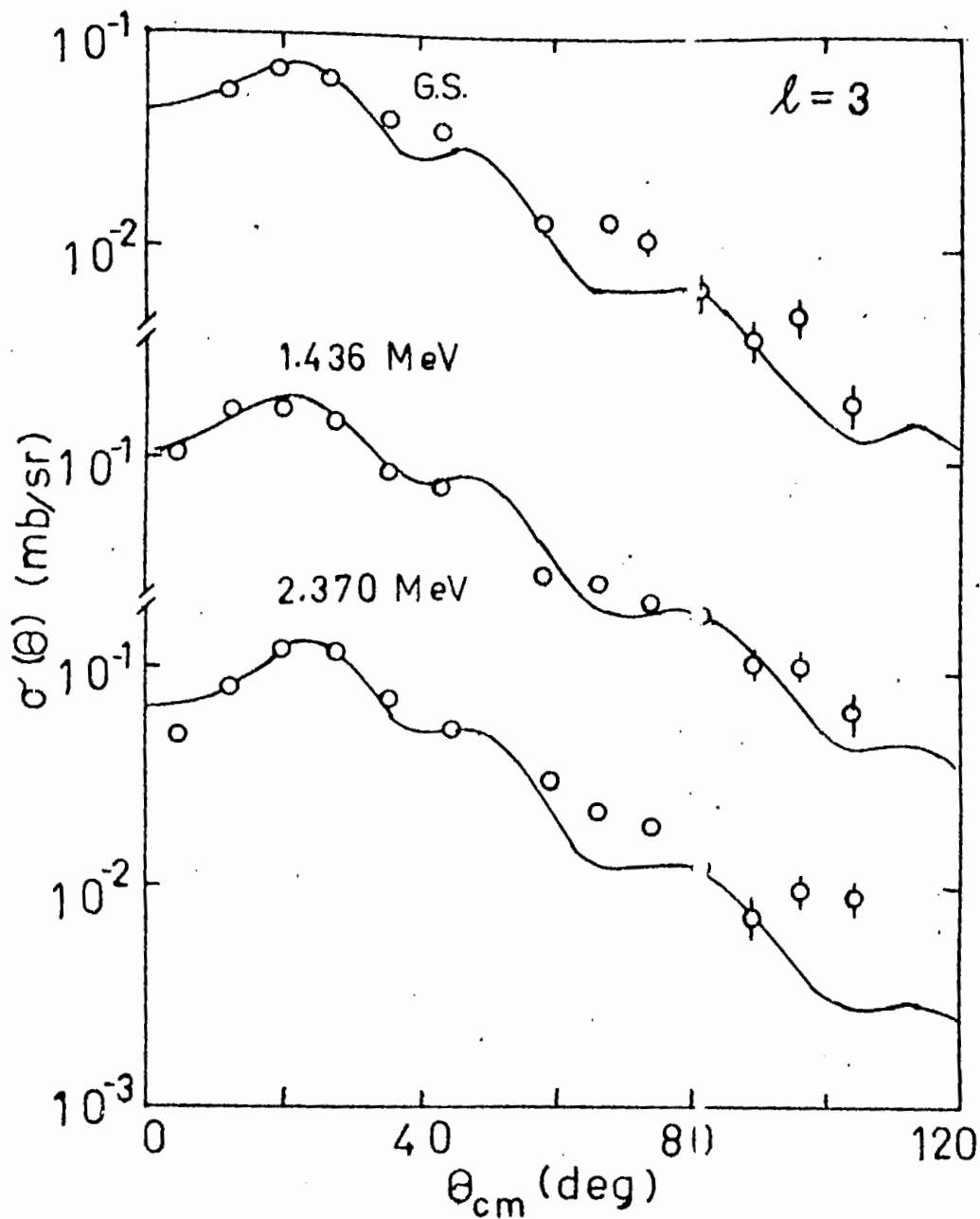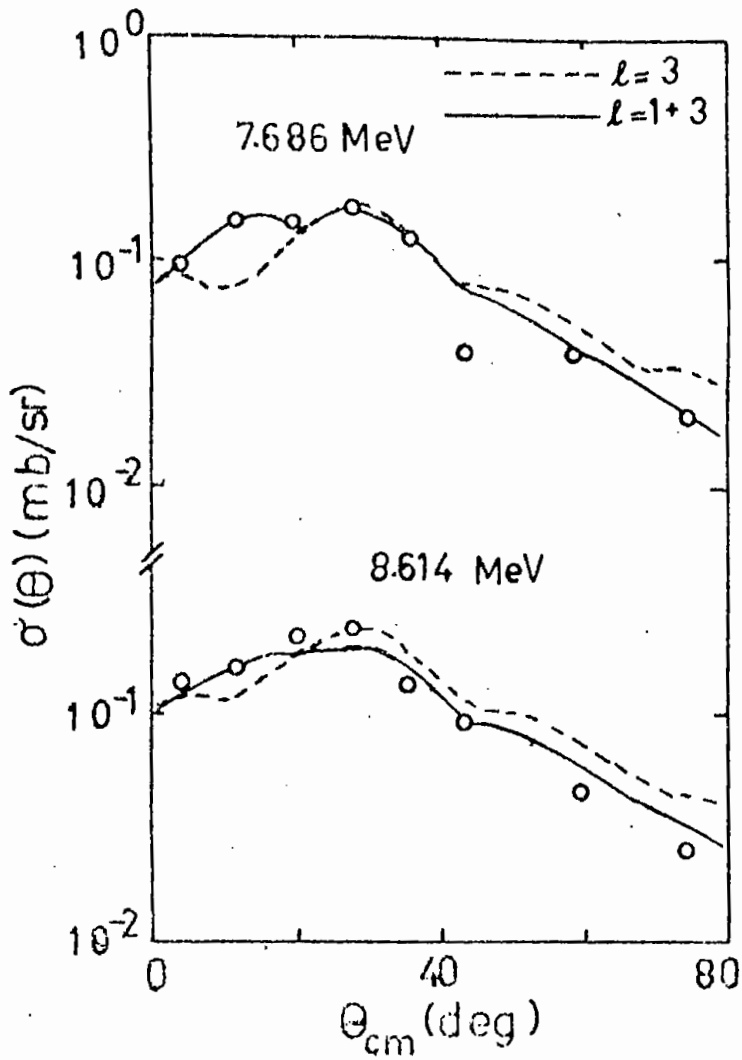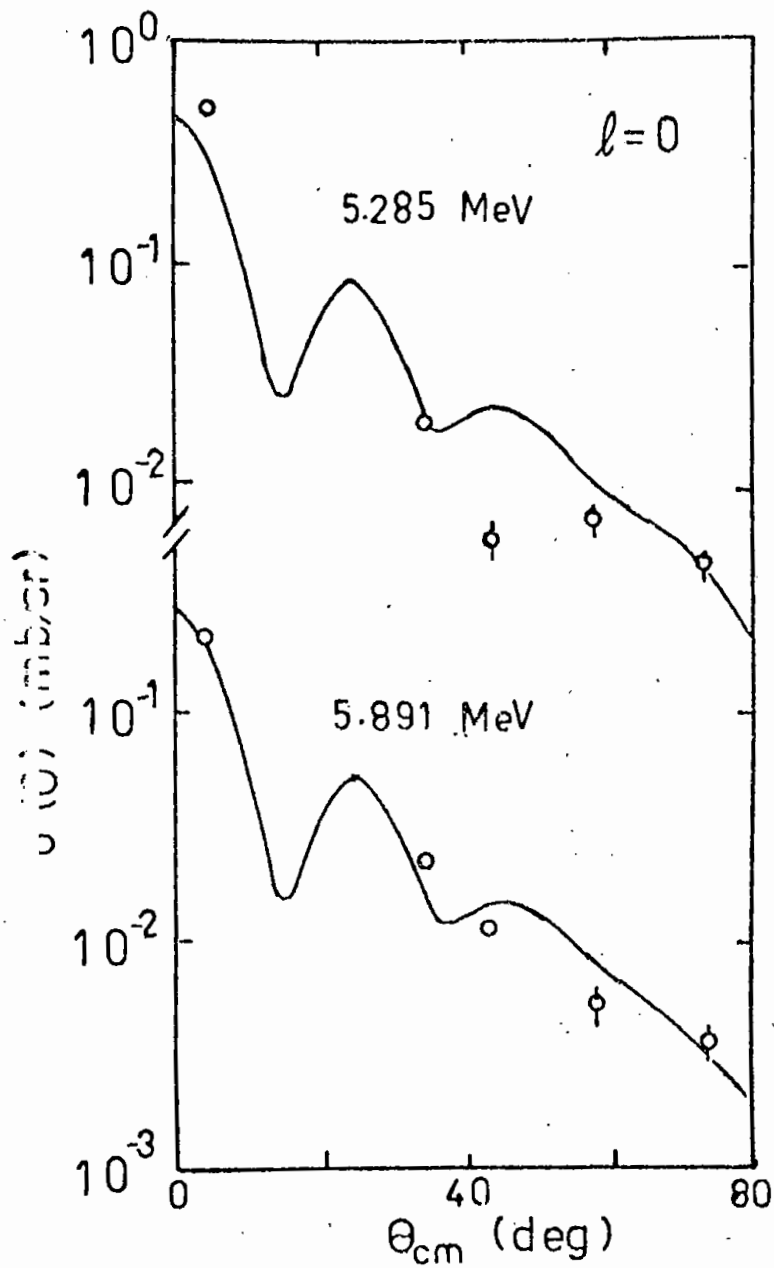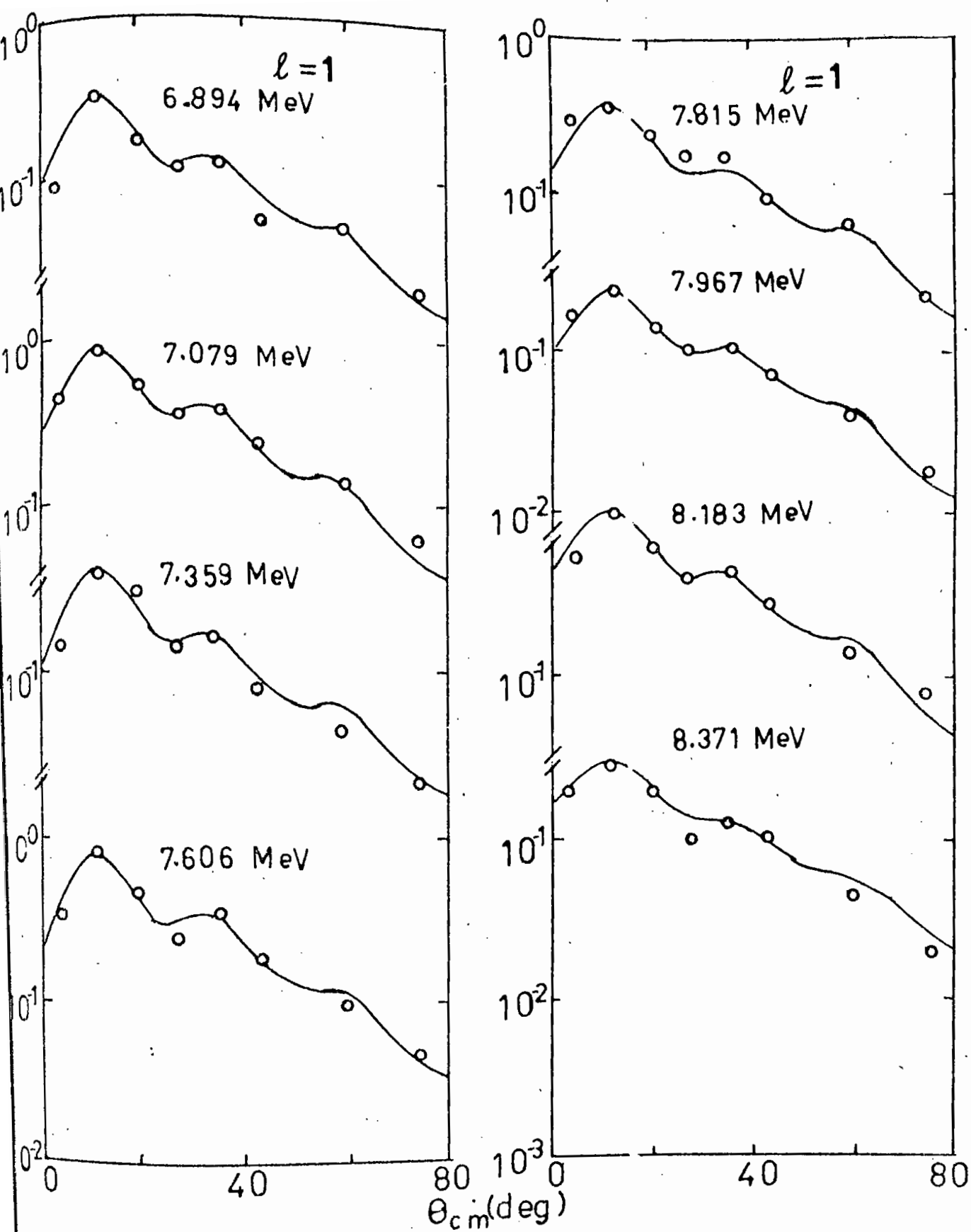
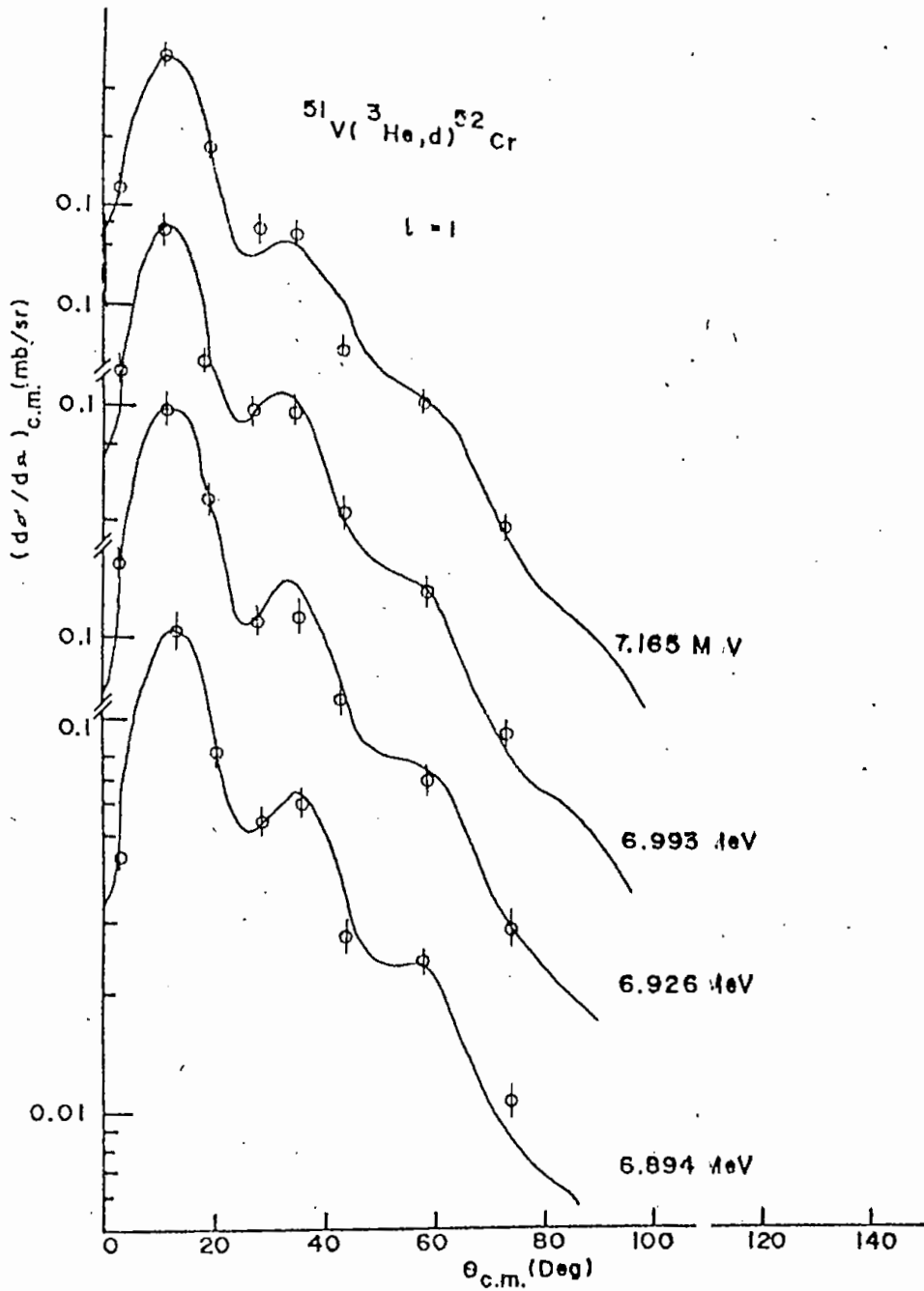Fig.5.4. The measured angular distributions fitted to l=1 DWBA curves.

Fig.5.5. Measured angular distributions compared to DWBA.
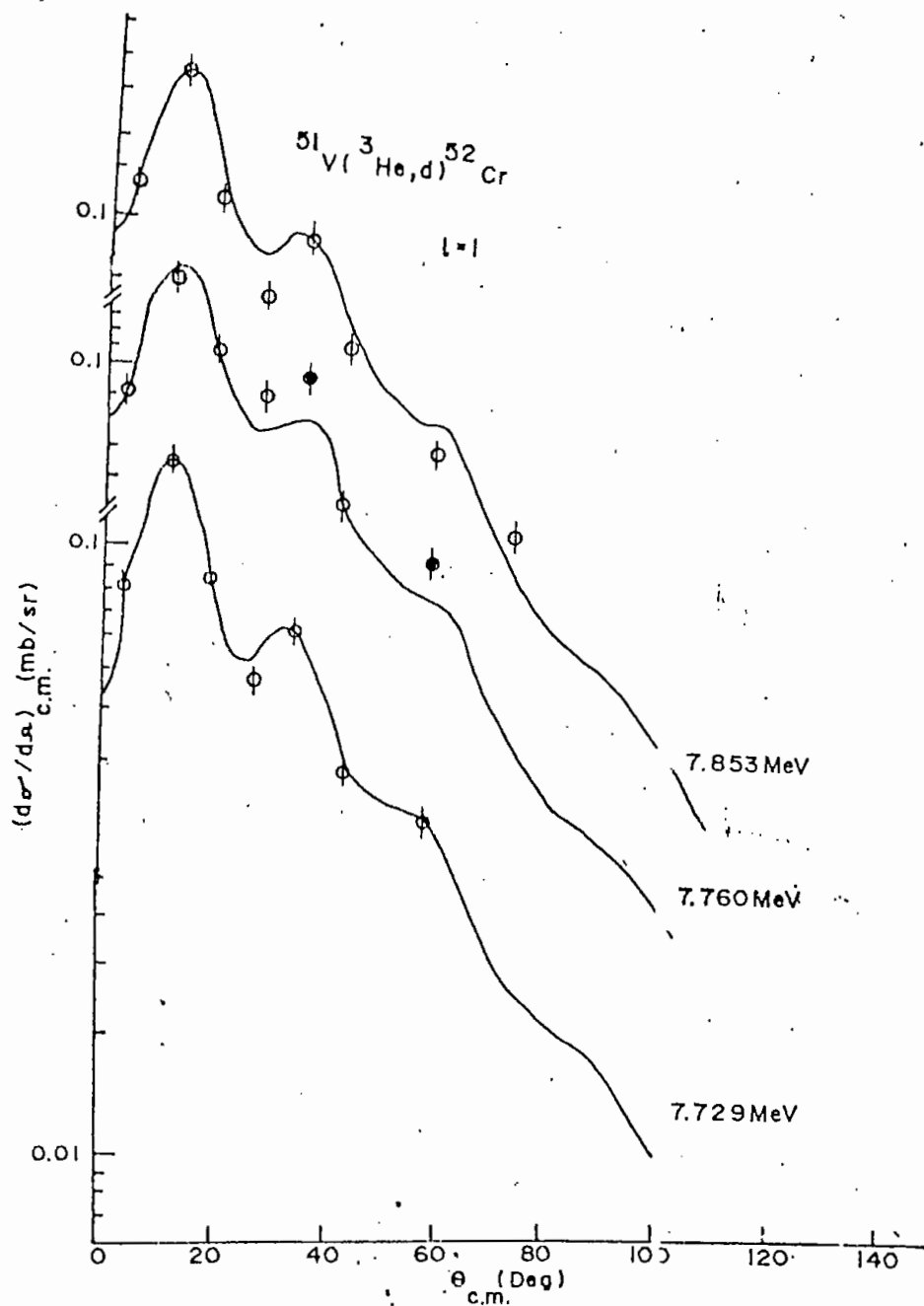
Fig. 5.7. Measured angular distributions compared to DWBA.
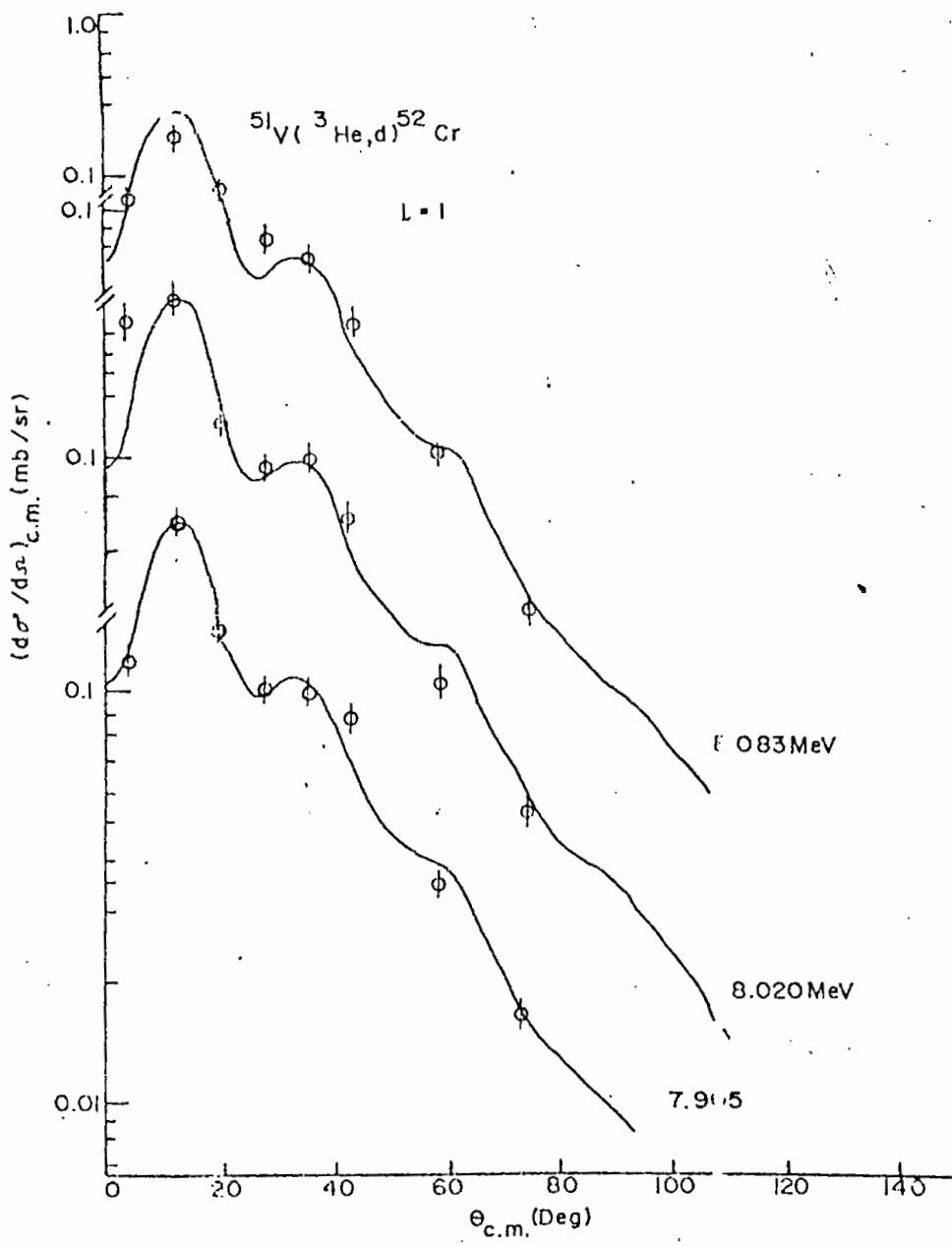
Fig. 5.8. Measured angular distributions compared to DWBA.
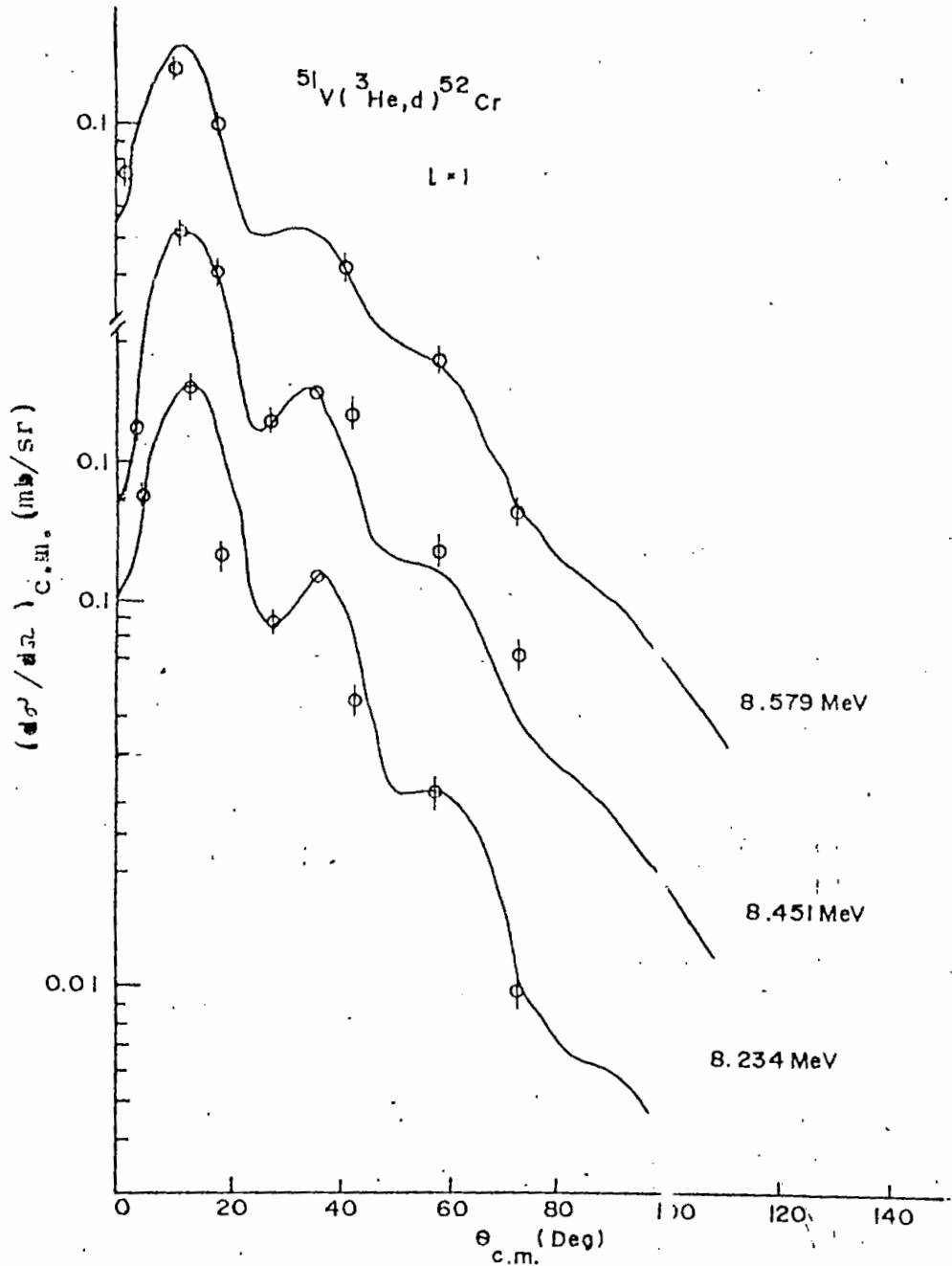
Fig. 5.9. Measured angular distributions compared to DWBA.
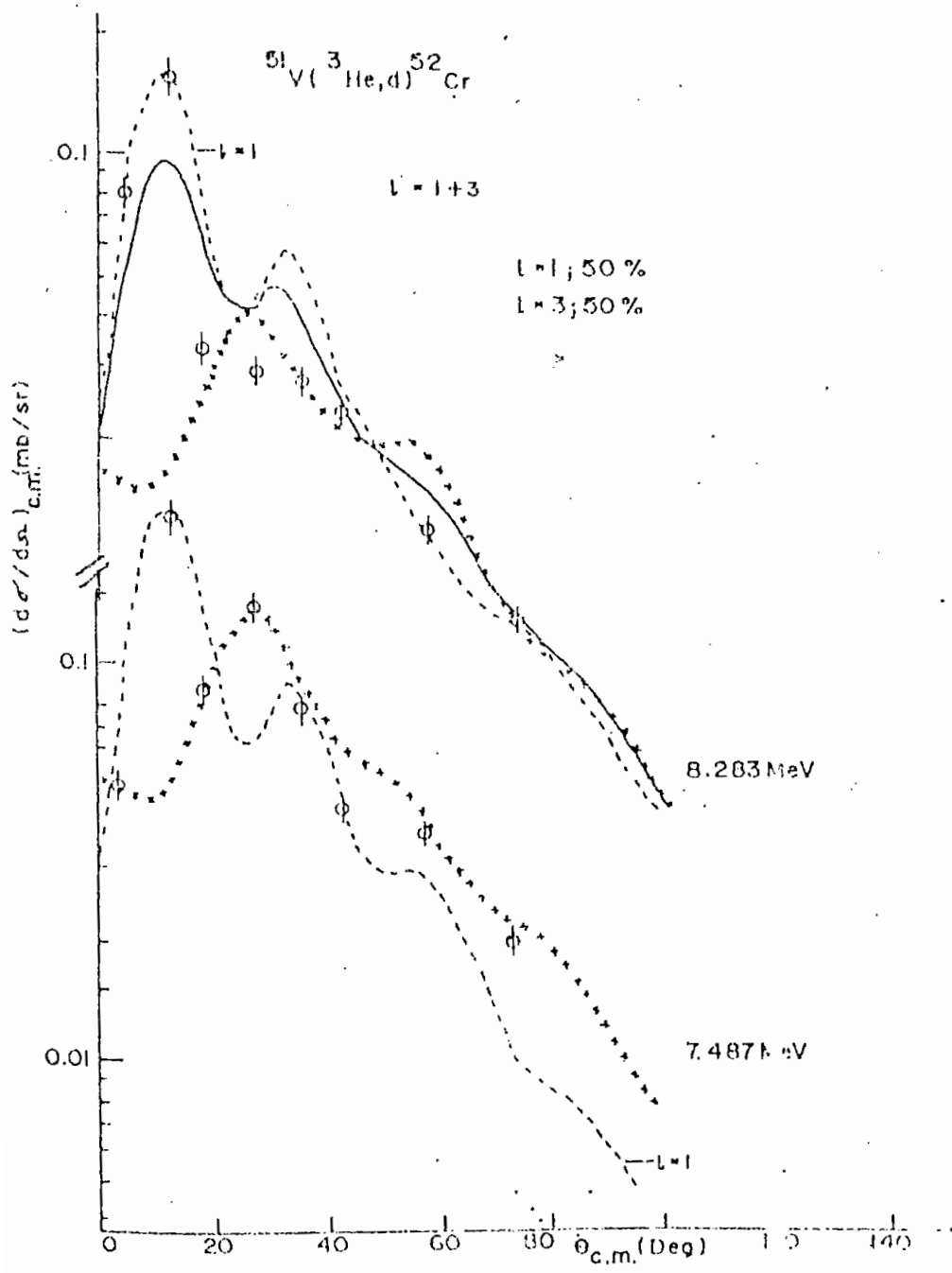
Fig. 5. 10. Measured angular distributions compared to DWBA.

5.3.2 Spectroscopic factors and the distribution of single particle strength

The relation between the experimental cross-section and that obtained by the use of DWBA code DWUCK4 is

$$\sigma_{exp}(\theta) = NG_j \ \sigma_{DW}(\theta) \ / \ (2j+1),$$

where the spectroscopic transition strength is

$$G_j = (2J_f+1) \ C^2S \ / \ (2J_i+1),$$

where J_i and J_f are respectively the angular momenta in the initial and final nuclear levels and j is the angular momentum of the transferred proton. The normalization constant N=4.42 was taken relevant to the Gunn-Irving wave function for the ^{3}He particle and the Hulthen wave function for the deuteron [Ba 66]. The results are summarized in Table 5.2. The dependence of the spectroscopic factor on the bound state geometries is known in the literature. For example, an increase in $´r_o´$ and/or $´a´$ of the bound state well amounts to extending the DWBA volume integral to a larger radius and thereby to decrease the spectroscopic factor. In the present work, the spectroscopic factors for transitions to the $1f_{7/2}$, $2p_{3/2}$ and $2p_{½}$ states decrease by approximately 40%, 20%, and 15% by changing the values of (r_o,a) from (1.17 fm, 0.70 fm) to (1.25 fm, 0.65 fm). The former geometrical parameters are considered in this work rather than the more conventional latter for reason of geometry matching. The spectroscopic factors are therefore subject to

the above uncertainties. This is of course usual of the DWBA calculations.

A few $L=3$, two $L=0$, and a large number of $L=1$ transitions are observed in the present work covering an excitation energy of about 8.6 MeV. The distribution of transition strength G_j over the components of a shell-model state is shown in Fig. 5.11 ($L=0$ is not included). Results of the sum rule analysis are shown in Table 5.3.

The $L=3$ transitions to the low-lying levels up to $E_x=3.11$ MeV were assumed to correspond to the $1f_{7/2}$ levels. These levels have well established J^π values [Si 76] and have a ono-to-one correspondence with the shell-model predictions [Pe 73]. The shell-model calculations were carried out by Pellegrini et al. [Pe 73], with good iso-spin wave functions [Os 71], and are based on the $(1f_{7/2})^4$ proton configurations with an inert ^{48}Ca-core. The positions of the levels are reproduced to better than 50 keV or so. The spectroscopic factors are also calculated for the proton stripping reactions on ^{51}V. The ground state of ^{51}V has a unique seniority quantum number $\nu=1$ and the proton stripping reactions on ^{51}V should populate levels in ^{52}Cr with $\nu=0$, $J^\pi=0^+$ and $\nu=2$, $J^\pi=2^+$, 4^+, and 6^+. The transition strengths for these levels as deduced from the (^{3}He,d) reaction (present work and refs. [Ar 65] and [Pe 73] and the (α,t) reaction [Ma 68] are compared with the shell-model theory [Pe 73] in Fig. 5.13. The G_j values from the (α,t)
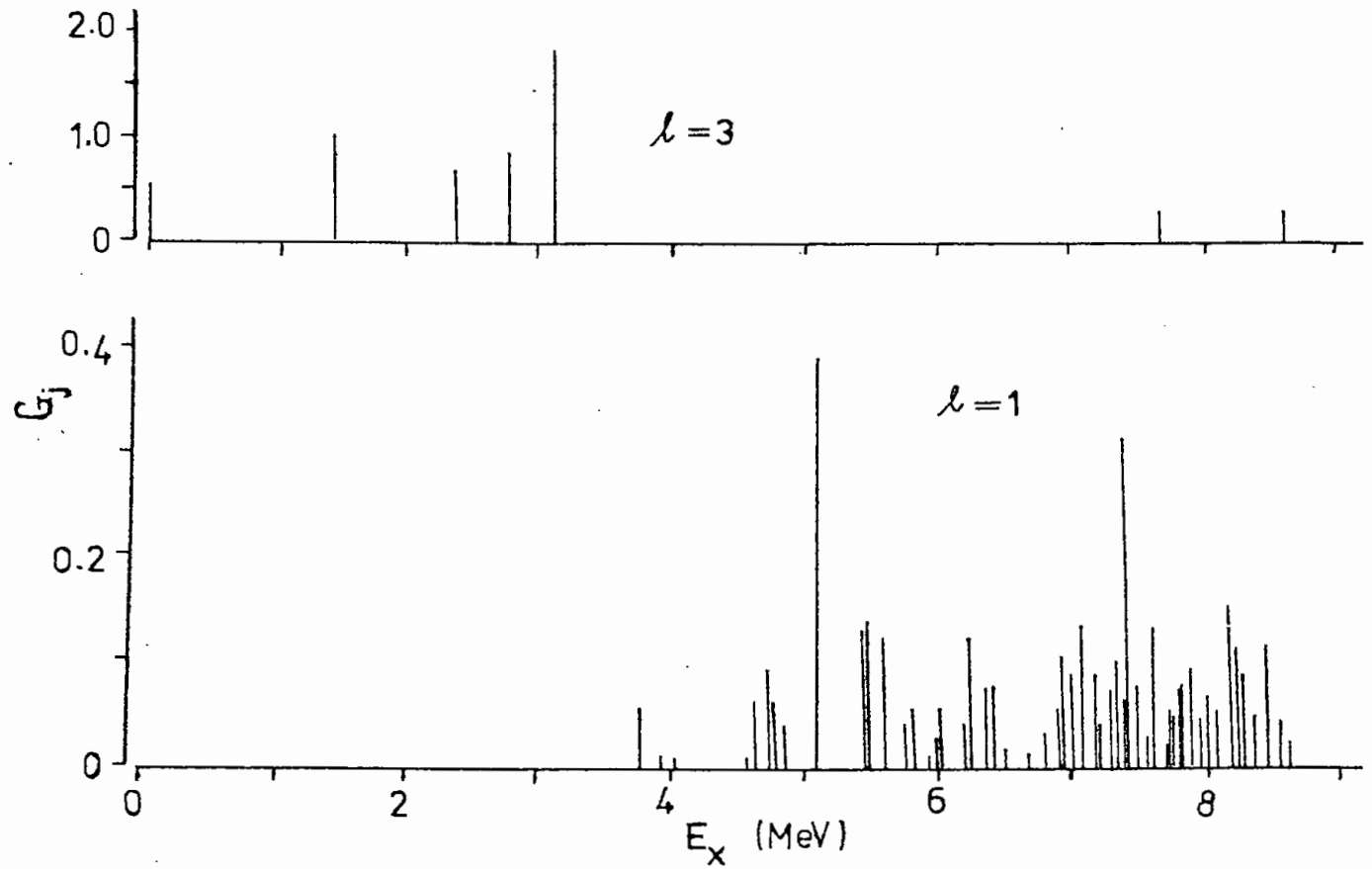
Fig. 5.11. The spectral distributions of the measured single particle strengths.

reaction are normalized to the shell-model prediction for the ground state transition. There is an excellent agreement between theory and experiment for the 0^+, 2^+, and 6^+ levels. The agreement for the two 4^+ states is qualitative in that the theory, in agreement with all measurements, predicts more strength in the second 4^+ level over the first. These strengths are a measure of the $\nu = 2$ components since the ($\nu = 4$, 4^+) state given by the $(1f_{7/2})^4$ scheme is not allowed in the (^{3}He,d) and (α,t) reactions because of the seniority selection rule ($\Delta\nu = 1$). Angular distributions of some of the $l = 1$ transitions are shown in Fig. 5.4. The 2p spectroscopic strength is fragmented over a large number of levels, as shown in Fig. 5.11. The spectrum is much more complicated than that given by the shell-model calculations [Pe 73]. The calculations [Pe 73] are again based on an inert ^{48}Ca-core as for the $1f_{7/2}$ transitions as mentioned earlier, but with a proton promoted to the $2p_{3/2}$ orbit. As an example three 2^+ levels are predicted up to $E_x \approx 4$ MeV, as against five (including a tentative one) observed experimentally [Si 76]. Two of these are populated in all the (^{3}He,d) reactions — one with $l = 3$ and the other with $l = 1$. The spectral distribution for $l = 1$ transfers (Fig. 5.11) can be very approximately represented by two Gaussians with considerable overlap. Therefore in deducing the transition strengths G_j (Table 5.2) it was arbitrarily assumed as in the previous (^{3}He,d) works [Ar 65, Pe 73] that the levels in ^{52}Cr up to $E_x \approx$ 7.2 MeV belong to the $2p_{3/2}$ state and those above to the $2p_{1/2}$

shell-model state. The summed strength ΣG_j comes to be 2.19 and 1.81 respectively for the $2p_{3/2}$ and $2p_{\frac{1}{2}}$ transitions. The former is somewhat smaller than the corresponding shell-model limit of 3.33 and the latter is within the uncertainty equal to the shell-model limit of 1.67. It then appears that the 2p strengths are just not exhausted up to $E_x = 8.6$ MeV and that some of the transitions beyond $E_x = 7.2$ MeV attributed to the $2p_{\frac{1}{2}}$, may belong to the $2p_{3/2}$ state. The spectroscopic factors are also given by the shell-model calculations [Pe 73] for the $2p_{3/2}$ transitions. In view of the complexity of the observed $2p_{3/2}$ spectrum, it is not possible to make a comparison of the measured spectroscopic factor with its prediction from theory. It is clear that configurations more complex than the simple $\pi(1f_{7/2}, 2p_{3/2})^4$ are involved.

In one of the previous (^{3}He,d) works [Ar 65], angular distributions to groups of levels at $E_x > 6.8$ MeV were summed over approximately 300 keV and these were found to have a mixture of $L=1$ and $l=3$ transfers. In the other (^{3}He,d) work [Pe 73] two $L=1+3$ mixtures were reported. Separate angular distributions are measured in the present work for all the levels and all of them were found to have a single L-transfer, namely $L=1$. The improved resolution of the present investigation would not explain the discrepancy. As the $L=3$ component of the $L=1+3$ mixture for the above transitions were

assumed to belong to the $1f_{5/2}$ shell-model state, the ΣG_j value for the $1f_{5/2}$ state according to Armstrong and Blair [Ar 65] is close to the single particle limit and is only 0.78 and 0.56 according to Pellegrini et al. [Pe 73] and the present work respectively (Table 5.3).

TABLE - 5.2

Summary of the $^{51}V(^3He,d)^{52}Cr$ reaction

Gr. No.	E_x (MeV) a	b	J^π b	$\sigma(\theta)$ c	L-transfer a	d	e	G_j a	d	e
00	0.000	0.000	0^+	0.054	3	3	3	0.500	0.50	0.18
01	1.436	1.434	2^+	0.100	3	3	3	0.970	0.67	0.68
02	2.370	2.370	4^+	0.047	3	3	3	0.650	0.57	0.53
		2.647	0^+							
03	2.767	2.768	4^+	0.079	3	3	3	0.820	0.91	1.02
04	2.965	2.965	2^+		NA					
05	3.113	3.114	6^+	0.180	3	3	3	0.180	2.13	1.96
		3.162	2^+							
		3.415	(4^+)							
		3.472	3^+							
		3.616	5^+							
		3.700	(2^+)							
06	3.770	3.772	2^+	0.074	1	1	1	0.054	0.11	0.09
07	3.938	3.946		0.009	1			0.0092		
		3.951	(1^+)							
		4.015	5^+							
08	4.033	4.038	4^+	0.010	1			0.0085		
09	4.565	4.563	3^-	0.016	1			0.0082		
10	4.628	4.627	5^+	0.098	1	1	1	0.060	0.48	0.17
11	4.701	4.706	2^+	0.236	1			0.090		
12	4.737	4.741	2^+-5^+	0.123	1		1	0.062		0.27

(continued)...

TABLE - 5.2 continued.

Gr. No.	E_x (MeV) a	E_x (MeV) b	J^π b	$\sigma(\theta)$ c	ℓ-transfer a	ℓ-transfer d	ℓ-transfer e	G_j a	G_j d	G_j e
		4.751	(8^+)							
		4.794	0^+							
		4.805	(6^+)							
		4.816	1,2,3							
13	4.835	4.837	(0^+)	0.037	1		1	0.040		0.05
		5.054								
		5.070								
14	5.101	5.097	4^+	0.772	1	1	1	0.390	0.38	0.37
		5.141	2^+							
		5.211								
15	5.285	5.281	$(2^+,3^-)$	0.602	0			0.0072		
		5.346								
		5.396	(7^+)							
		5.410	$(^+)$							
16	5.435	5.432	(2^+)	0.278	1	1	1	0.130		
17	5.467	5.450	4^+	0.186	1			0.140	0.35	0.34
		5.571	3^-							
18	5.594	5.584		0.257	1	1	1	0.120	0.18	0.17
		5.600	0^+							
		5.650	0^+							
		5.664	2^+							

TABLE - 5.2   continued

Gr. No.	E_x (MeV) a	b	J^π b	$\sigma(\theta)$ c	L-transfer a	d	e	G_j a	d	e
		5.724	$+$							
		5.737	(4^+)							
19	5.751			0.088	1	1	1	0.040	0.13	0.05
		5.770	2^+-5^+							
		5.775	0^+							
		5.798								
		5.812								
		5.818	(3^-)							
20	5.828	5.830	2^+-5^+	0.116	1		1	0.054		0.06
		5.853								
		5.865								
		5.879	(2^+)							
21	5.891	5.916		0.210	0			0.0052		
		5.924								
22	5.945	5.953		0.030	1	1		0.0082	0.15	
		5.961								
23	5.992	5.996		0.047	1		1	0.026		0.06
24	6.026	6.026	2^+-5^+	0.032	1			0.048		
		6.035								
		6.057	2^+							
		6.065								
25	6.089	6.106	0^+	0.030	NS					

TABLE - 5.2   continued

Gr. No.	E_x (MeV) a	b	J^π b	$\sigma(\theta)$ c	L-transfer a	d	e	G_j a	d	e
		6.145								
		6.153	2^+							
		6.164								
		6.175	2^+							
26	6.192	6.193		0.060	1	1		0.040	0.26	
		6.205								
		6.210								
		6.220								
27	6.232	6.233	2^+-5^+	0.231	1		1	0.120		0.17
		6.252								
		6.272								
		6.282								
		6.293								
		6.324								
		6.356	$(3^-,4^+)$							
28	6.364	6.372	2^+-5^+	0.135	1	1	1	0.074	0.21	0.16
29	6.388	6.392		0.128	1			0.074		
		6.437								
		6.462								
30	6.500	6.490		0.051	1			0.020		
		6.493								
		6.541								

TABLE - 5.2 continued

Gr. No.	E_x (MeV)		J^π	$\sigma(\theta)$	l-transfer			G_j		
	a	b	b	c	a	d	e	a	d	e
		6.568								
		6.585	3^-							
31	6.625			0.091	NS					
32	6.676			0.025	1	1		0.012	0.09	
		6.700	$(1-6)^-$							
33	6.814	6.810	2^+	0.112	1			0.031		
34	6.894			0.079	1			0.051		
35	6.928	6.920	2^+-5^+	0.280	1		1	0.10		0.05
36	6.993	7.010		0.222	1			0.085		
		7.060	3^-							
37	7.079	7.070		0.368	1		1+3	0.13		0.05+0.44
38	7.165	7.180		0.205	1		1+3	0.085		0.04+0.34
39	7.223			0.068	1			0.036		
40	7.273			0.175	1			0.067		
41	7.322			0.221	1			0.096		
42	7.359			0.130	1			0.060		
43	7.400	7.400		0.623	1			0.30		
		7.450	$0^+,2^+$							
44	7.487			0.086	1			0.071		
45	7.536			0.133	1			0.025		
46	7.606	7.600		0.271	1			0.125		

(continued)...

TABLE - 5.2 continued

Gr. No.	E_x (MeV) a	E_x (MeV) b	J^π b	$\sigma(\theta)$ c	l-transfer a	l-transfer d	l-transfer e	G_j a	G_j d	G_j e
47	7.686			0.089	1+3			0.016+0.25		
48	7.729	7.730	3^-	0.144	1			0.047		
49	7.760			0.145	1			0.046		
50	7.815			0.284	1			0.068		
51	7.853			0.212	1			0.073		
52	7.905	7.900	$+$	0.217	1			0.086		
53	7.967			0.161	1			0.043		
54	8.020			0.387	1			0.068		
55	8.083			0.187	1			0.047		
56	8.183	8.200	$+$	0.485	1			0.144		
57	8.234			0.324	1			0.106		
58	8.283			0.312	1			0.080		
59	8.371			0.180	1			0.043		
		8.400	$+$							
60	8.451			0.226	1			0.106		
61	8.579			0.131	1			0.038		
		8.600	3^-							
62	8.614			0.145	1+3			0.021+0.29		

a   Present work

b   Summary [Si 84]

c   c.m. cross section (mb/sr) at 3.75° (lab)

d   Armstrong and Blair [Ar 65], data analyzed for several groups of unresolved levels summed over approximately 300 keV with l=1+3

e   Pellegrini et al. [Pe 73].

f   c.m. cross section (mb/sr) at 11.25° (lab); data at 3.75° missing

NA Poor data; not analyzed.

NS non-stripping angular distribution.

5.3.3 The level spectrum of ^{52}Cr

The observed level spectrum of ^{52}Cr has been compared with the theoretical spectra calculated by Pellegrini et al. [Pe 73]. Assuming for ^{51}V, a pure $(1f_{7/2})_{J=7/2,T=5/2}$ configuration, the ^{52}Cr levels excited in the ^{51}V(^{3}He,d) reaction by $1f_{7/2}$ and $2p_{3/2}$ transfers, are expected to be simply described in terms of $(1f_{7/2})^{11}$ $(2p_{3/2})^{1}$ configurations. With this scheme, they [Pe 73] have performed shell-model calculations with good iso-spin wave functions. Fig. 5.12 shows the results of these calculations spectrum (a), with iso-spin treated correctly, has been obtained using effective two-body interactions parameters of Osnes [Os 71]. The spectrum (b) has been calculated without good iso-spin wave functions using the two-body interaction parameters of Lips and McEllistrem [Li 70]. It is evident that the position of the predicted second 0^{+} level is in a better agreement with the experimental one [Si 76] only when the iso-spin was taken correctly into account. The 0^{+}, 2^{+}, 4^{+}, 4^{+}, 2^{+}, 6^{+}, and 2^{+} levels (present) show good agreement with theory and experiment.

The transition strengths G_{j} for the levels in ^{52}Cr with $(1f_{7/2})^{4}$ configuration have been compared with the works of several authors. In Fig. 5.13, 'A' represents work done by Pellegrini et al. [Pe 73] using shell-model theory; 'B' represents the present work; 'C' represents the work of Armstrong and Blain [Ar 65]; 'D' represents the work of
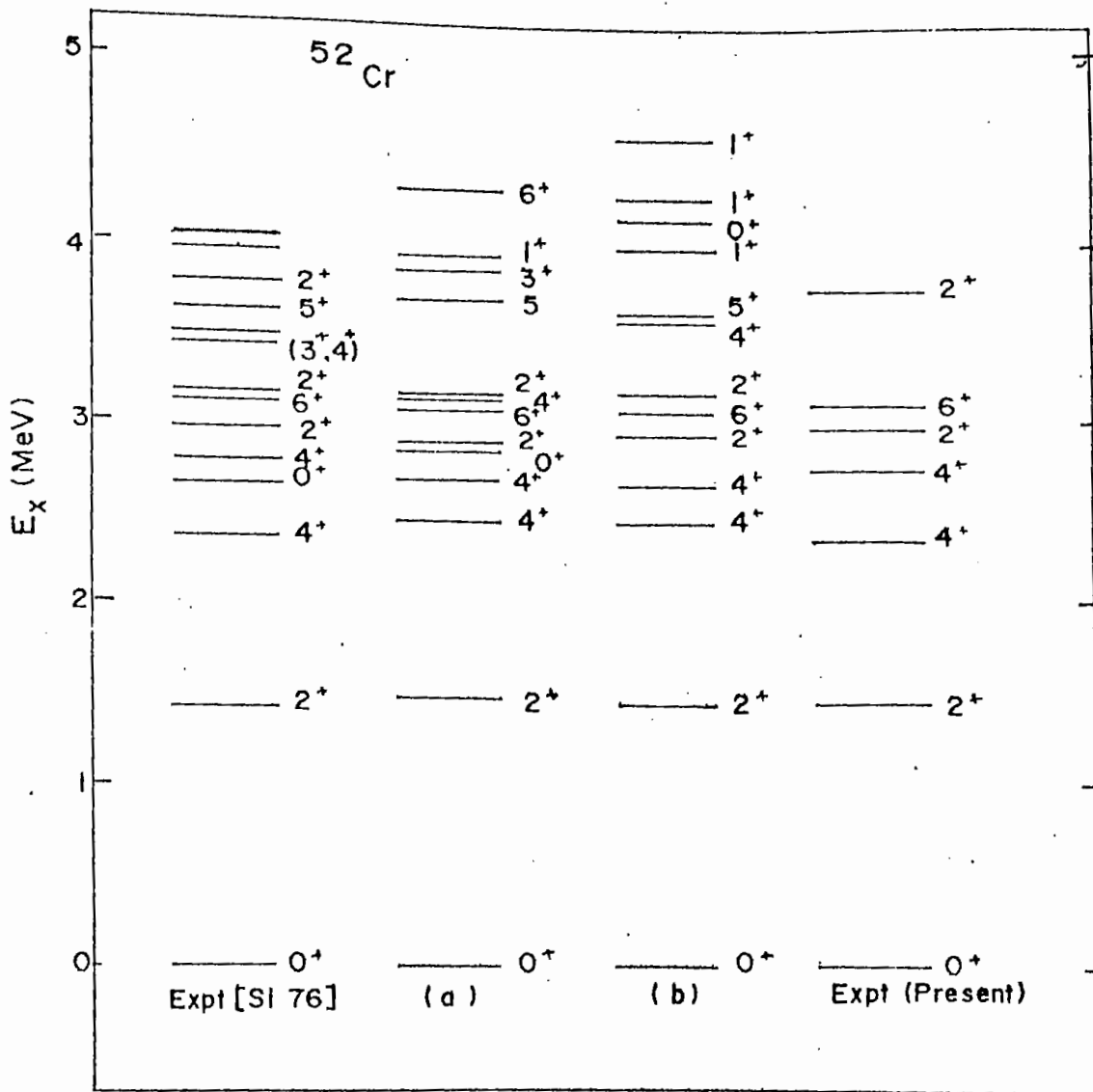
Fig. 5.12. Comparison of the experimental and theoretical spectra of ^{52}Cr.

(a) and (b) represent calculations with and without good isospin wave functions, respectively.
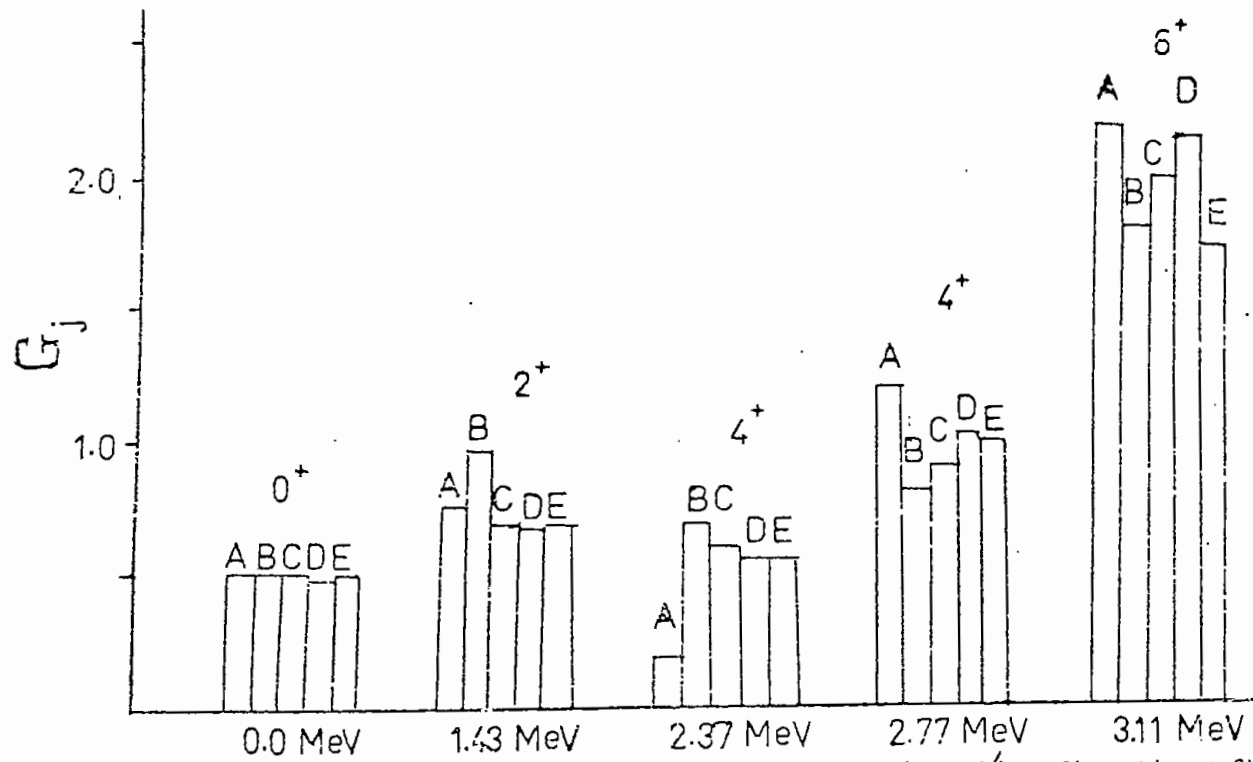
Fig. 5. 13. The transition strength G_j for the levels with $(1f_{7/2})^4$ configuration. A: Shell model theory [Pe 73], B: Present work, C: Armstrong and Blair [Ar 65], D: Pellegrini et al. [Pe 73], E: Matoba [Ma 68] (normalized to the g.s. transition strength).

Pellegrini et al. [Pe 73] and 'E' represents the work of Masaru Matoba [Ma 68]. It is observed that the transition strength for the ground state in ^{52}Cr is in excellent agreement with those works; but for the levels at 1.43 and 2.37 MeV, it is higher than that of others. For the 2.37 MeV level, the strength calculated by Pellegrini et al. [Pe 73] using shell-model theory, is much smaller than that of others; whereas it is for the 2.77 and 3.11 MeV levels, higher.

CHAPTER 6

THE $^{62}Ni(^{3}He,p)^{64}Cu$ REACTION

CHAPTER 6

THE ^{62}Ni(^{3}He,p)^{64}Cu REACTION

6.1 Introduction

Two-nucleon transfer reactions are highly sensitive to the details of the wave functions, as many different configurations of the transferred nucleon pair can contribute to the process. These reactions are less selective than the single nucleon transfer reactions. The present work is concerned with a study of the ^{62}Ni(^{3}He,p)^{64}Cu reaction at 18 MeV. This reaction was studied before by Young and Rapaport [Yo 68], but details are not available. This reaction should supplement the information on the level structure of ^{64}Cu given from the ^{66}Zn(d,α)^{64}Cu reaction studied by Park and Daehnick [Pa 69]. The dominant configurations may not be identical in the two reactions.

Due to the relatively large angular momentum mismatch between the entrance and exit channels, the (d,α) reaction favours the transfer of the larger angular momenta. Also the spin and iso-spin selection rules and the anti-symmetrization requirement in the two nucleon transfer reaction allow the transfer of only spin triplet in the (d,α) reaction in contrast to both the spin triplet and a singlet in the (^{3}He,p) reaction.

In the present study, a total of 69 levels in ^{64}Cu have been observed, covering an excitation energy up to $E_x \sim 8.2$ MeV.

Angular distributions have been measured for all the levels. The data for the stripping levels have been analyzed in terms of the DWBA theory. The predicted differential cross-sections have been normalized to the experimental cross-sections using the expression [Na 71]:

$$\sigma_{exp}(\Theta) = N \; \frac{(2J_f+1)}{(2j_i+1)} \sum_{LJST} b_{ST}^{\;2} \; |D_{ST}|^2$$

$$(T_i \; T_{iz} \; T_0 \; | \; T_f \; T_{fz})^2 \; X \; \frac{\sigma_{DW}(\Theta)}{(2J+1)}$$

The LJST refer to the transferred particles and $(T_i \; T_{iz} \; T_0 \; | \; T_f \; T_{fz})$ is an iso-spin Clebsch-Gordan co-efficient. The quantity b_{ST}^2 is essentially a spectroscopic factor for light particles, being 1/2 for both the spin state and $|D_{ST}|^2$ is the weighting factor which following Nann [Na 71] was taken as 0.72 and 0.30 respectively for S=0 and S=1 transfers. N is the normalization constant which is not correctly given by the DWBA method for two-nucleon transfer reactions. It is expected that the relative value of N should nevertheless be fairly independent of the transition, provided the nuclear structure information has been properly included in the DWBA calculations. Results on the values of N for three levels at 0.0, 6.821 and 8.188 MeV are summarized in Table — 6.1(a) for potential parameters H1P2.

TABLE-6.1 (a)

The normalization constant.

E_x(MeV)	J^{π}	Potential	The value of NC^2S
0.000	1^+	H1P2	159
6.821	$0^+,T_>$	H1P2	156
8.188	$2^+,T_>$	H1P2	666

Then L-transfers and J^{π}-values have been examined for 46 levels. Two analogue states have been identified. Properties of the levels of ^{64}Cu have been compared with the prediction based on shell-model calculations.

6.2 DWBA analysis

The local zero-range DWBA analyses were carried out using the code DWUCK4 due to Kunz. The optical-model potential used in the DWBA analysis was of the same form as mentioned in Section 5.2.

The optical-model potentials were of the standard Woods-Saxon form for the real part of ^{3}He-particles and for the protons; while a Woods-Saxon derivative was employed for the imaginary part of the ^{3}He potentials and both Woods-Saxon and Woods-Saxon derivative were considered for the imaginary part of proton potentials. A spin-orbit term of the usual Woods-Saxon derivative form was added to the proton potential.

Three sets of optical model potential parameters were used from ^{3}He particles in the DWBA analysis, as shown in Table-6.1. The potential parameters H1, H2 and H3 are the potentials given by Shepard et al. [Sh 77] and the parameters P1 and P2 are the proton-potentials given by Becchetti et al. [Be 69a] and Menet et al. [Me 71] respectively.

The DWBA calculations using the parameter combination H1P2 was found to fit best the measured angular distributions.

There is no unique choice for the bound-state wave functions in the case of two-nucleon transfer reaction [Ne 60]. The wave function for neutron-proton transferred particles was calculated by assuming a (real) Woods-Saxon potential well having geometric parameters $r = 1.25$ fm and $a = 0.65$ fm including a Thomas-Fermi spin-orbit term of strength $\lambda = 25$. The potential well depths are adjusted by the DWBA programme so as to reproduce the appropriate separation energy given as follows for each of the transferred nucleons:

$\frac{1}{2}$ [E_B (final) $-$ E_B (initial) $-E_x$] MeV   for singlet spin,

and $\frac{1}{2}$ [E_B (final) $-E_B$ (initial) $-E_x-2.23$] MeV for triplet spin.

The ground state binding energy for the n-p in ^{64}Cu was taken to be -12.966 MeV.

The effect of the finite range interaction and the non-locality of the optical model potentials can be introduced in the DWBA calculations in the local energy approximation using a finite range correction factor $F_R \approx 0.80$ fm and non-localities $\beta_p \approx 0.85$ fm for proton, $\beta_d \approx 0.54$ fm for deuteron, and $\beta_\tau \approx 0.2-0.3$ fm for ^{3}He. But for the (^{3}He,p) reaction, the finite range interaction correction was not effective in DWBA programme using the code DWUCK4, because the transferred neutron-proton pair was considered to be stripped off with a zero-range interaction. Only the non-local correction was introduced in the reaction.

All calculations were carried out with the help of Alpha-micro computer of the University of Rajshahi, Bangladesh. The summary of the results on the levels in ^{64}Cu have been shown in Table-6.2.

TABLE-6.1

Optical model parameters (depth in MeV and lengths in fm)

Par-ti-cle	Nota-tion	V	r_o	a	W_D	r_1	a_1	r_c
^{3}He	H1	156.13 +.0543E_L	1.20	.720 -.000644E_L	29.458 -.0809E_L	1.257 -.00216E_L	.806 +.00166E_L	1.25
	H2	163.88 +.0386E_L	1.676	.751 -.000578E_L	32.596 -.123E_L	1.293 -.00252E_L	.7212 +.00265E_L	1.25
	H3	179.74 -.0591E_L	1.108 +.00027E_L	.784 -.0154E_L	32.344 -.120E_L	1.299 -.003161E_L	.7184 +.00215E_L	1.25

	V	r_o	a_o	W	W_D	r_w	a_w	V_{so}	r_{so}	a_{so}	r_c
P1	58.127 -.32E	1.17	.75	.22E-2.7 or zero whichever is greater.	12.390 -.25E	1.32	.544	6.2	1.01	.75	1.30
P2	54.145 -.22E	1.16	.75	.12-.09E	4.962 -.05E	1.37	.789 -.008E	6.04	1.064	.78	1.25

In the programme, the ground state binding energy for n-p in ^{64}Cu was taken as 12.966 MeV. The bound state parameters for the transferred n or p were r_o = 1.25 fm and a_o = 0.65 fm).

The ^{3}He potentials are from [Sh 77] and their proton potentials P1 and P2 are respectively from [Be 69] and [Me 71].

TABLE- 6.2

Summary of the $^{62}Ni(^{3}He,p)^{64}Cu$ reaction.

Gr. No.	E_x(MeV) a	b	$\sigma_{cm}(\theta)(\mu b/sr)$ c	d	L-transfer a	f	J^π b
00	0.000	0.000	40.37	26.00	0+2	0+(2)	1+
01	0.160	0.159	14.18	5.34	2	2+(0)	2^+
02	0.278	0.278	6.20	2.67	2	2	2^+
		0.342				weak	1^+
03	0.362	0.362	16.36	7.82	2	4	3^+
04	0.574	0.574	18.44	6.61	2	4	4^+
05	0.608	0.608	10.20	4.74	2	2	2^+
06	0.663	0.663	4.60	2.11	2	4	1^+
		0.739					2^+
07	0.745	0.746	44.99	17.68	2	2+(4)	3^+
08	0.878	0.879	4.86	3.03	weak	weak	(0^+)
09	0.927	0.927	106.50	30.25	2	0+(2)	1^+
10	1.243	1.241	16.42	4.95		(0+2)	$2^+(1^+)$
		1.288					$(3^+,4^+)$
11	1.299	1.298	120.40	26.16	0	0+2	(1^+)
12	1.322	1.320	21.52	7.77	2		(0–3)
13	1.359	1.354	13.44	3.83	2	V.weak	(3^+)
		1.364				V.weak	
14	1.440	1.438	18.35	7.81	2	0+(2)	1^+
		1.462				3	

TABLE- 6.2   continued

Gr. No.	E_x(MeV) a	b	$\sigma_{cm}(\theta)(\mu b/sr)$ c	d	L-transfer a	f	J^π b
		1.499				2+(4)	$2^-(1-)$
15	1.509	1.521	13.62	5.44	2		
16	1.551	1.551	37.29	14.85	2	2	$(1^+-3^+)^f$
		1.594					6^-
		1.594					(3^+)
17	1.602	1.607	25.72	7.44	(0+2)	0+(2)	(1^+)
	1.616						
18	1.689	1.683	196.30	73.70	(0+2)	0+2	$(1^-,2^-);(1^+)$
	1.701 $\longrightarrow$					3	$(3^-,4^-)$
	1.707 $\longrightarrow$						
	1.737 $\longrightarrow$					4	
19	1.741	1.742	51.71	12.39			(3^+)
20	1.775	1.770	15.82	4.66			
		1.780					$3^+,(4^+)$
21	1.853	1.852	9.52	3.34	2	4	(3^+)
22	1.907	1.909	47.34	11.03	0	(0+2)	$(1^+)2^+$
23	1.952	1.940	19.56	4.59	0	2+(0)	(1^+-3^+)
		1.979				4	(3^+-5^+)
		2.022					$2^+(3^+,1^+)$
24	2.047	2.053	21.33	9.45	2	4+(2)	3^+
		2.072					5^-

TABLE- 6.2   continued

Gr. No.	E_x(MeV) a	b	$\sigma_{cm}(\theta)(\mu b/sr)$ c	d	L-transfer a	f	J^π b
25	2.092	2.092	10.26	6.05		2+(0)	(1^+-3^+)
26	2.146	2.145	4.08	1.94	2	4+(2)	(3^+)
		2.226					(3^+-4^+)
27	2.246	2.251	19.99	8.62	2	(2)	$?^{f)}$
		2.263					$(3^-,4^-)$
		2.275					
28	2.290	2.301	29.62	12.58	2	2	$?^{f)}$
		2.309					(3^+)
29	2.323	2.322	14.29	5.92	(0+2)	not seen	$(4^+,6^+)$
		2.356				2	
30	2.369	2.378	10.40	4.77			$(7^-,5^+)$
	2.386 $\rightarrow$					0+(2)	
31	2.414	2.417	40.32	7.62			(3^+-5^+)
32	2.455	2.457	21.02	5.42	0	(1)	$(1^+,2^+)$
		2.491				3	(2^+-4^+)
		2.504					
33	2.515	2.522	28.60	7.58			$(1^+,2^-);(1^+)$
		2.534				(0+(2))	$(1^+,2^+);(1^+)$
		2.550				4+(2)	(3^+-5^+)
		2.586				4+(2)	(3^+-4^+)
		2.596				(0+2)	(1^+)

TABLE- 6.2   continued

Gr. No.	E_x(MeV) a	b	$\sigma_{cm}(\theta)$(μb/sr) c	d	L–transfer a	f	J^π b
34	2.608	2.607	31.00	9.53			$(1^-–2^-);(3^+–5^+)$
		2.622				0+2	(1^+)
		2.631					$(1^+);0^-–4^-$
		2.644					
		2.654					
35	2.679	2.670	22.07	9.17	2	(3+(1))	$(2^-,1^-)$
		2.692					$(1^-–2^-);(3^+)$
36	2.718	2.716	14.40	5.98	2	2	
		2.720					$(1^-–2^-)$
37	2.762	2.757	16.60	5.81			$(1^-–2^-);(3^+)$
38	2.801	2.800$^{f)}$	13.15	4.34	0	not seen	
39	2.827	2.823$^{f)}$	18.64	7.01			
40	2.875	2.876$^{f)}$	15.72	7.02	(2+4)	4	
41	2.907	2.913$^{f)}$	16.71	5.36	(0+2)	(0+2)	
42	2.990	2.985$^{f)}$	20.66	8.65	2+4		
		3.050					
43	3.066	3.055$^{f)}$	9.93	5.02			
44	3.130	3.127	28.19	10.40	2		
45	3.189	3.190	23.87	9.41	2		8^-
46	3.231		20.16	5.53	2		
47	3.265		9.69	4.70			

TABLE- 6.2   continued

Gr.	E_x(MeV)		$\sigma_{cm}(\theta)(\mu b/sr)$		L—transfer		J^π
No.	a	b	c	d	a	f	b
48	3.302		11.02	5.12	2		
49	3.397		23.28	10.80			
50	3.472		30.10	11.33	2		
51	3.513		20.94	6.97			
52	3.607		25.76	12.20			
53	3.686		31.69	10.56			
54	3.713		21.37	10.20	4		
55	3.767		40.15	23.23			
56	3.802	3.799	119.40	34.72	2		9^-
57	3.902		60.35	17.31			
58	3.973	3.987	29.54	12.98	2		
59	4.028		51.77	18.50	2		
60	4.137		45.43	17.35	1		
61	4.257^N		28.10	15.63	1+3		
62	4.316^N		60.36	25.13			
63	4.425		42.32	16.60			
64	4.571	4.570^*	46.03	24.07			
65	6.171^N	6.810	81.93	35.50			0^+
66	6.821^{++}	6.826	483.30	131.63	0		0^+
67	7.339	7.320^*	288.60	89.34	2		
68	8.188^{++}		281.90	115.50	2		

Footnotes to table:

a   Present work

b   Summary [Si 84]

c   Maximum cross-section

d   Average over 5° — 80° (c.m.s.)

f   From (d,α) reaction given by (Park and Daehnick [Pa 69]

*   means ref. [Lu 69]

++   means Analogue state

N   Not found in literature (new)

h   Ref. [Br 92].

6.3 Results and discussions

6.3.1   The angular distributions

A large number of levels in ^{64}Cu are identified up to $E_x \approx$ 8.2 MeV. The DWBA analyses were carried out for 46 levels. The cross-section data for the remaining levels could be measured over only a narrow angular range so that a DWBA comparison was not considered meaningful.

The measured angular distributions are presented in Figs. 6.1-6.18 and compared with the DWBA curves.

It is noted that the slopes of the experimental distributions are reasonably well reproduced by the DWBA theory even when there is a lack of an oscillatory feature in the angular distributions. It is well-known from literature that the shapes of the angular distributions are mainly dependent on the orbital angular momentum transfer, whereas the finer details and absolute magnitudes of these cross-sections are affected by the spins and the configurations.

DWBA analyses were usually done using a pure configuration (Figs. 6.1-6.12 and 6.14). Only for the ground state and the two analogue states (E_x=6.821 and 8.188 MeV), DWBA calculations were done using the spectroscopic amplitudes given by Brown [Br 92] based on the shell model calculations (Figs. 6.13 and 6.15-6.18).

The maximum cross-sections are listed in Table 6.2. The average differential cross-section is around 16 μb/sr. The angular distributions are mainly featureless.

Some of the populated states in ^{64}Cu is discussed below in details.

A. The L=0 transitions

Up to $E_x \approx 8.2$ MeV, only two levels namely, $E_x = 6.810$ and 6.821 MeV, are known to have $J^\pi=0^+$ [Si 84], while a 0^+ is tentatively assigned to the level $E_x=0.878$ MeV. Of these, the 0.878 MeV level is extremely weakly excited in the present work and the level at 6.810 MeV does not appear to have been excited. Only the 6.821 MeV level is strongly populated. The latter is the ground state analogue of ^{64}Ni [Si 84]. These features are similar to the several previous studies of the (^{3}He,p) reaction and are consistent with the selection rules for a 0^+-0^+ transition (i.e. transition to the final states with $J^\pi=0^+$, $T_<$ are forbidden).

The L=0 transitions observed in the present work (exccept to the ground state analogue) may probably be considered to correspond to $J^\pi=1^+$. Many of these were in fact excited in the ^{66}Zn(d,α) reaction with L=0+2 transfers [Pa 69]. Such a mixture of L transfers was however not found necessary in the present work (Fig. 6.1). Similarly, levels in ^{64}Cu populated in the

above (d,α) reaction with L=2+4 or even pure L=4 are usually found to have a pure L=2 transfer in the present work as discussed below. One can associate these differences in the two reactions to the momentum mismatch in the (d,α) reaction.

The 2.455 MeV level populated in the $(^3He,p)$ reaction with L=0 transfer (Fig. 6.1) was found to have a tentative L=1 transfer in the (d,α) reaction [Pa 69]. The present work is thus consistent with the positive parity of the level [Si 84] and suggests further a J=1.

B. The L=2 transitions

A large number of L=2 transitions are observed in the $^{62}Ni(^3He,p)$ reaction, and in most cases the L=2 transfer is consistent with the J^π-values or limits quoted by Singh [Si 84].

Several new assignments of L=2 transfers are made in the present work, thus giving J^π-limits (1^+-3^+) to some of the levels. The L=2 transitions observed in the present work in many of the cases were found to have either L=4 or L=2+4 in the (d,α) reaction, as mentioned above (e.g. E_x = 0.362, 0.574, 0.663, 0.745, 1.853, 2.047, and 2.146 MeV). Some of these transitions to levels with known $J^\pi=3^+$ (E_x = 0.362, 0.745, 1.853, 2.047 and 2.146 MeV) can perhaps be attributed to the momentum mismatch in the (d,α) reaction. In some cases, the present L=2 transfer is inconsistent with the J^π assignments [Pa 69], namely the levels

at 0.574, 2.679, 3.189, 3.802 MeV. The DWBA fits in the present work to all but the 0.574 MeV level is reasonably good (Figs. 6.6-6.8).

The L=2 assignment made in the present work to the latter level is only tentative (Fig. 6.6) and we do not therefore propose to contradict the $J^{\pi}=4^+$ assignment [Si 84]. One way to account for the disagrement in the remaining three cases would be to assume them to be doublets.

Two levels, namely 0.927 and 1.440 MeV were populated in the $^{66}Zn(d,\alpha)$ reaction [Pa 69] with L=0 transition having a small contribution from L=2. In the present case, angular distributions of these two levels on the other hand are well reproduced by a pure L=2 transfer and there is no necessity of a mixture of any other L-value (Figs. 6.7 and 6.8).

C. The L=4 transition

Only one level, E_x = 3.713 MeV was found to be populated by an L=4 transition and a reasonable fit is obtained (Fig. 6.11). The level was not reported earlier [Si 84]. The presenbt work thus gives a J^{π} limit of (3^+-5^+).

D. The L=1 transition

The level at 4.137 MeV was excited in the $(^3He,p)$ reaction with angular distribution reasonably well fitted by an L=1 transfer (Fig. 6.11). The level is new and we assign $J^{\pi}=0^--2^-$ to it.
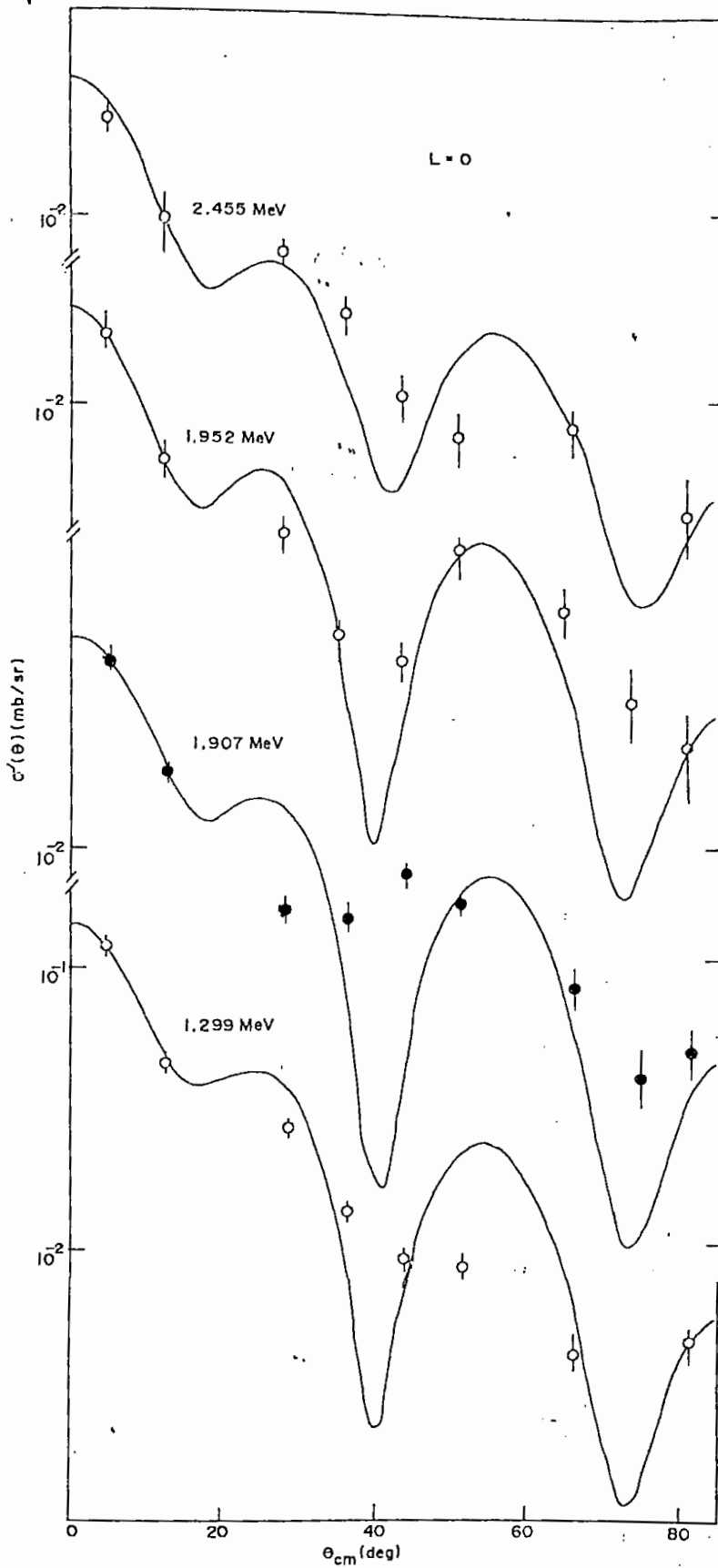
Fig. 6.1. Measured angular distributions compared to DWBA.
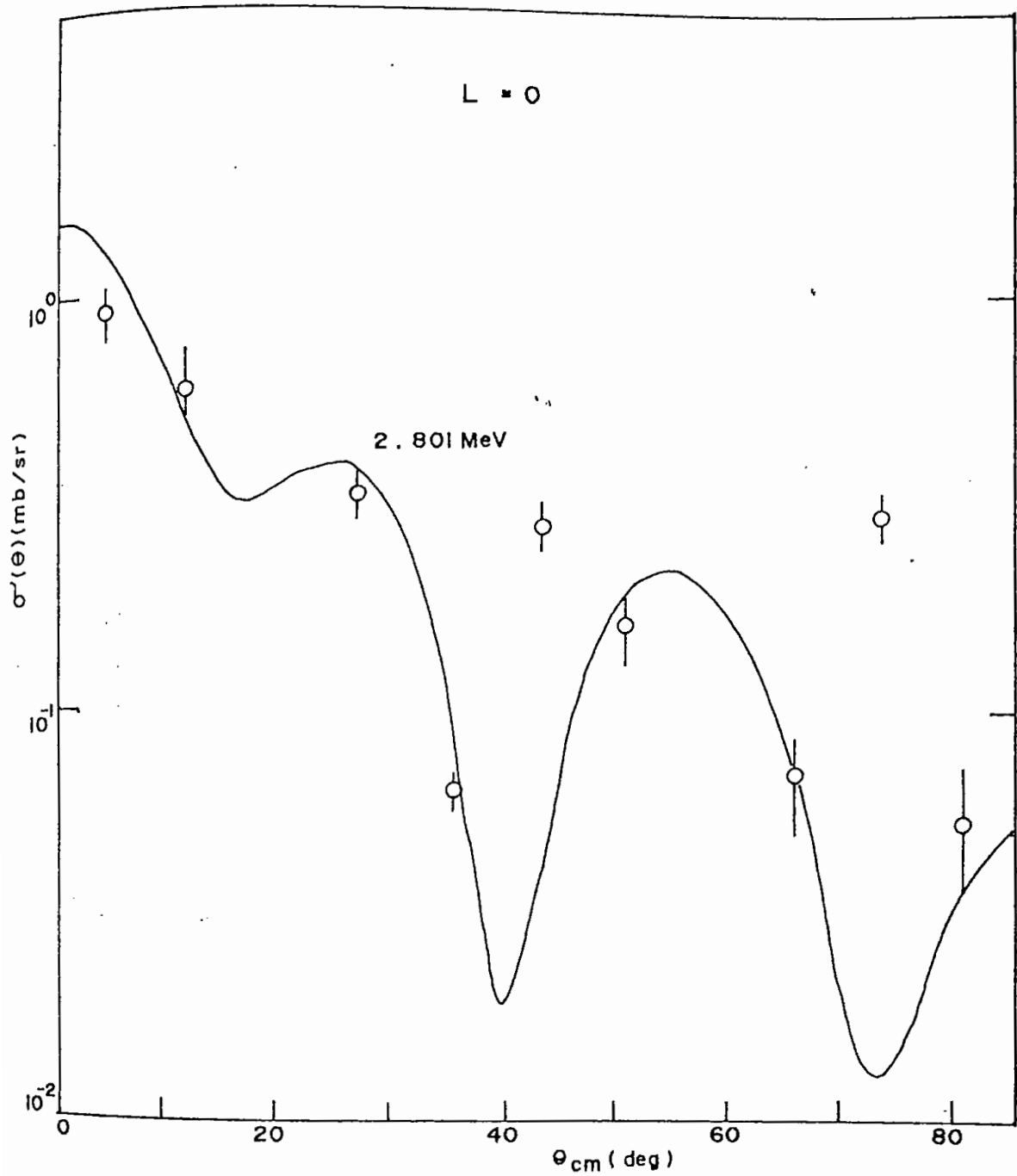
Fig. 6.2. Measured angular distributions compared to DWBA.
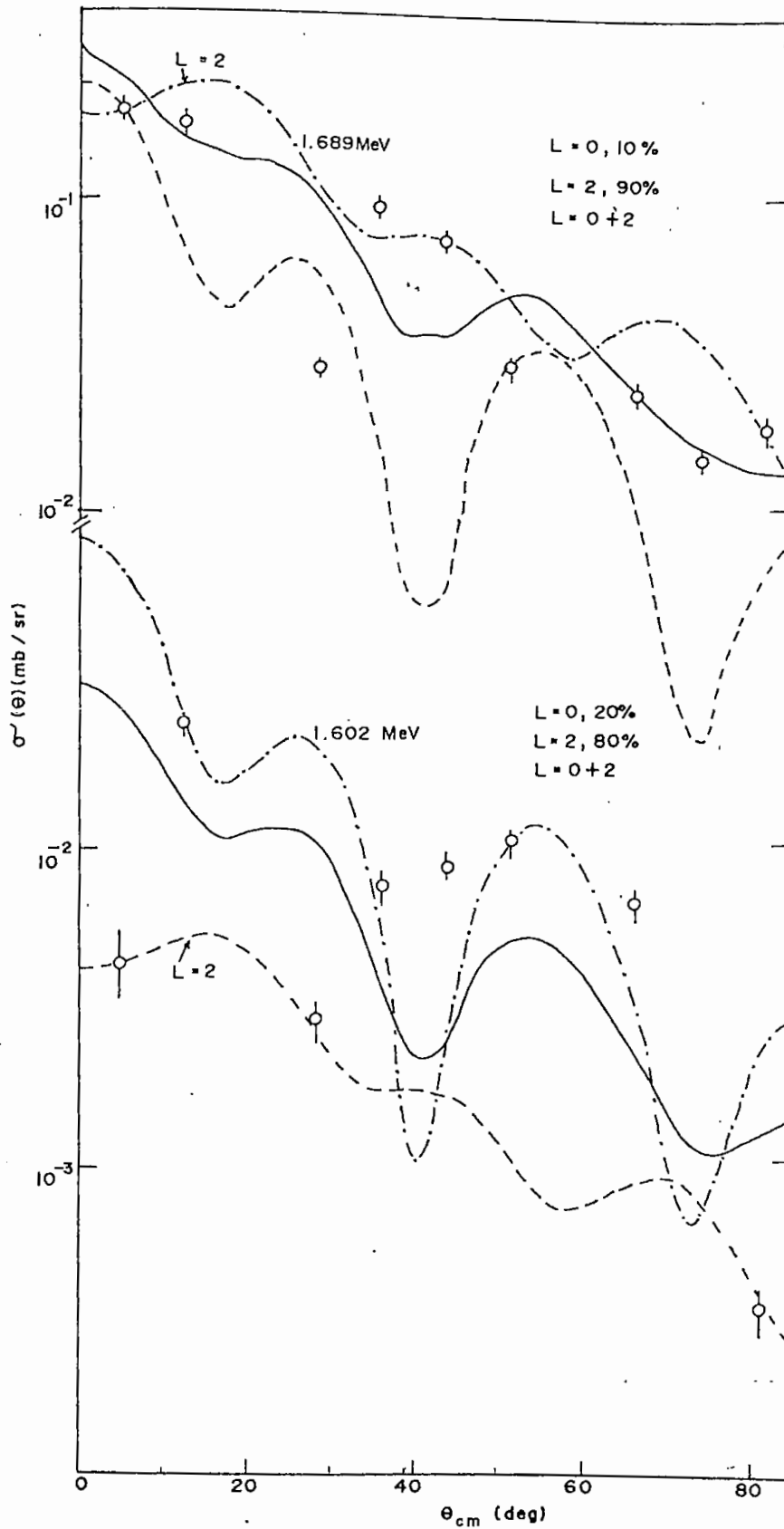
Fig. 6.3. Measured angular distributions compared to DWBA
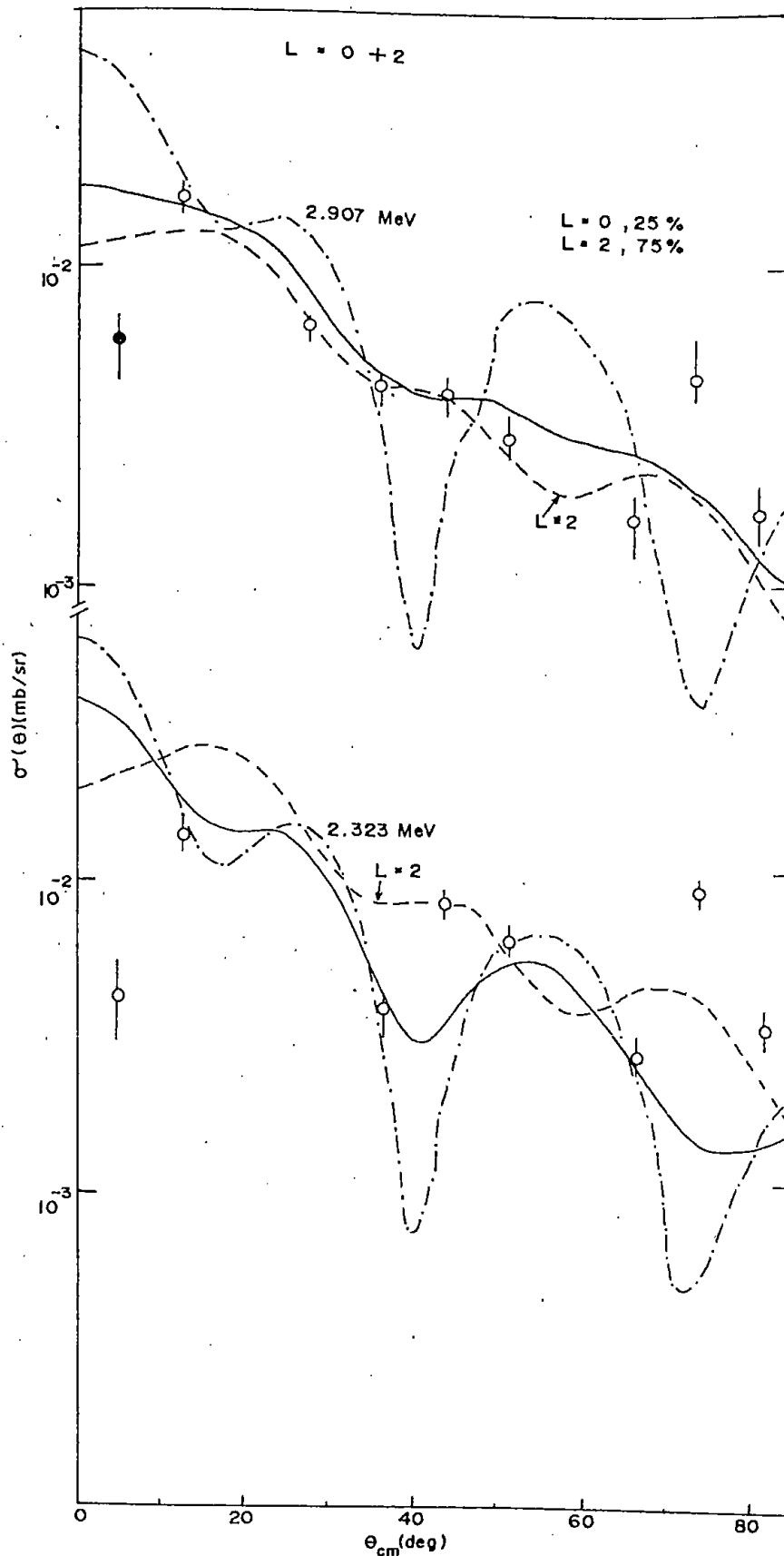
Fig. 6.4. Measured angular distributions compared to DWBA.
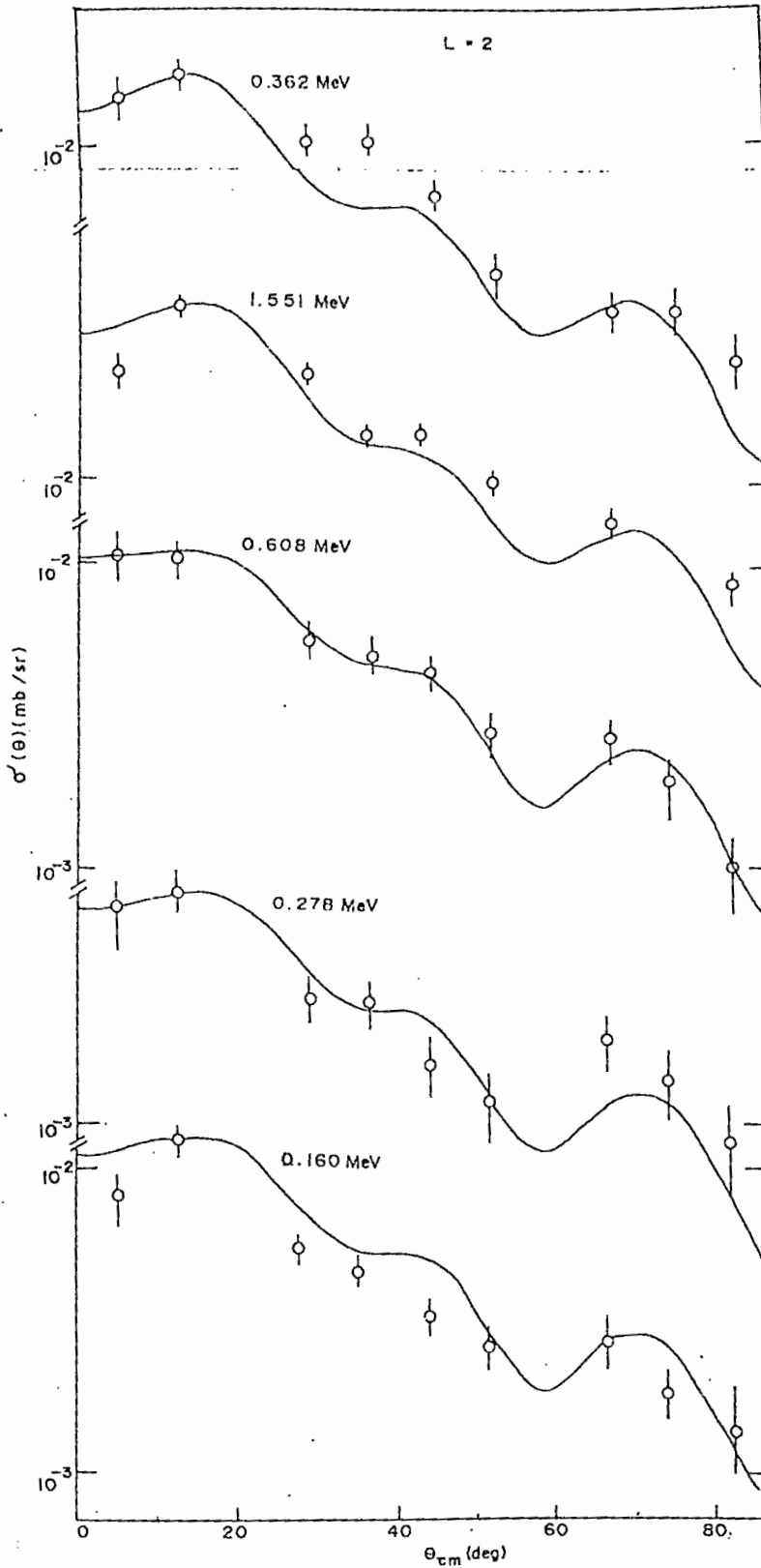
Fig. 6.5. Measured angular distributions compared to DWBA.
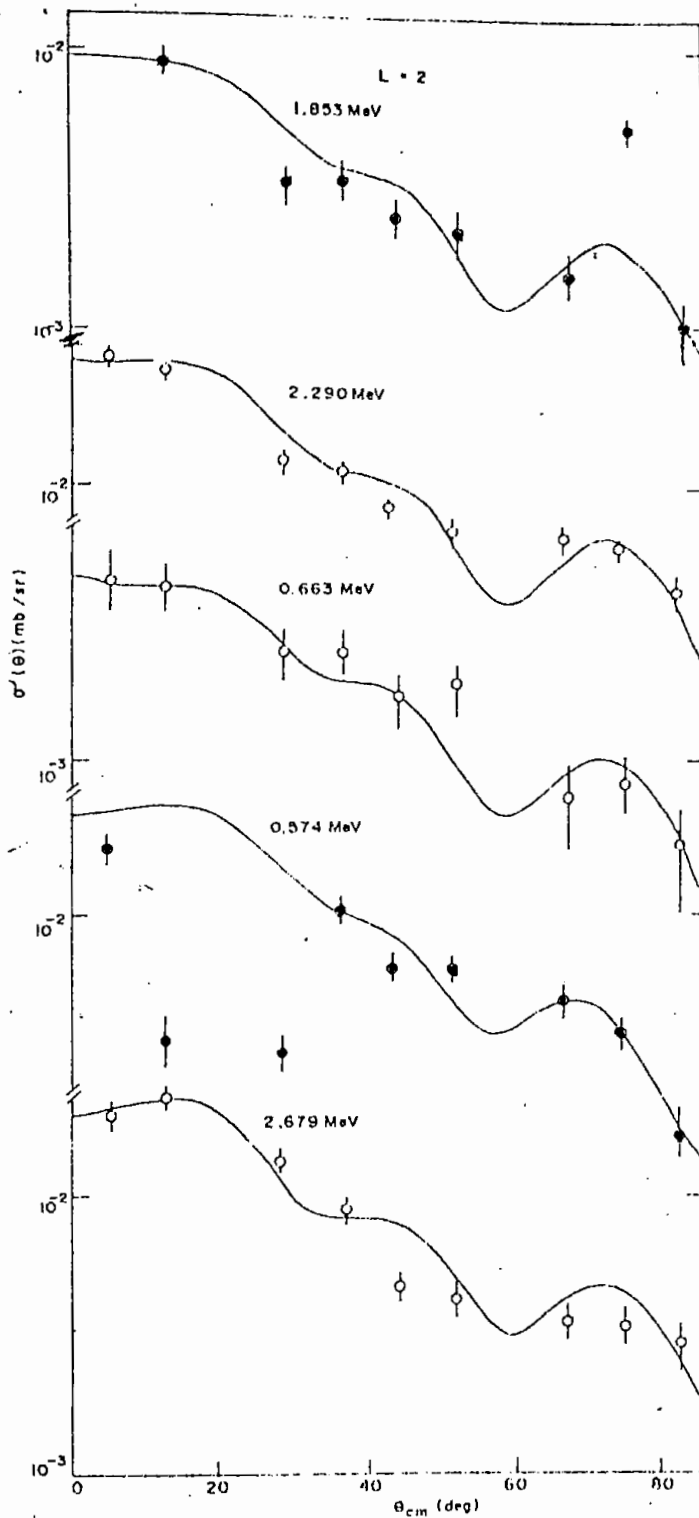
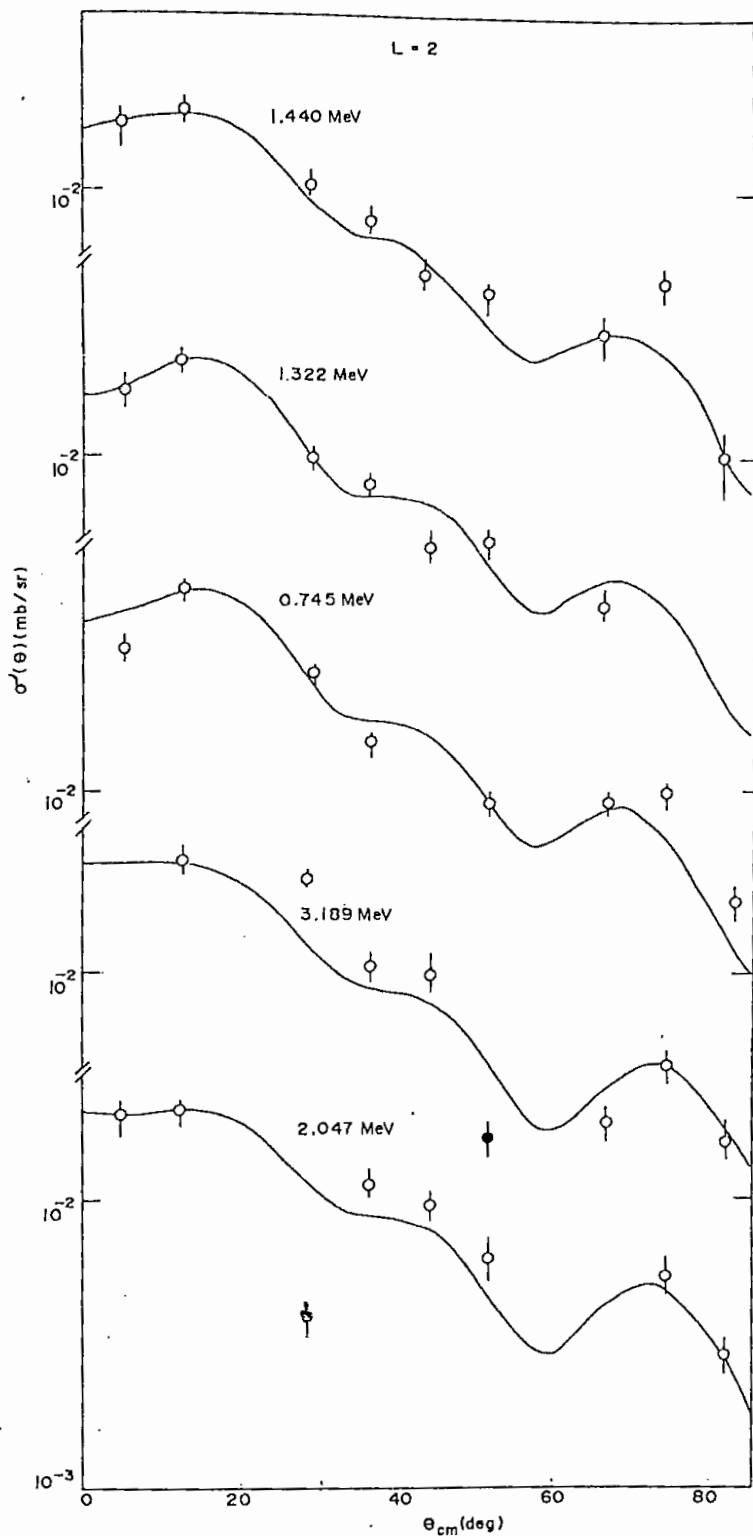Fig. 6.6. Measured angular distributions compared to DWBA.

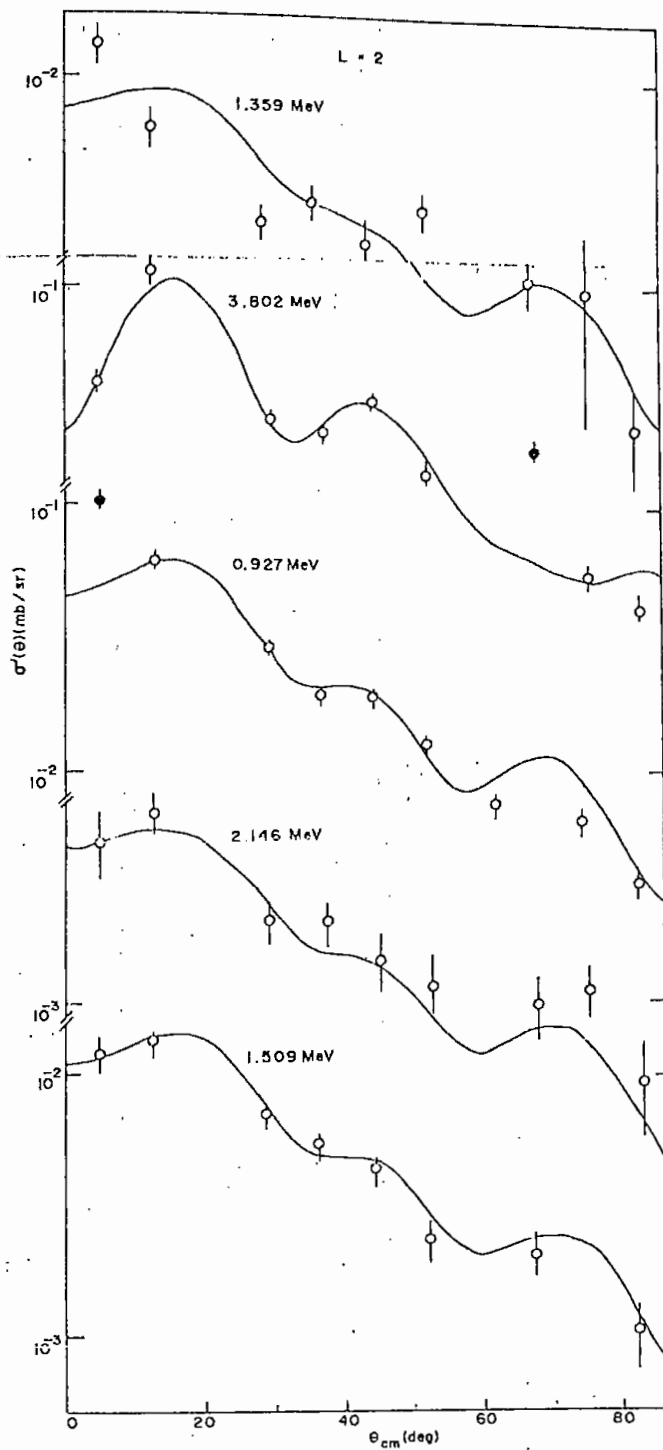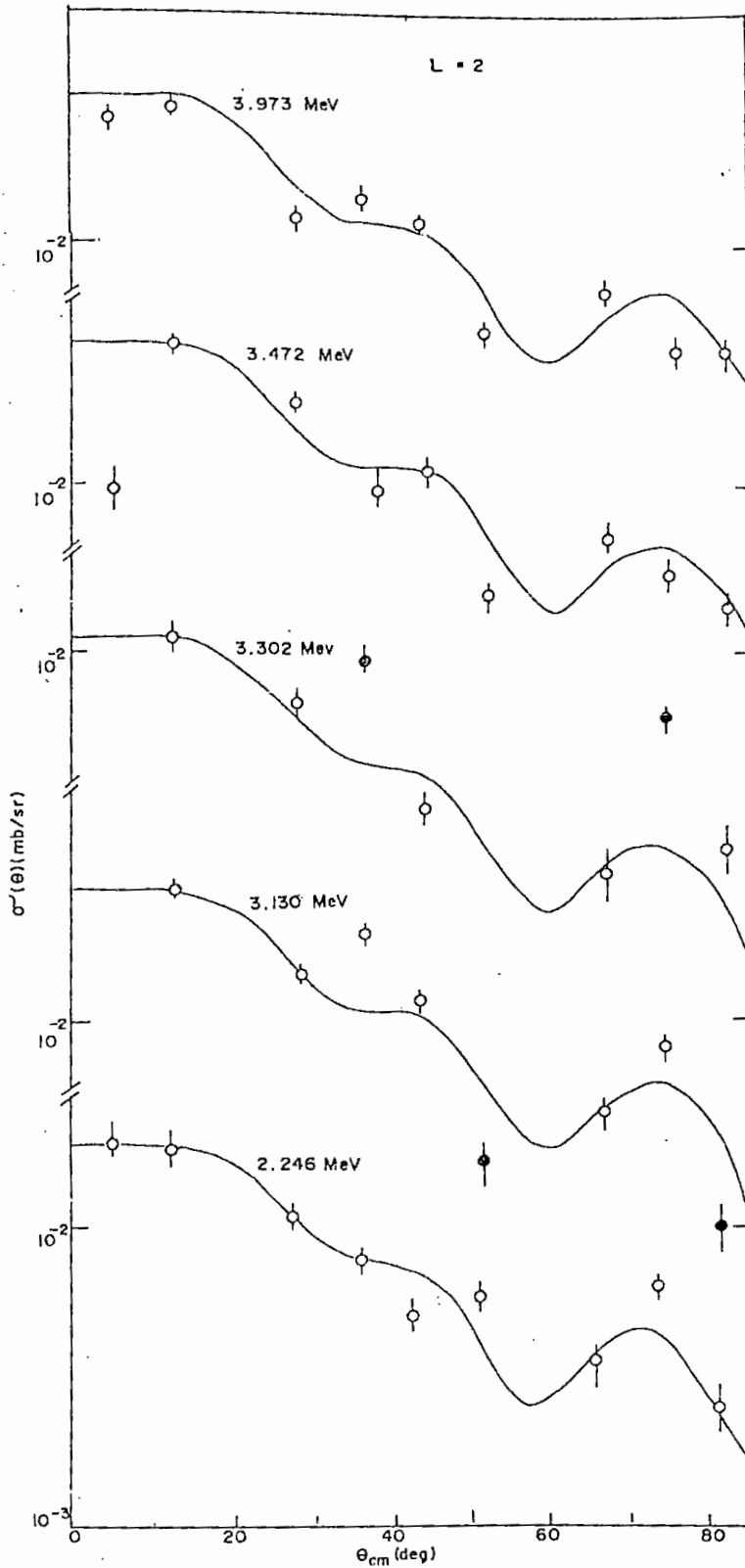Fig. 6.7. Measured angular distributions compared to DWBA.

Fig. 6.8. Measured angular distributions compared to DWBA.

E. The L=0+2 transitions

The angular distribution to the ground state is well fitted
(Figs. 6.13 and 6.14) by the DWBA calculations for the L=0+2
transition based on both a pure configuration as well as the
spectroscopic amplitudes given by Brown [Br 92]. These
amplitudes are based on a shell-model calculation using a closed
^{56}Ni core with the extra-core nucleons distributed to the
$2p_{3/2,1/2}$ and $1f_{5/2}$ shells. This is discussed in Section 6.3.3.
The L=0+2 transfer is also consistent with the values observed in
the (d,α) reaction [Pa 69].

F. The L=1+3 transition

The 4.257 MeV level has its angular distribnution typical of
L=1+3 transition (Fig. 6.12). The present work thus suggests
$J^{\pi}=2^{-}$ to the level. The level was not observed in any previous
studies.

G. Angular distribution to levels at E_x = 1.602,
    1.689, 2.323, 2.875, 2.907, and 2.990 MeV

Angular distributions were also measured for these levels.

Attempts were made to fit the distributions to four of the
levels, namely 1.602, 1.689, 2.323, and 2.907 MeV levels. Of
these the 1.602, 1.689, and 2.907 MeV levels were populated in
the ^{66}Zn$(d,\alpha)^{64}$Cu reaction with angular distribution
characteristics of L=0+(2), 0+2 and (0+2) transfers respectively,

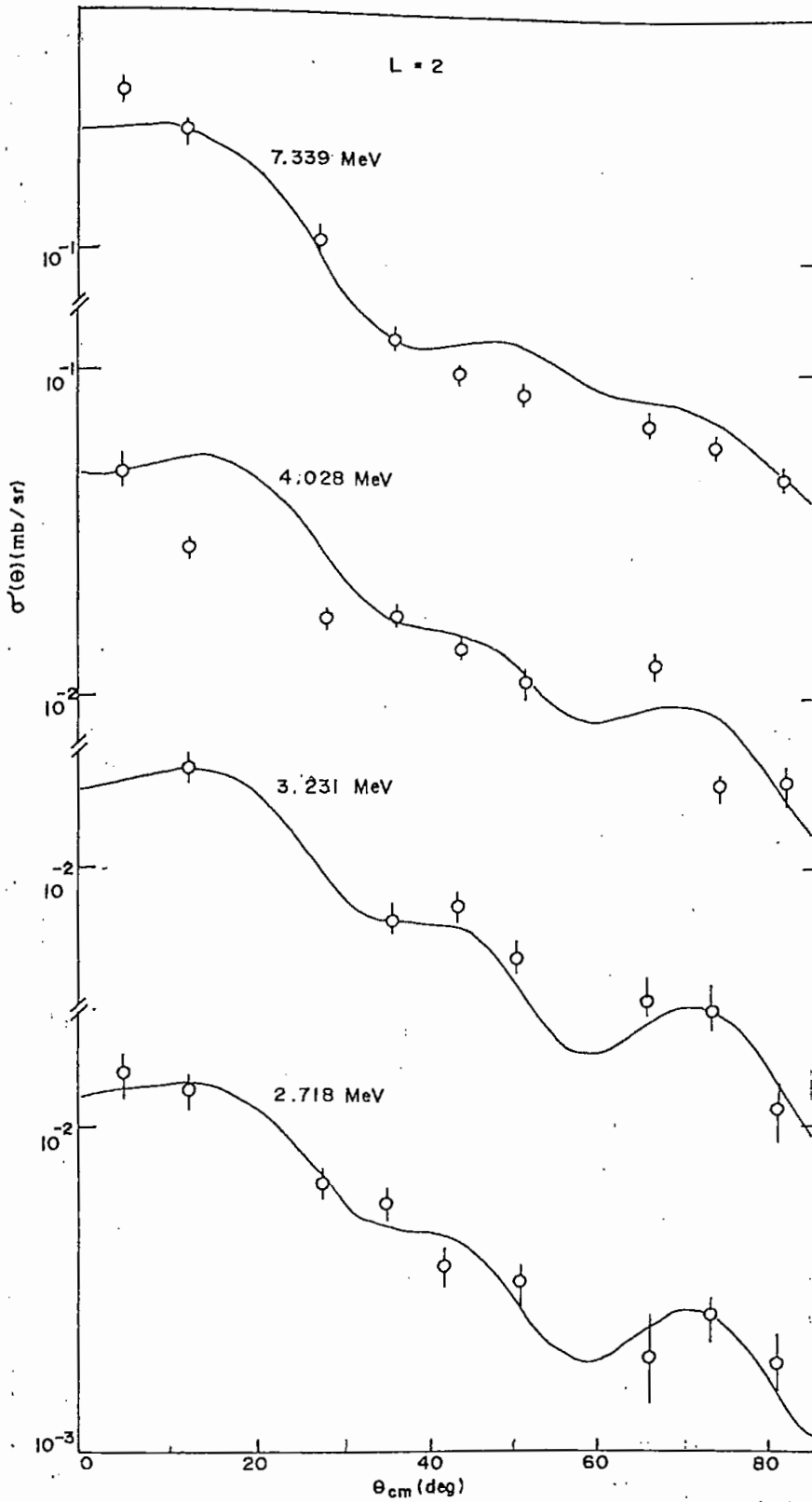Fig. 6.9. Measured angular distributions compared to DWBA.

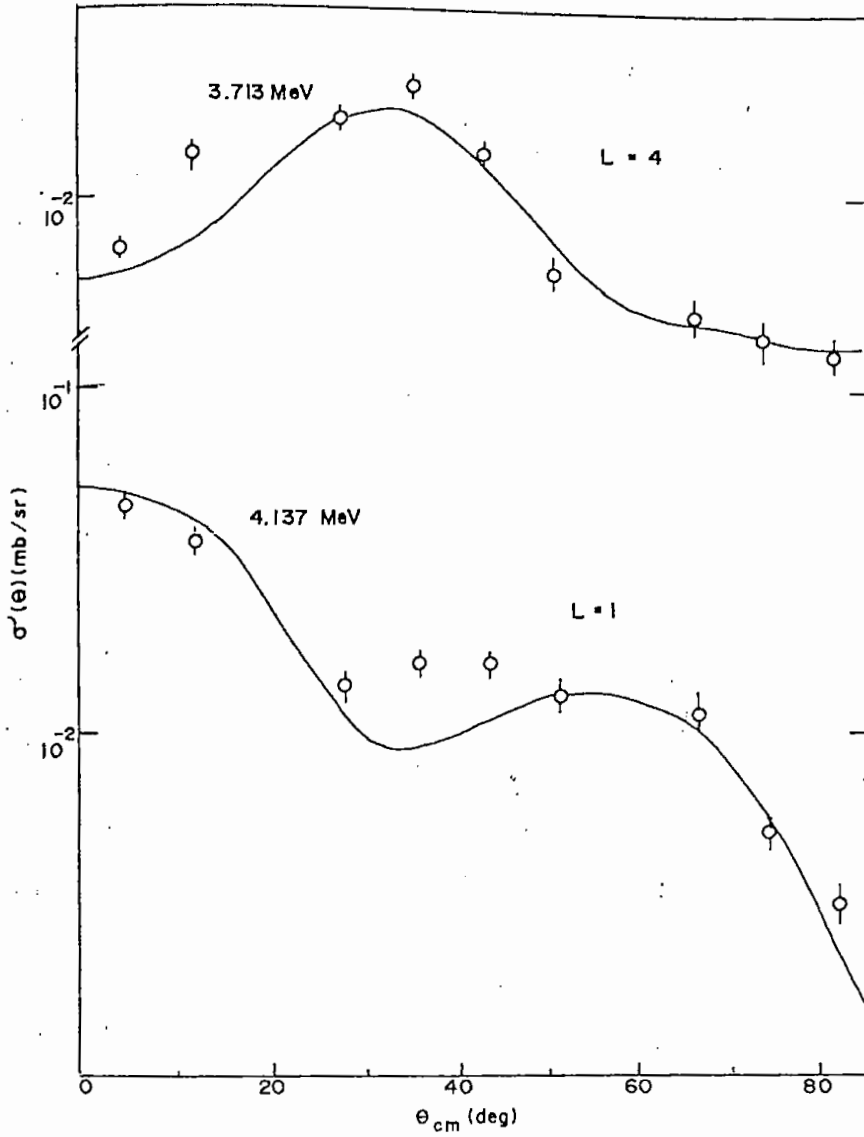Fig. 6.10. Measured angular distributions compared to DWBA.

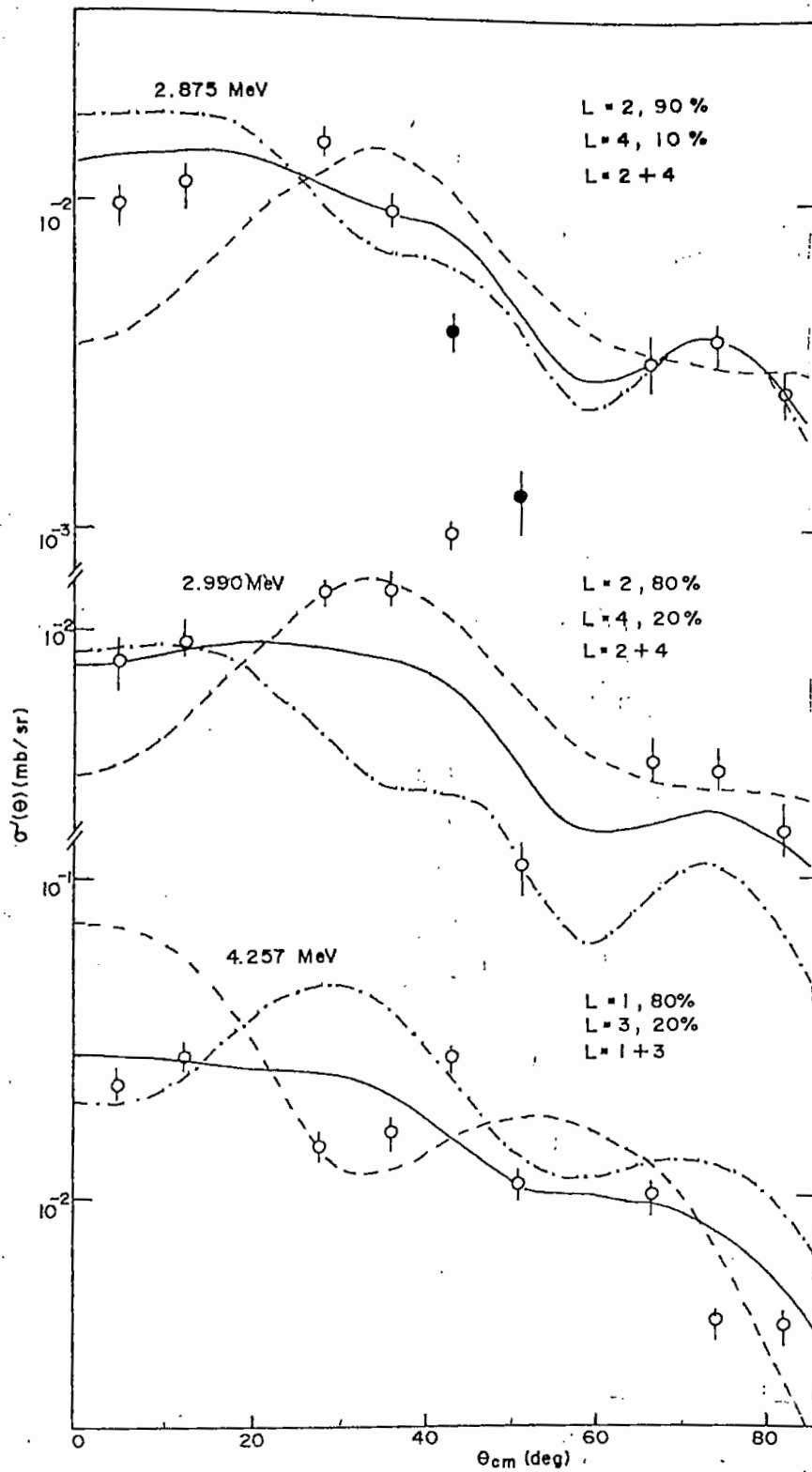Fig. 6.11. Measured angular distributions compared to DWBA.

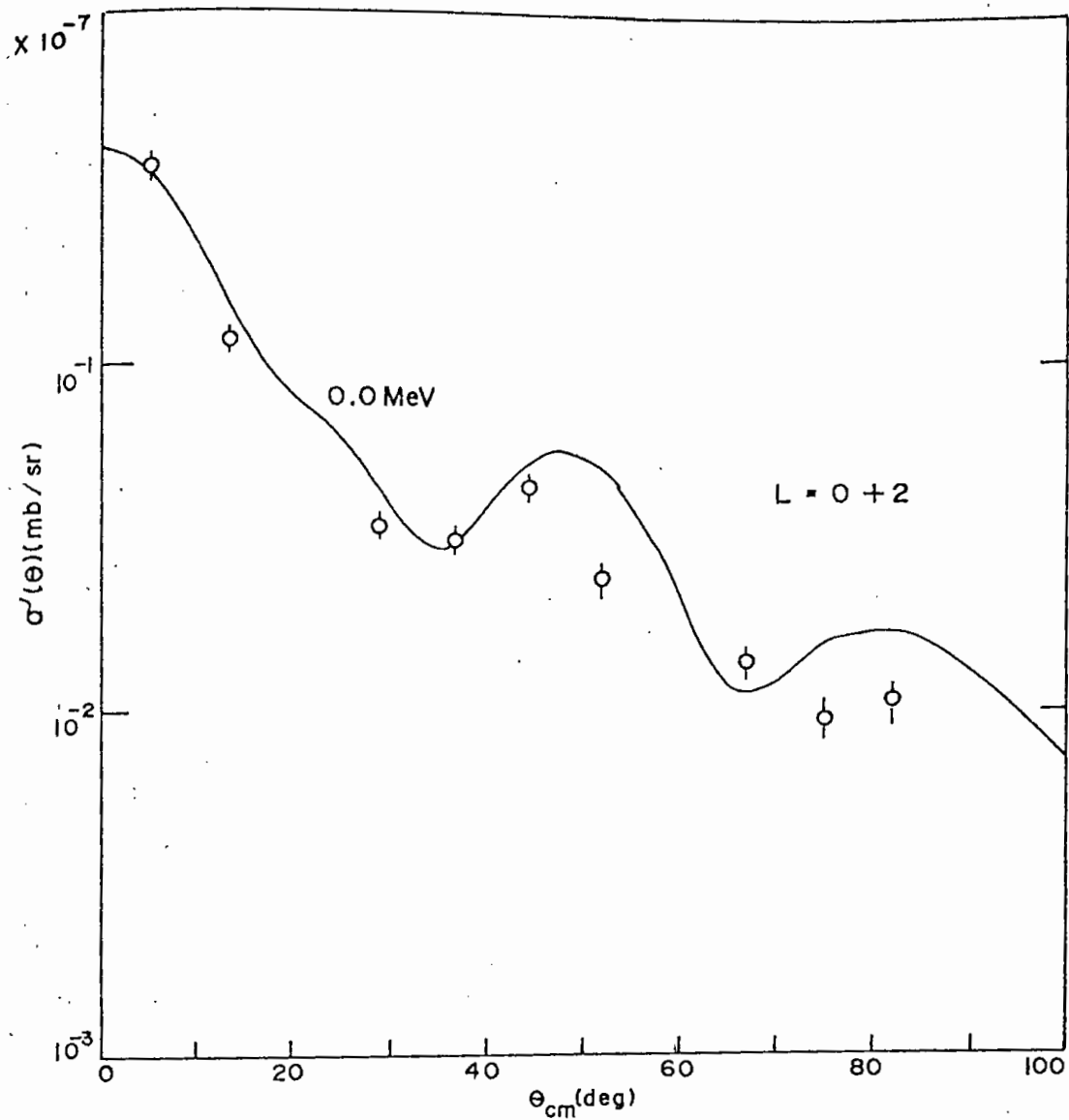Fig. 6.12. Measured angular distributions compared to DWBA.

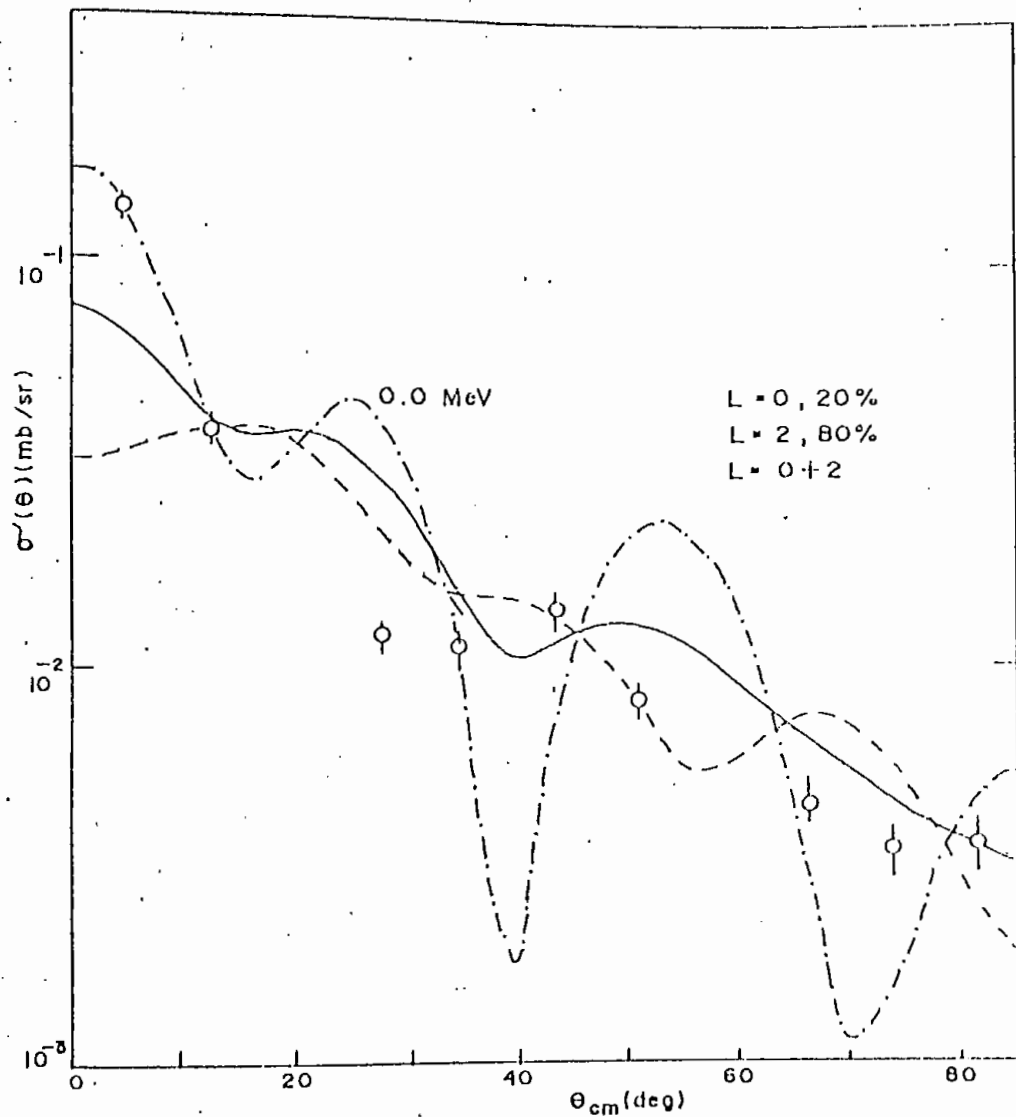Fig. 6. 13. Measured angular distribution compared to DWBA.

Fig. 6.14. Measured angular distributions compared to DWBA.

while the level at 2.323 MeV were not observed. The L=0+2 to these distributions are tentative in the present case (Figs. 6.3 and 6.4).

Similarly neither a single L transfer nor a mixture of two L-values could reproduce the angular distributions to the levels at 2.875 and 2.990 MeV. Tentative fits with L=2+4 are shown in Fig. 6.12. The 2.875 MeV level was however found to have L=4 character in the (d,α) reaction [Pa 69], while the other level was not previously reported. No further comments can be made.

6.3.2   Isobaric analogue states

The criteria used for the identification of the analogue states in the experiment were as follows:

(a) The difference in excitation energy between two levels were approximately equal to the energy difference between the corresponding levels in the parent nucleus;

(b) and that the L-values of the levels were consistent with the J^{π}-values of the corresponding parent levels.

Using the relation of Anderson et al. [An 65], the Coulomb displacement energy for the isobaric pair (^{64}Ni-^{64}Cu) was calculated as $\triangle E_c$=9.159 MeV.

Based on the above criteria the levels at 6.821 and 8.188 MeV are identified as the analogus of the ground state (J^{π}=0$^+$) and the first excited state (J^{π}=2$^+$) of ^{64}Ni.
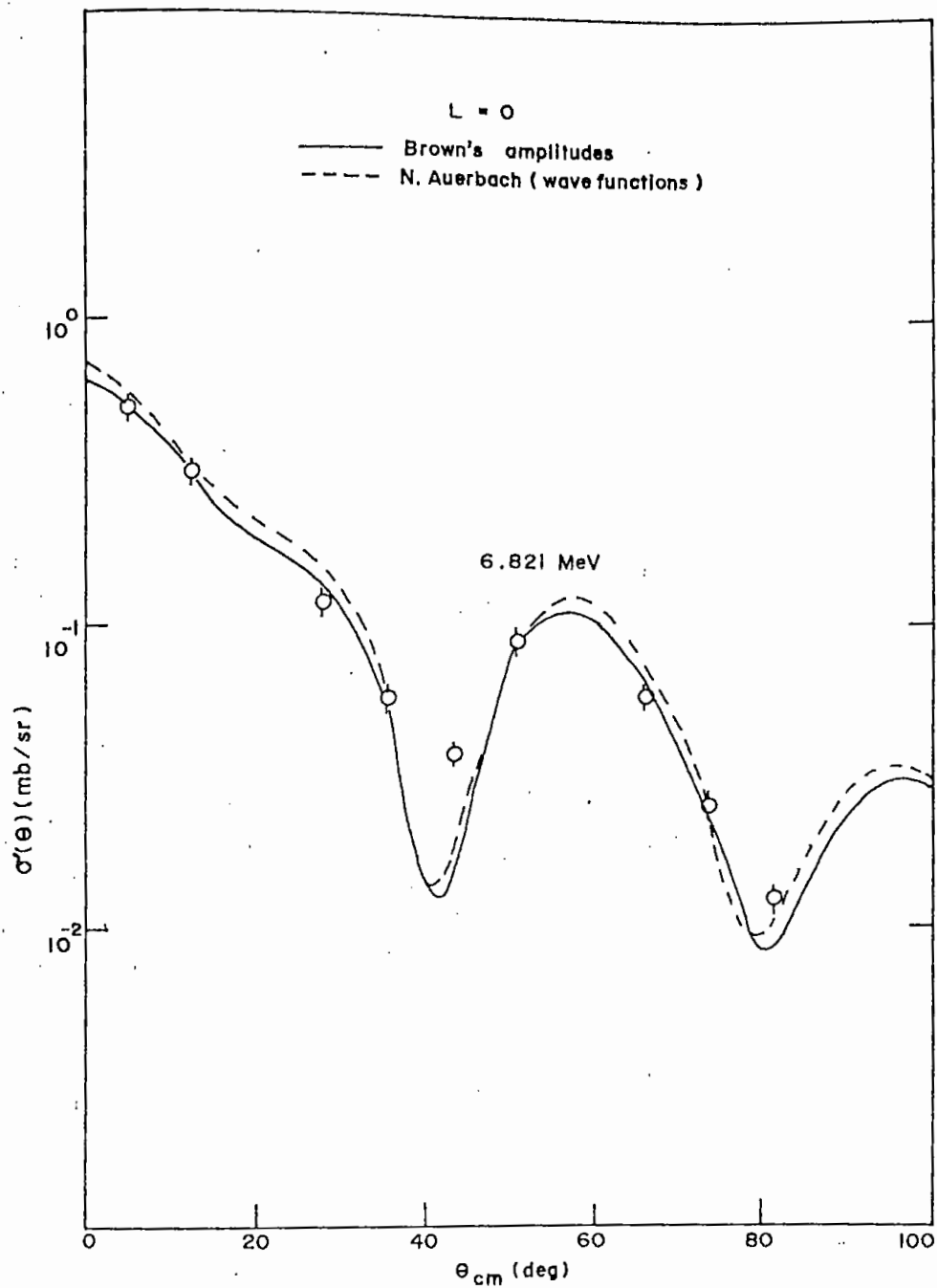
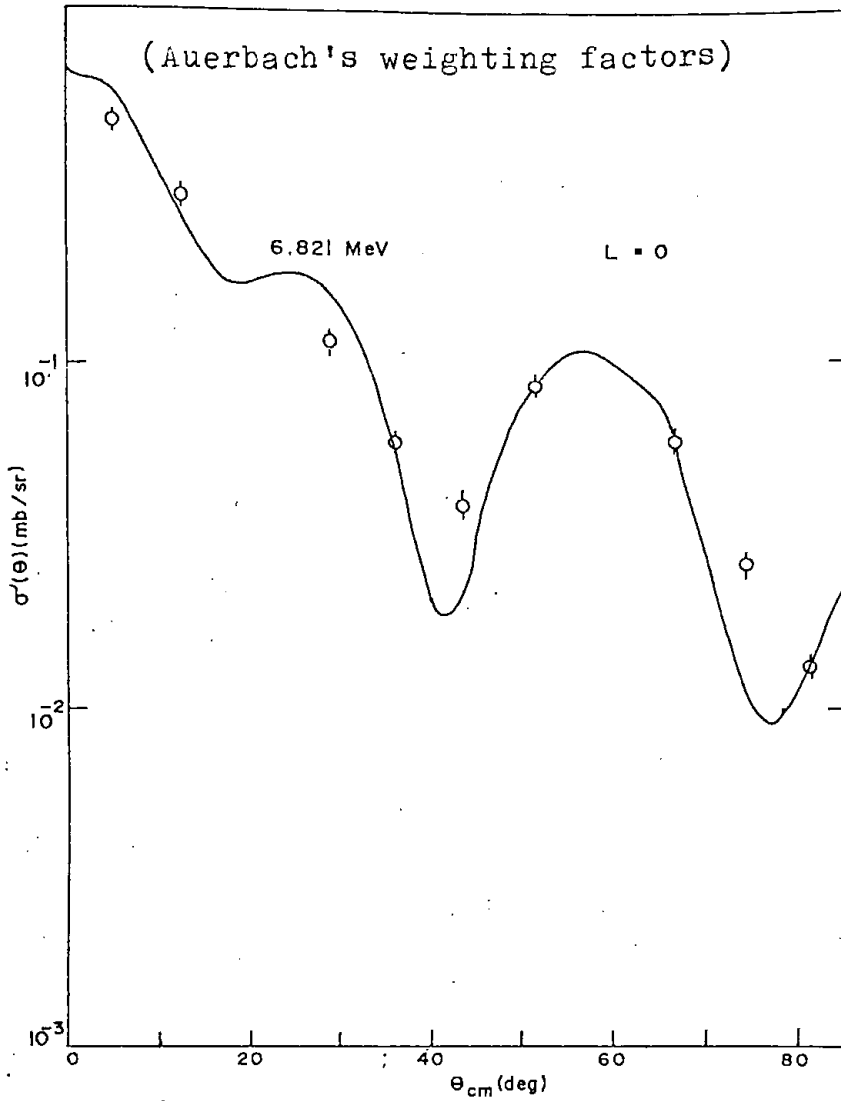Fig. 6.15. Measured angular distributions compared to DWBA

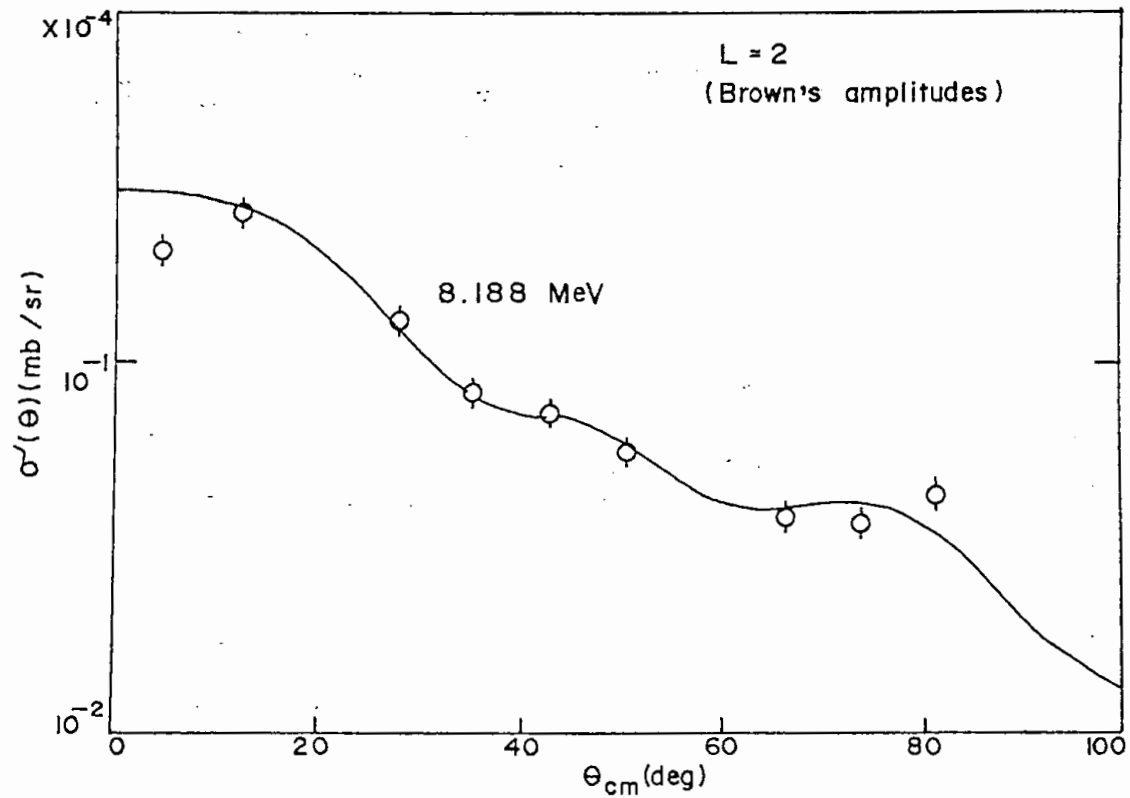Fig. 6.16. Measured angular distribution compared to DWBA.

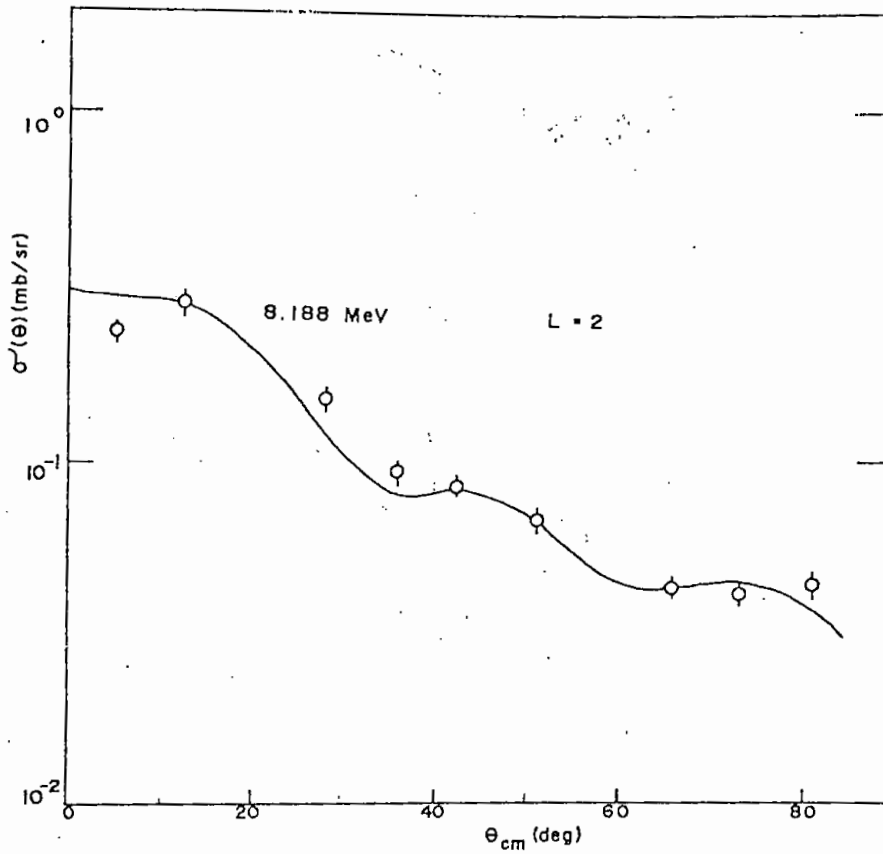Fig. 6.17. Measured angular distribution compared to DWBA..

Fig. 6.18. Measured angular distribution compared to DWBA.

The angular distribution to the level at 6.821 MeV was analyzed in terms of the DWBA theory using the spectroscopic amplitudes of Brown [Br 92] and separately with the weighting factors of Auerbach (Appendix A). But the angular distribution to the 8.188 level was analyzed in terms of the DWBA model using both a pure configuration and the spectroscopic amplitudes of Brown [Br 92]. The fits are shown in Figs. 6.15-6.18.

The ground state analogue was observed earlier in the charge exchange reactions, as summarized by Singh [Si 84]. This is confirmed in the present work and the 8.188 MeV level is identified as the analogue of the 1.344 MeV level (i.e. the first excited state) of ^{64}Ni. The (^{3}He,p) cross-section to the isobraic analogue states of the isotopic nuclei are expected to vary in the same way as the (t,p) cross-sections to the parent states except for the factor due to the square of isospin Clebsh-Gordan co-efficient. This has been confirmed by Caldwell et al. [Ca 73] and references theirin to be approximately valid for many nuclei. The (t,p) reaction data on Ni-isotopes [Da 71] do not quote the absolute corss-sections. It is therefore not possible to compare the present work with the (t,p) reaction data.

6.3.3   The level spectrum

Shell model calculations for ^{64}Cu have been performed in a complete $2P_{3/2}-1f_{5/2}-2p_{1/2}$ basis [Br 92] as mentioned in Section
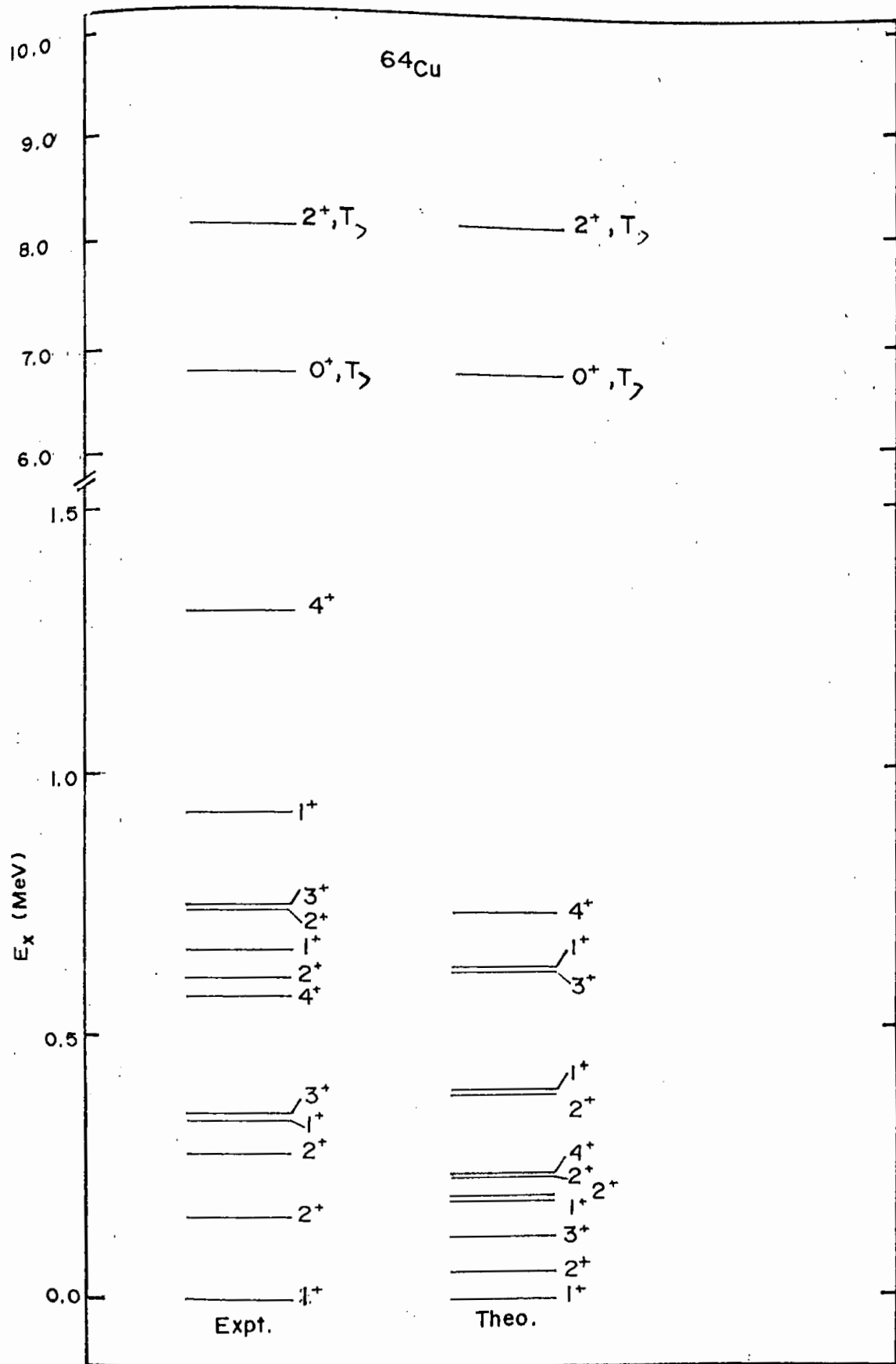
Fig. 6.19. Comparison of the experimental and theoretical spectra of ^{64}Cu .

6.3.1. Fig. 6.19 shows a comparison of the observed level spectrum of ^{64}Cu with the calculations due to Brown [Br 92].

The ground state J^π-value ($=1^+$) of ^{64}Cu is reproduced in the shell model calculations.

All the positive parity levels upto E_x~1.3 MeV except the 0.878 MeV ($J^\pi=0^+$) and the 1.243 MeV ($J^\pi=2^+$, (1^+)) levels are reproduced by the shell model theory [Br 92].

If it is assumed that the 1.288 MeV levels has $J^\pi=4^+$, and/or 3^+, then the calculated position is lowered by about 600 keV. The other levels are reproduced to within reasonable limits although the levels do not appear always in the right sequence.

The two analogue states at 6.821 and 8.188 MeV are well given by the calculations.

CHAPTER 7

CONCLUSION

CHAPTER 7

CONCLUSION

The aim of the present work was to investigate the spectroscopic properties of ^{52}Cr and ^{64}Cu nuclei respectively through the ^{51}V(^{3}He,d) and ^{62}Ni(^{3}He,p) reactions. The conclusions drawn from the results of the investigations are presented in this chapter.

The ^{51}V(^{3}He,d) reaction has been studied using ^{3}He-particles of energy 15 MeV. A total of 63 levels in ^{52}Cr, including several new levels, up to an excitation energy $E_x \approx$ 8.6 MeV, have been observed. The present work was done with a much more improved energy resolution than the previous ones [Ar 65,Pe 73].

The (^{3}He,d) reaction has an advantage over other proton stripping reactions like (d,n) and (α,t) and should provided information on the levels in final nuclei having dominant single-proton configuration. In the present work, the positive parity levels in ^{52}Cr with $(1f_{7/2})^n$ and $(1f_{7/2})^{n-1}(2p_{3/2})$ shell-model configurations, are excited.

The (^{3}He,d) reaction is well established as a useful tool for studying analogue states. But in the present case, the analogue states are known to lie at $E_x >$ 11 MeV. We could not study the levels beyond $E_x \approx$ 8.6 MeV. The level density starts

increasing and it was, therefore, not possible to identify the levels at still higher excitation.

Several levels in the nucleus ^{52}Cr observed in other reactions below $E_x \approx 6.6$ MeV (summarized by Singh [Si 84]) are not populated in the (^{3}He,d) reaction, while several new levels above $E_x \approx 6.6$ MeV are identified. Angular distributions for 63 levels are measured in the present work. The data for 34 levels are studied in terms of the DWBA theory. The DWBA analysis immediately gives the L-transfers, the parity, the spectroscopic factors, and J-limits. The single particle strengths are fragmented. A few low lying L=3 transitions are observed followed by two L=3 transitions at high excitation with a clear gap of about 5 MeV between the two groups. The latter two are assumed to belong to the $1f_{5/2}$ shell model state and the others to the $1f_{7/2}$ shell model states. The L=1 transitions are heavily fragmented with no such clear division between the $2p_{3/2}$ and $2p_{1/2}$ states. The $1f_{7/2}$ strength is exhausted and around 80% of the total 2p single particle strength is reached. The $1f_{5/2}$ strength in agreement with Pellegrini et. al. [Pe 73], but in disagreement with Armstrong and Blair [Ar 65], just begins to appear within the excitation energy covered in the present work.

The (^{3}He,p) reaction on ^{62}Ni has been studied using ^{3}He-particles of energy 18 MeV. A total of 69 levels in ^{64}Cu were identified. These include the two isobaric analogue states and

several new levels up to $E_x \approx 8.2$ MeV. The energy resolution was found to be ≈ 36 kev. Angular distributions for all the levels have been measured. Of these, 46 levels are analyzed in terms of the DWBA theory; L-transfers, the parity and the J-limits are obtained.

The $(^3He,p)$ reaction is known to populate levels with dominant two nucleon correlations. In the present experiment the levels with fp shell-model configurations are excited mostly with positive-parity states. A reasonably good account of the shape of the measured angular distributions are given by the DWBA method using two-nucleon spectroscopic amplitudes from fp shell model calculations as well as the DWBA calculations using a pure configuration. Properties are presented for several of the levels (Table 6.2). In order to get a meaningful comparison with experiment, care was taken in choosing the right optical-model parameters.

The $(^3He,p)$ reaction is also a useful tool for studying the analogue states. The levels at 6.821 and 8.188 MeV have been identified as the isobaric analogue states of the ground state $(J^\pi=0^+)$ and the first excited state $(J^\pi=2^+)$ of ^{64}Ni. Only the former level is adopted as the analogue of the ground state of ^{64}Ni [Si 84]. The latter identification is made for the first time. The $^{62}Ni(^3He,p)^{64}Cu$ reaction was previously studied by

Young and Rapaport [Yo 68] and Lee et al. [Le 73]. Only in the former a few strong transitions were studied, but details are not given. The present work thus gives information on the level structure of ^{64}Cu based on the (^{3}He,p) reaction.

We hope to have given information on the spectroscopy of the nuclei ^{52}Cr and ^{64}Cu.

REFFERENCES

REFFERENCES

[Ah 72]   N. Ahmed, M.A. Rahman, M. Rahman and H.M. Sen Gupta, *Nuovo Cim.*, **A11** (1972) 478.

[Aj 83]   F. Ajenberg-Selove, *Nucl. Phys.*, **A392** (1983) 1.

[Al 75]   W.P. Alford, R.A. Lindgren, D. Elmore and R.N. Boyd, *Nucl. Phys.*, **A243** (1975) 269.

[An 65]   J.D. Anderson, C. Wong and J.W. McClure, *Phys. Rev.*, **B138** (1965) 615.

[Ar 65]   D.D. Armstrong and A.G. Blair, *Phys. Rev.*, **B140** (1965) 1226.

[Ar 67]   D.D. Armstrong and A.G. Blair, *Phys. Rev.*, **155** (1967) 1254.

[Au 66]   N. Auerbach, *Nucl. Phys.*, **76** (1966), 331.

[Ba 53]   G.A. Bartholomew and B.B. Kinsey, *Phys. Rev.*, **89** (1953) 386.

[Ba 66]   R.H. Bassel, *Phys. Rev.*, **149** (1966) 791.

[Ba 71]   W.T. Bass and P.A. Stelson, *Phys. Rev.*, **C2** (1971) 2154.

[Ba 74]   F.T. Baker, S. Davis, C. Glashansser and A.B. Robbins, *Nucl. Phys.*, **A233** (1974) 409.

[Be 69]   F.D. Becchetti, Jr. and G.W. Greenless, *Phys. Rev.*, **182** (1969) 1190.

[Be 81]   U.E.P. Berg, D. Ruck, K. Ackermann, K. Bangert, C. Blasing, K. Kobras, W. Naatz, *Phys. Letters*, **B103** (1981) 301.

[Bi 81]   J.A. Bieszk and S.E. Vigdor, *Phys. Rev.*, **C23** (1981) 1404.

[Bl 72]   J. Black, R. Butt, K.H. Lindenberger, W. Ribbe and W. Zeitz, *Nucl. Phys.*, **197** (1972) 620.

[Bo 36]   Neils Bohr, "Neutron Capture and Nuclear Constitution", *Nature*, **137** (1936) 344.

[Bo 75]   W. Bohne, H. Fuchs, K. Grabisch, D. Hiescher, D. Jahnke, H. Kluge, T.G. Masterson and H. Morgenstern, *Nucl. Phys.*, **A245** (1975) 107.

[Bo 81]   J.J. Bowles, R.H. Hott, H.E. Jackson, R.M. Iaszewski, R.D. McKeown, A.M. Nathan and J.R. Specht, *Phys. Rev.*, **C24** (1981) 1940.

[Br 56]   C.P. Browne and W.W. Buchner, *Rev. Sc. Instr.*, **27** (1956) 899.

[Br 57]   D.A. Bromley, E. Almaquist, H.B. Grove, A.E. Litherland, E. Paul and A.J. Fargusen, *Phys. Rev.*, **105** (1957) 957.

[Br 92]   J.D. Brown, University of Pitsburgh, U.S.A., private communication (1992).

[Bu 50]   S.T. Butler, *Phys. Rev.*, **80** (1950) 1095.

[Bu 51]   S.T. Butler, *Proc. Roy. Soc.*, **A208** (1951) 559.

[Bu 58]   S.T. Butler et al., *Phys. Rev.*, **112** (1958) 1227.

[Ca 72]   Cage et al., *Nucl. Phys.*, **A183** (1972) 449.

[Ca 73]   T. Caldwell, O. Nathan, O. Hansen and H. Bork, *Nucl. Phys.*, **A202** (1973) 225.

[Ce 62]   Joseph Cery, Bernard G. Harway and H. Rehl Richardson, *Nucl. Phys.*, **29** (1962) 128.

[Co 63]   H. Collard and R. Hofstadter, *Phys. Rev.*, **131** (1963) 416.

[Da 70]   W.F. Davidson et al., *Nucl. Phys.*, **A142** (1970) 167-176.

[Da 71]   W. Darcey, R. Chapman and S. Hinds, *Nucl. Phys.*, **A170** (1971) 253.

[De 85]   M.G. Delfini and P.J. Brussaardy, *Nucl. Phys.*, **11** (1985) 113-117.

[Dj 83]   C. DJalali, N. Marty, M. Morlet, A. Willis and J.C. Jowdain, *Nucl. Phys.*, **A410** (1983) 399.

[Ev 74]   D. Evers, W. Assmann, K. Rudolph and S.J. Skorka, *Nucl. Phys.*, **A230** (1974) 109.

[Fi 58]   R.P. De Figueiredo et al., *Phys. Rev.*, **112** (1958) 873.

[Fu 85]   M. Fujiwara, Y. fujita, S. Imanishi, S. Morinobu, T. Yamazaki and H. Ikegami, *Phys. Rev.*, **C32** (1985) 830.

[Ga 74]   C. Gaarde et al., *Nucl. Phys.*, **A221** (1974) 238.

[Gi 52]   W.M. Gibson et al., *Proc. Roy. Soc.*, **A210** (1952) 549.

[Gl 62]   N.K. Glendenning, *Nucl. Phys.*, **29** (1962) 109.

[Gr 56]   T.S. Green and R. Middleton, *Proc. Phys. Soc.*, **A69** (1956) 28.

[Gr 76]   P.W. Green et al., *Nucl. Phys.*, **A274** (1976) 125-140.

[Hi 59]   S. Hinds et al., *Proc. Phys. Soc.* (London), **74** (1959) 196.

[Ho 55]   H.D. Holmgreen et al., *Phys. Rev.*, **100** (1955) 436.

[Hs 85]   C.C. Hsu, S.C. Yeh, and J.C. Wang, *Phys. Rev.*, **C31** (1985) 49.

[Hu 56]   W.J. Huiskamp, M.J. Steenland, A.R. Miedema, H.A. Talhock and C.J. Gorter, *Physica*, **XXII** (1956) 587-594.

[Jo 58]   R.L. Johnston, *Phys. Rev.*, **109** (1958) 884.

[Jo 85]   I.P. Johnstone, Dean Halderson, J.A. Carr and F. Petrovich, *Phys. Rev.*, **C35** (1985) 103.

[Ko 65]   J. Kopecky et al., *Nucl. Phys.*, **68** (1965) 449-462.

[Ko 84]   R.L. Kozub, C.B. Chitwood and D.J. Fields, *Phys. Rev.*, **C30** (1984) 1324.

[Le 80]   I.S. Lee, B.L. Cohen, T. Congede and H.N. Jow, *Nucl. Phys.*, **A344** (1980) 409-420.

[Li 50]   B.A. Lippmann and J. Schwinger, *Phys. Rev.*, **79** (1950) 299.

[Li 61]   A.E. Litherland and A.J. Ferguson, *Can. J. Phys.*, **39** (1961) 788.

[Li 64]   C.L. Lin and H. Yoshida, *Prog. Theor. Phys.*, **32**
            (1964) 885.

[Li 70]   K. Lips and M.T. McEllistrem, *Phys. Rev.*, **c1** (1970)
            1009

[Li 73]   C.L. Lin, S. Yamaji and H. Yoshida, *Nucl. Phys.*,
            A209 (1973) 135.

[Lu 69]   Lu, Zizman and Harvey, *Phys. Rev.*, **186** (1969) 1086.

[Ma 57]   H. Mazari, W.W. Bucchner and A. Sperduto, *Phys. Rev.*,
            107 (1957) 1383.

[Ma 68]   Masaru Matoba, *Nucl. Phys.*, **A118** (1968) 207.

[Ma 68]   Nolan F. Mangelson, *Nucl. Phys.*, **A119** (1968) 79-96.

[Me 71]   Menet et al., *Phys. Rev.*, **C4** (1971) 1114.

[Mi 62]   R. Middleton and S. Hinds, *Nucl. Phys.*, **34** (1962)
            405.

[Mo 68]   C.F. Monahan, N. Lawley, C.W. Thomas and P.J. Twin,
            Nucl. Phys., **A120** (1968) 460.

[Mu 84]   K. Muto and H. Horie, *Phys. Letters*, **B138** (1984) 9.

[Na 57]   M. El Nadi, *Proc. Phys. Soc.*, **A70** (1957) 62.

[Na 60]   M. El Nadi, *Phys. Rev.*, **119** (1960) 242.

[Na 71]   H. Nann, B. Hubert and R. Bass, *Nucl. Phys.*, **A176**
            (971) 553.

[Ne 52]   H.C. Newns, *Proc. Phys. Soc.*, **A65** (1952) 916.

[Ne 60]   H.C. Newns, *Proc. Phys. Soc.*, **A76** (1960) 489.

[Ne 67]   E. Newman, L.C. Becker, B.M. Preedom and J.C.
            Hiebert, *Nucl. Phys.*, **A100** (1967) 225.

[Op 35]   J. Oppenheimer and Phillips, *Phys. Rev.*, **48** (1935)
            500.

[Os 71]   E. Osnes, Proc. Topical Conference on the Structure
            of the $1f_{7/2}$ Nuclei, ed. R.A. Ricci (Enditrice
            Compositri, Bologna, Italy, 1971) 79.

[Pa 61]   F. Pellegrini, *Nucl. Phys.*, **24** (1961) 372.

[Pa 69]   Y.S. Park and W.W. Daehnick, *Phys. Rev.*, **180** (1969) 1082.

[Pe 73]   F. Pellegrini, I. Filisofo and M.I. El Zaiki, I. Gabrielli, *Phys. Rev.*, **C8** (1973) 1547.

[Pe 75]   R.J. Peterson and R.A. Risitinen, *Nucl. Phys.*, **A246** (1975) 402.

[Ph 69]   Phys. Letters, **B29** (1969) 327.

[Po 59]   C.F. Powell et al., *The Study of Elementary Particle by Photographic Emulsion*, Pergamon Press (1959).

[Re 68]   L.P. Remsberg, *Phys. Rev.*, **174** (1968) 1338.

[Ro 30]   S. Rosenblum, "Progess Recents: dans I´Etude du Spectra Magnetigue des Rayons L", *J. Phys. et Radium*, **1** (1930) 438.

[Ru 61]   M.L. Rustigi, *Nucl. Phys.*, **25** (1961) 169.

[Ru 70]   A. Ruh and P. Marmier, *Nucl. Phys.*, **A151** (1970) 479.

[Ry 78]   T.B. Ryves, P. Kolkowski, and K.J. Zieba, *Metrologia*, **14** (1978) 127-135.

[Sa 64]   G.R. Satchler, *Nucl. Phys.*, **55** (1964) 1-33.

[Sc 64]   L.I. Schiff, *Phys. Rev.*, **133** (1964) B802.

[Se 70]   K.K. Seth, J. Picard and G.R. Satchler, *Nucl. Phys.*, **A140** (1970) 577.

[Se 86]   H.M. Sen Gupta, M.A. Zaman, F. Watt and M.J. Huest, *Nuovo Cim.*, **A93** (1986) 222.

[Sh 68]   E.B. Shera and Bolotin., *Phys. Rev.*, **169** (1968) 940.

[Sh 77]   J.R. Shepard, W.R. Zimmerman and J.J. Kraushaar, *Nucl. Phys.*, **A275** (1977) 189.

[Si 84]   B. Singh, Adopted Levels, ENSDF version, February 1984 (Kuwait Institute of Scientific Research, May 1984).

[Sk 58]   V.V. Skliarveskii, E.P. Stepanov and B.A. Obiniakov, *Atomuaia Energia*, **5** (1958) 454.

[Sm 73]   J.W. Smith, L.M. Schutzmeister, T.H. Braid and P.P. Singh, *Phys. Rev.*, **C7** (1973) 1104.

[Sm 83]   Ph.B. Smith and W. Segeth, *Nucl. Phys.*, **A398** (1983) 397.

[So 85]   D.I. Sober, B.C. Metsch and W. Knupfer et al., *Phys. Rev.*, **C31** (1985) 2054.

[St 67]   R. Stock, R. Bock, P. David, H.H. Duhm and T. Tamura, *Nucl. Phys.*, **A109** (1967) 136.

[To 61]   S.J. du Toit and L.M. Bollinger, *Phys. Rev.*, **123** (1961) 629.

[Tr 57]   G. Trumphy, Jener Publications, **13** (1957).

[Tr 87]   Hans-Jochen Trost, Peter Lezoch and Udo Strobbusch, *Nucl. Phys.*, **A462** (1987) 333.

[Ur 71]   P.P. Uroni et al., *Nucl. Phys.*, **A167** (1971) 383-400.

[Ve 61]   J. Vervier, *Nucl. Phys.*, **26** (1961) 10.

[Wa Un]   D.L. Watson, University of Bradford, private communication.

[We 71]   C.C. Welborn et al., Phys. Rev., C3 (1971) 153.

[Wi 62]   R.R. Wilson, A.A. Bartlett, J.J. Kraushaar, J.D. McCullen and R.A. Ristinen, Phys. Rev., 125 (1962) 1254.

[Yo 68]   Helen J. Young and J. Rapaport, *Bu. Am. Phys. Soc.*, **13** (1968) 105.

APPENDIX

APPENDIX

A.   <u>CALCULATION OF WEIGHTING FACTOR</u>

[Ref.[Au 66]: N.Auerbach, Nuclear Physics, <u>76</u> (1966) 331]

for the ^{62}Ni(^{3}He,p) ^{64}Cu reaction:

$$\langle \Psi\, ^{64}\text{Cu} \quad \Psi\, ^{64}\text{Cup} \,|V|\, \Psi\, ^{3}\text{He}, \Psi\, ^{62}\text{Ni}\, \chi\, ^{3}\text{He}^{62}\text{Ni} \rangle$$

$$|^{62}\text{Ni}\rangle_{g.s.} = |^{62}\text{Ni}\rangle_{core}\,\{0.508\,(p_{3/2})^4\,(f_{5/2})^2 - 0.526(p_{3/2})^2$$

$$+(f_{5/2})^4 - 0.183(f_{5/2})^6 + 0.502(p_{3/2})^2\,(f_{5/2})^2$$

$$(p_{\frac{1}{2}})^2 + 0.337\,(p_{\frac{1}{2}})^2\,(p_{3/2})^4 - 0.259\,(f_{5/2})^4(p_{\frac{1}{2}})^2\}.$$

$$|^{64}\text{Ni}\rangle_{g.s.} = |^{56}\text{Ni}\rangle_{core}*\,\{0.549\,(p_{3/2})^4\,(f_{5/2})^4 - 0.561(p_{3/2})^2$$

$$(f_{5/2})^4\,(p_{\frac{1}{2}})^2 - 0.429(p_{3/2})^2 - 0.219(p_{\frac{1}{2}})^2(f5_{5/2})^6$$

$$+ 0.339\,(p_{\frac{1}{2}})^2\,(p_{3/2})^4\,(f_{5/2})^2\}.$$

1(a). $(p_{3/2})^4\,(f_{5/2})^2\,\dfrac{0.508\text{x}\,(-0.549)}{(f_{5/2})^2}\,(p_{3/2})^4(f_{5/2})^4$

1(b). $(p_{3/2})^4\,(f_{5/2})^2\,\dfrac{0.508\text{x}0.391}{(p_{\frac{1}{2}})^2}\,(p_{\frac{1}{2}})^2(p_{3/2})^4(f_{5/2})^2$

2(a). $(P_{3/2})^2$ $(f_{5/2})^4$ $\dfrac{-0.526 \times (-0.549)}{(P_{3/2})^2}$ $(P_{3/2})^4 (f_{5/2})^4$

2(b). $(P_{3/2})^2$ $(f_{5/2})^4$ $\dfrac{-0.526 \times (-0.561)}{(P_{1/2})^2}$ $(P_{3/2})^2 (f_{5/2})^4 (P_{1/2})^2$

2(c). $(P_{3/2})^2$ $(f_{5/2})^4$ $\dfrac{-0.526 \times (-0.429)}{(f_{5/2})^2}$ $(P_{3/2})^2$ $(f_{5/2})^6$

3(a). $(f_{5/2})^6$ $\dfrac{-0.183 \times (-0.429)}{(P_{3/2})^2}$ $(P_{3/2})^2$ $(f_{5/2})^6$

3(b). $(f_{5/2})^6$ $\dfrac{-0.183 \times (-0.219)}{(P_{1/2})^2}$ $(P_{1/2})^2$ $(f_{5/2})^6$

4(a). $(P_{3/2})^2 (f_{5/2})^2 (P_{1/2})^2$ $\dfrac{0.502 \times (-0.561)}{(f_{5/2})^2}$ $(P_{3/2})^2$ $(f_{5/2})^4$ $(P_{1/2})^2$

4(b). $(P_{3/2})^2 (f_{5/2})^2 (P_{1/2})^2$ $\dfrac{0.502 \times 0.391}{(P_{3/2})^2}$ $(P_{1/2})^2 (P_{3/2})^4$ $(f_{5/2})^2$

5. $(P_{1/2})^2 (P_{3/2})^4$ $\dfrac{0.337 \times 0.391}{(f_{5/2})^2}$ $(P_{1/2})^2 (P_{3/2})^4$ $(f_{5/2})^2$

6. $(f_{5/2})^4 (P_{1/2})^2$ $\dfrac{-0.259 \times (-0.219)}{(f_{5/2})^2}$ $(P_{1/2})^2$ $(f_{5/2})^6$.

WEIGHTING FACTOR

(1) for $(f_{5/2})^2$

   $0.508 \times (-0.549) + (-0.526) \times (-0.429) + 0.502 \times (-0.561)$

   $+ 0.337 \times 0.391 + (-0.259) \times (0.219) = -0.146 \approx -0.15$

(2) for $(p_{3/2})^2$

   $-0.526 \times (-0.549) + (-0.183) \times (-0.429) + 0.502 \times 0.391 = 0.563 \approx 0.56$

(3) for $(p_{1/2})^2$

   $0.508 \times 0.391 + (-0.526) \times (-0.561) + (-0.183) \times (-0.219) = 0.533 \approx 0.53.$

103